Model-Based Approach for Optimizing Operational Flexibility of Integrated Multi-Energy Industrial Clusters

I.R. Zuijderwijk

Delft University of Technology

TU Delft

Port of Rotterdam

Model-Based Approach for Optimizing Operational Flexibility of Integrated Multi-Energy Industrial Clusters

by

I.R. Zuijderwijk

The present thesis was submitted to the Delft University of Technology in partial fulfillment of the requirements for the degree of Master of Science in Sustainable Energy Technology.

Student number:	4978579	
Project duration:	September, 2024 – June, 2025	
Thesis committee:	Dr. ir. J.L. Rueda Torres	TU Delft, committee chair & supervisor
	Dr. Z. Qin	TU Delft, committee member
	Dr. P. Procel Moya	TU Delft, committee member
External advisors:	Ir. R. Weterings	Port of Rotterdam, external supervisor
	Ir. M. Fruytier	Port of Rotterdam, external supervisor

TU Delft

Disclaimer

The research work shown in this dissertation has received funding from the Port of Rotterdam. It reflects only the author's view, and the above indicated organization is not responsible for any use that may be made of the information it contains in.

Acknowledgment

The completion of this thesis marks the end of my time as a student — a valuable period during which I have come to better understand myself and my interests. I started with a bachelor's in Molecular Science and Technology, and I quickly discovered that my passion lies in sustainability. This realization led me to apply my technical background to this field through the master's program in Sustainable Energy Technologies.

This time has not only shaped my academic and professional direction, but also brought me deep and lasting friendships, which I hope will continue well beyond this chapter.

This final thesis project marks the conclusion of a valuable learning journey. While the thesis is an individual project, I would like to acknowledge the contributions of several people. I thank my academic supervisor, José Rueda Torres, for his time, guidance, and for providing thoughtful and constructive feedback that helped me move forward throughout the process. I am grateful for the time and effort he invested in helping publish my research, which marks a meaningful milestone at the close of this chapter.

I also had the opportunity to carry out this thesis in collaboration with the Port of Rotterdam. I am especially grateful to my supervisors there, Marthe Fruytier and Randolf Weterings, for the engaging weekly meetings, where I could always ask questions and discuss ideas openly. These meetings were extremely helpful in shaping the direction of my project and making steady progress. I would also like to thank my colleagues at the Port of Rotterdam for the enjoyable coffee and lunch breaks, as well as the fun team activities.

Finally, I would like to thank my friends and family for their support throughout the entire process. A special thanks goes to my sister Noa, who made time to reflect with me, challenge my ideas, and help me move forward throughout my studies and once again during this thesis.

I.R. Zuijderwijk
Delft, May 2025

Abstract

Achieving carbon-neutral energy systems in industrial clusters necessitates fundamental restructuring of existing energy systems. This transition is accompanied by several significant challenges. In pursuit of carbon neutrality, there is an increasing demand for industrial electrification, as well as a rising demand for green electricity and sustainable energy carriers, such as hydrogen and ammonia. The integration of variable renewable energy sources (VRES) is critical to address the growing demand for clean energy and enable the critical shift away from fossil fuel dependence. However, the intermittent nature of VRES, in combination with grid congestion issues, poses a challenge to the reliability of energy supply, a crucial element in fostering an attractive investment climate. Moreover, the development of new energy infrastructure is constrained by several factors, including limited access to new grid connections, investment uncertainty, and spatial limitations. Conventional energy planning and operation approaches, which treat energy sectors in isolation, are unable to address these complex, system-wide challenges. These approaches limit the ability to optimize across various energy sectors and fail to harness the potential synergies between energy carriers. Conversely, a more flexible and integrated approach provided by multi-energy systems (MESs) has been shown to effectively mitigate VRES intermittency, alleviate grid congestion through alternative energy pathways, and enhance cross-sector synergies and infrastructure utilization. However, the realization of these benefits necessitates a deeper understanding of the operation and organization of such systems.

To provide these insights, this research develops a model-based optimization approach for the cost-effective operation of MESs. The modeled system represents a synthetic, future-oriented energy system for an industrial cluster, drawing inspiration from the Maasvlakte area in the Port of Rotterdam. The research introduces a new operation strategy to support the transition towards a carbon neutrality, addressing key barriers currently limiting the decarbonization of industrial clusters.

A detailed conceptual model for the synthetic MES was developed to reflect the existing infrastructure of the Maasvlakte area, planned projects, and potential future developments. This conceptual model was translated into an operational optimization model implemented in Python using the PyPSA toolbox. The MES integrates five energy carriers—electricity, natural gas, hydrogen, ammonia, and heat—within a unified model through the energy hub approach that facilitates sector coupling, conversion, and storage within multi-energy carrier networks. The electricity system is modeled with physic-based power flow constraints to capture technical feasibility in the power system, and the non-electrical carrier networks are modeled using the energy hub approach. The entire system is optimized through a single-objective cost minimization, with mixed-integer linear programming, using hourly resolution over a one-year horizon. To test the system's performance under varying renewable energy supply, three weather-dependent scenarios were formulated and optimized, reflecting variability in wind and solar conditions and its implications for system operation.

Based on the system's optimal performance across all scenarios, this research proposes a new operation strategy that enables flexible and cost-effective operation of a multi-energy industrial cluster, representing a paradigm shift from conventional approaches. Instead of relying on static, price-driven, and siloed sectoral operation, the proposed strategy emphasizes cross-sector economic optimization, dynamic dispatch response to system states, enhanced system flexibility through integrated conversion and storage technologies, and continuous energy supply to industrial consumers.

Key outcomes include the development of an operation strategy that minimizes costs while ensuring energy supply to industrial consumers and technical feasibility, the identification of ammonia as key flexibility provider, and actionable insights into flexibility management, the role of conversion technologies, and infrastructure planning. The results have important implications for decarbonization pathway of industrial clusters, offering a cost-effective and actionable approach to integrated energy system operation.

Contents

Nomenclature

Abbreviations

Abbreviation	Definition
AC	Alternating Current
ATR	Autothermal Reforming
Capex	Capital Expenditures
CCUS	Carbon Capture, Utilization, and Storage
CHP	Combined Heat and Power
CO_2	Carbon Dioxide
COP	Coefficient of Performance
DC	Direct Current
DNLP	Dynamic Nonlinear Programming
DR	Demand Response
DSM	Demand Side Management
H_2	Hydrogen
HV	High Voltage
HV	High Voltage Alternating Current
HHV	Higher Heating Value
KNMI	Koninklijk Nederlands Meteorologisch Instituut
LH_2	Liquid Hydrogen
LHV	Lower Heating Value
LP	Linear Programming
LNG	Liquid Natural Gas
LOHC	Liquid Organic Hydrogen Carrier
MES	Multi-Energy System
MILP	Mixed Integer Linear Programming
MINLP	Mixed Integer Non Linear Programming
MIQP	Mixed Integer Quadratic Programming
MMES	Maasvlakte Multi-Energy System
N/A	Not Applicable / Not Available
NG	Natural Gas
NH_3	Ammonia
NLP	Non-Linear Programming
Opex	Operational Expenditures
P2X	Power-to-X
PSO	Particle Swarm Optimization
PyPSA	Python for Power System Analysis
RES	Renewable Energy Sources
RO	Robust Optimization
Ref.	Reference
VPP	Virual Power Plant
VRES	Variable Renewable Energy Sources
ZC-MES	Zero Carbon Multi-Energy System

Symbols

Symbol	Definition	Unit
t	Time	[h]
E	Energy	[MWh]
Q	Thermal energy / heat	[MW] or [MWh]
P	Power	[MW]
S	Apparent power	[MVA]
V	Voltage	[V]
I	Electric current	[A]
m	Mass	[kg] or [tonne]
V	Volume	[m^3]
c	Specific heat capacity	[J/(kg·K)]
η	Efficiency	[-]
x_n	Longitude of node n	[degrees]
y_n	Latitude of node n	[degrees]
T	Temperature	[K] or [°C]
ΔT	Temperature difference	[K] or [°C]
λ	Standing loss coefficient	[h^{-1}]
θ	Voltage phase angle	[radians]
r	Resistance	[Ω]
x	Reactance	[Ω]
z	Impedance	[Ω]
b	Susceptance	[S]
g	Conductance	[S]
z	Admittance	[S]
E_{nom}	Nominal Energy	[MWh]
P_{nom}	Nominal Power	[MW]
LHV	Lower Heating Value	[MJ/kg] or [MWh/tonne]
Capex	Capital expenditure	[€/MW] or [€/MWh]
Opex	Operating expenditure	[€/MW] or [€/MWh]

1 Introduction

1.1. Energy Transition in Industrial Clusters

The transition to low-carbon energy systems is among the most pressing global challenges of the 21st century. Despite the existence of international climate agreements, including the United Nations Framework Convention on Climate Change of 1992, the Kyoto Protocol of 1997, and the Paris Agreement of 2015, emissions continue to reach alarming levels in numerous sectors [1]. Among these sectors, the industrial sector is of significant importance, as it is responsible for approximately 30% of global CO_2 emissions, a share that has steadily grown over the past two decades [2].

In this context, industrial clusters—geographically concentrated networks of interconnected industries, suppliers, and institutions—present both a challenge and an opportunity for sustainable transformation. These clusters typically support a multitude of energy-intensive processes such as chemical manufacturing, steel production, oil refining, and heavy manufacturing, predominantly powered by fossil fuels. Beyond being significant energy consumers, these industrial clusters frequently serve as the primary sites where energy is generated, converted, and distributed at large scale for end-use applications, owing to their strategic locations, high energy demand, and extensive existing energy infrastructure. Consequently, these industrial clusters often function as critical energy hubs for regional and national energy systems. The significance of decarbonizing these clusters thus extends beyond reducing carbon emissions in the industrial sector itself. Their transformation plays a crucial role in facilitating the broader energy transition, with downstream impacts on other end-use sectors, such as transport and buildings. Achieving carbon neutrality in these clusters is thus a fundamental component of a successful transition to a low-carbon economy.

Furthermore, this energy transition within industrial clusters is not only essential for reducing carbon emission, but also has significant implications for the economic future of the regions in which they are embedded. It presents an opportunity to build economies based on sustainable energy while also enhancing economic resilience and strategic autonomy. By pioneering new clean energy value chains, industrial clusters can establish leadership positions, unlock opportunities for knowledge export and international collaboration, and support substantial workforce expansion through the creation of new jobs. Consequently, beyond the environmental benefits, the energy transition in industrial clusters offers significant social and economic opportunities through new value chains, innovation potential, and strategic positioning in emerging sustainable markets. To achieve these benefits, industrial clusters must foster an investment climate that not only retains existing businesses but also actively stimulates sustainable innovation across all sectors.

1.2. Barriers to Industrial Cluster Decarbonization

The decarbonization of industrial clusters demands a shift from fossil fuel dependence to renewable energy sources. However, this transition faces several challenges. The increasing integration of variable renewable energy sources (VRES) introduces intermittent energy production, placing strain on the operational limits of current power infrastructure and system balancing capabilities. This challenge arises as the variable output of renewables is often misaligned with real-time demand patterns, creating temporal mismatches between energy supply and demand. This intermittent nature of energy production undermines the reliability of energy supply, which is a critical factor for maintaining an attractive investment climate in industrial regions.

Simultaneously, grid congestion is already a significant challenge in many regions and is projected to intensify as the rate of renewable energy deployment and electrification surpasses the capacity for grid reinforcement.

Consequently, new developments for sustainable energy infrastructure encounter delays in initiation due to the inability to secure grid connection, resulting in extended waiting periods. The establishment of necessary infrastructure therefore represents one of the most pressing challenges in decarbonizing industrial clusters [3].

The transition is further complicated by limited affordability and low current market demand, which often contribute to delayed investments in new energy infrastructure. The realization of new energy infrastructure and sustainability initiatives is further complicated by spatial constraints, permitting processes, environmental regulations, and inadequate execution capacity. The aforementioned issues collectively contribute to the difficulty of achieving carbon-neutral and economically competitive energy systems [3].

1.3. Multi-Energy Systems

In order to address the challenges associated with the transition toward carbon neutrality, it is essential to consider more than strengthening the existing energy infrastructure. A fundamental restructuring of the way energy systems operate is necessary. A key limitation of traditional energy systems is their sectoral separation, where electricity, natural gas, and heating networks function independently in terms of planning, operation, and regulation [4]. This siloed approach not only impedes system flexibility, required for large-scale renewable integration and the decarbonization of industrial processes, but also creates barriers to cross-sectoral optimization, limiting the potential for synergistic solutions that could address multiple challenges simultaneously. So to address the challenges regarding the transition towards carbon-neutral energy systems, there has been an increasing focus on the concept of integrated or multi-energy systems (MES).

An energy system that exhibits optimal interaction between multiple energy sectors at various levels is defined as an integrated or multi-energy system (MES) [4]. Given that the majority of energy systems are inherently multi-energy, i.e. existing of multiple energy carrier networks, the concept of a multi-energy system is understood as a comprehensive approach to optimization and evaluation across economic, environmental, and technical levels. In practice, the implementation of such a system necessitates the integration and coordination of energy production, consumption, infrastructure with energy services, and enabling new technologies [5].

The consideration of energy systems from this whole-system perspective can yield numerous advantages. The integration of different energy carriers in multi-energy systems enhances the flexibility of energy systems by facilitating sector coupling through conversion and storage technologies, allowing energy to exist in various forms across different carriers. This addresses the challenge of maintaining a constant balance between electricity supply and demand, which becomes increasingly relevant with the increasing share of VRES in energy systems, due to their unpredictability and intermittency of energy production. Therefore, overcoming these balancing issues can significantly enhance the uptake of these technologies, contributing to a substantial reduction in carbon emissions. Additionally, the flexibility of energy flow between carriers enables the optimal use of existing infrastructure, reducing the need for costly expansion and thereby lowering overall system costs. Furthermore, by enhancing the flexibility of energy use across different carriers, multi-energy systems improve the utilization of primary energy sources, ultimately increasing overall system efficiency [4].

1.4. Problem Statement

Achieving carbon-neutral energy systems within industrial clusters necessitates a comprehensive restructuring of their current energy systems. In pursuit of carbon neutrality, industrial electrification is increasing alongside a rising demand for green electricity and sustainable energy carriers such as hydrogen and ammonia. Integration of VRES is essential to address the growing demand for clean energy and enable the critical shift away from fossil fuel dependence. However, the intermittent nature of VRES, together with grid congestion issues, poses a challenge to reliable energy supply, a crucial element in fostering an attractive investment climate.

Beyond intermittency, this transition is further constrained by barriers such as grid congestion, limited access to new grid connections, uncertainty in investment, spatial constraints, and regulatory obstacles. Conventional energy operation and planning approaches, which treat energy sectors in isolation, are unable to address these complex, system-wide challenges, as they limit the ability to optimize across various energy sectors and fail to harness the potential synergies between energy carriers.

A more flexible and integrated approach, characterized by optimal integration of multiple energy carriers into a MES, can mitigate VRES intermittency, alleviate grid congestion through alternative energy pathways, and enhance cross-sector synergies. By enabling sector coupling, a MES can reduce dependence on fossil fuels,

improve infrastructure utilization, and optimize energy flows throughout system operations. However, realizing these benefits requires a deeper understanding of how such systems operate and are organized.

The objective of this thesis is to develop a novel modeling approach for the optimization of integrated multi-energy systems within industrial clusters. The modeled system is a synthetic, future-oriented MES inspired by the Maasvlakte area in the Port of Rotterdam. This location is an ideal case study due to the available space for the development of new energy infrastructure and the presence of major planned energy projects, including a hydrogen conversion park and new offshore wind connections. However, while these investments are in the pipeline, it remains unclear how they can best be integrated and which investments are most critical to the operation of the system. Rather than focusing on a specific target year, this research will incorporate multiple potential infrastructure developments to assess their influence on system performance. By doing so, emphasis will be placed on the integration of future developments rather than simulating a specific point in time.

This research develops an operation strategy for carbon-neutral multi-energy industrial clusters that minimizes overall system costs, ensures continuous energy supply, and maintains technical feasibility within the power system. By optimizing system operation under varying scenarios, the modeling results offer insights into the optimal operation of MESs, identifying critical components, necessary infrastructure, and high-priority investments.

1.5. Research Questions

The main research question is stated as follows;

> *"How can a model-based approach be developed to advance the optimization of multi-energy systems in industrial clusters and support decision-making regarding system operation strategies?"*

In order to answer the main research question, a set of sub-questions has been defined, focusing respectively on system modeling, system operation, and the development of a flexible operation strategy.

1. How can multi-energy systems be modeled to represent existing infrastructure and future developments, and what methodological advances does this research offer in the broader context of multi-energy system modeling?
2. What are the operational constraints of the system, and how can weather-related uncertainties be effectively incorporated into the optimization model to ensure consistent and cost-effective system operation under varying weather conditions?
3. How can multi-energy systems enhance energy system flexibility, and what operation strategies enable flexible and cost-effective operation of multi-energy systems?

1.6. Thesis Outline

In order to address the stated research objective and respond to the research questions, the thesis first establishes a theoretical foundation of energy system flexibility and energy system modeling. Chapter 2 presents the background and literature review, exploring the role of flexibility in future energy systems and reviewing current modeling approaches. This chapter identifies significant gaps in the extant literature on MES modeling. These gaps inform the research design and support the development of the optimization model proposed in this thesis. Chapter 3 builds on the foundation established in the preceding chapter by introducing the research methodology, which provides a structured approach to developing the optimization model. The chapter provides an explanation of the selection of the Maasvlakte as a case study, the development of the conceptual model, and its translation into the optimization model. Furthermore, the chapter elaborates on the development of scenarios designed to evaluate system operation under varying weather conditions. Chapter 4 presents and analyzes the results of the optimization experiments. The system behavior is evaluated across the different scenarios, and an operation strategy for multi-energy industrial clusters is introduced based on modeled outcomes. While derived from the case study, this strategy provides generalizable principles for the cost-effective energy system operation in industrial clusters. In addition, this chapter presents a critical reflection on the study's findings and discusses its limitations. Finally, Chapter 5 synthesizes the key findings in relation to the research questions and provides recommendations for future research.

2

Background and Literature Review

2.1. Introduction

This chapter establishes the theoretical foundation for developing the optimization model for MESs. The chapter begins by examining the critical role of flexibility in energy systems during the ongoing energy transition in Section 2.2, thereby highlighting the growing relevance of MESs. Section 2.3 then explores how MESs can be described through energy system modeling, discussing the classification, modeling approaches and aggregation concepts, covering the theoretical foundation for MES modeling. The section concludes with a structured literature review that establishes the state-of-the-art of MES modeling and identifies critical gaps in current literature.

2.2. Flexibility in Energy Systems

The incorporation of VRES within energy systems has undergone substantial expansion in recent years, driven by two primary factors. Firstly, there has been an increase in electricity demand, owing to the electrification of the energy system. Secondly, there has been an increase in the share of VRES in the electricity grid, as part of the broader transition towards a renewable energy future. As a result, the importance of flexibility in energy systems to enhance the resilience of the energy system to the variable and unpredictable energy production associated with VRES is increasing.

Research conducted by the Netherlands Organization for Applied Scientific Research (TNO) indicates that the demand for flexibility and system integration is expected to increase more than sixfold from 2015 to 2050 [6]. In this study, flexibility is defined as ”the ability of the energy system to respond to the variability and uncertainty of the residual load within the limits of the electricity system”. The study identifies three specific factors that are driving the growing need for flexibility in the energy system. These drivers are the variability of the residual power load—i.e. the electricity demand that needs to be met by sources other than VRES—when VRES supply is insufficient to meet demand, the increasing uncertainty of electricity supply due to the unpredictable output of VRES, and grid congestion. This section presents a comprehensive analysis of the methods by which flexibility can be provided in power systems—Section 2.2.1—and in MESs—Section 2.2.2.

2.2.1. Flexibility in Power Systems

The adoption of flexibility in power systems is becoming increasingly important for the management of variability in renewable energy generation and the maintenance of a stable balance between supply and demand. There are several solutions for increasing the flexibility of the power system. In their book, Schmidt and Staffell identify four main technical options for providing flexibility to power systems: flexible generation, interconnection, demand response, and electricity storage [7].

Flexible generation refers to measures that facilitate the adaptability of power generation units, thereby allowing them to adjust their output in response to fluctuations in electricity demand. Presently, this necessity for flexible generation is predominantly met by gas-fired power plants, which possess the technical capacity to regulate their output with ease, thereby contributing to the stability of the power system [8]. However, as fossil fuels are being phased out, there is an increasing need for alternative flexibility options in power generation. This is especially relevant during periods of low renewable energy production, such as during periods of limited sunlight or wind.

Network interconnection enhances the flexibility of power systems by enabling efficient and dynamic power

flows across various power networks [7]. Network interconnection refers to the global interconnection of electrical transmission systems, a strategy that has been identified as a means of addressing geographical mismatches in the power sector. This approach enables the transmission of electricity between countries and continents, thereby contributing to the stabilization of overall demand and generation patterns.

Another flexibility option is demand response (DR) or demand-side management (DSM), which allows end-users to adjust their electricity consumption in response to changes in supply, thereby helping to balance the system. These responses are typically triggered by market signals and can be price- or incentive-based [9].

Finally, electricity storage incorporates a variety of technologies that facilitate the storage of surplus electricity and its subsequent release during periods of energy deficit. This temporal adjustment in energy consumption and production generates flexibility within the power system.

When the scope is expanded beyond the limitations of power systems alone, additional flexibility options emerge. This flexibility is attributable to the MES's capacity to facilitate energy flows across carriers, thereby enabling dynamic responses to fluctuations in supply and demand. The subsequent section will delve into the flexibility introduced by MESs, offering a more comprehensive understanding of how integrated multi-energy networks contribute to a more resilient and adaptable energy system.

2.2.2. Flexibility in Multi-Energy Systems

Multi-energy systems have been demonstrated to augment the flexibility of energy systems through the integration of energy carrier networks, a concept frequently referred to as sector coupling [10]. This integration facilitates the conversion and storage of energy in various forms, thereby ensuring the maintenance of power balance through the injection or absorption of energy into or from other sectors. Kleinschmidt et al. propose a categorization of MES flexibility solutions into three distinct categories: conversion, storage, and DSM [11]. Notably, the incorporation of conversion capabilities offers an additional flexibility solution that differs from those previously discussed in the context of power systems alone.

Conversion, defined as the transformation of energy from one form to another, is enabled by conversion technologies. When integrated with the electricity system, these technologies are commonly referred to as Power-to-X (P2X) devices [10]. The integration of these technologies facilitates the flow of energy between different energy sectors, thereby enhancing system flexibility. During periods of surplus generation, electricity can be converted and stored in alternative carriers such as gas, hydrogen (carriers), renewable fuels, or heat. These carriers can be utilized either directly for energy consumption or converted back into electricity when there is a shortfall in power generation. The conversion capabilities of these technologies therefore support the integration of VRES into the energy system.

The ability to dynamically balance supply and demand is a key benefit of conversion facilitated by MESs. This contribution to energy efficiency and reliability is significant, as is the reduction in costs that results from the ability to store energy in less expensive carriers. This is the second type of flexibility that MESs can provide, namely the ability to store energy for later use in different energy carriers, such as gas, hydrogen (carrier) and thermal storage. When compared to large-scale battery storage, alternative forms of energy storage offer compelling potential for cost reduction. As shown by the authors in [12], storing energy in natural gas and heat can be significantly more cost-effective than storing electricity in batteries. This capability further highlights the benefits of MESs in optimizing energy use across sectors and reducing overall system costs.

Demand-side management (DSM) is also recognized as a critical form of flexibility in the context of MESs. In contrast to traditional DSM, which focuses on electricity consumption profiles, DSM in MESs extends to the consumption of other energy carriers within the system. Notably, DSM in MESs has the potential to reduce peak loads, lower operational costs, and improve overall system efficiency [12]. In addition to enabling DSM across multiple energy carriers, the MES provides other possibilities for adapting consumption patterns. A MES enables consumers to directly use alternative energy carriers such as hydrogen or heat, depending on system conditions, thereby enhancing flexibility and offering consumers more efficient and cost-effective energy use options.

2.3. Multi-Energy System Modeling

Having established the importance of flexibility in energy systems and the role that MESs play in providing it, it is now essential to explore how these systems can be described through energy system modeling in order

to create the optimization model for this study and investigate their operation.

Energy system models serve as mathematical representations of energy systems that are used to assess interactions both within energy systems and with external economic and environmental systems [13]. These models facilitate detailed exploration of energy systems despite significant uncertainties in their design, such as economic developments, societal changes, resource costs, technological advances, and policy developments [14]. Consequently, models can provide a framework for assessing the potential impacts of innovations and guiding decision-making processes under conditions of uncertainty. In the field of energy system analysis, modeling is a wide-used approach. This section explores how energy system modeling is defined in existing literature (Section 2.3.1 - 2.3.4) , identifies what studies have already been conducted using MES models (Section 2.3.5), and identifies current gaps in MES modeling studies (Section 2.3.6).

2.3.1. Analytical Approach

Energy models can be categorized into three analytical approaches: bottom-up, top-down, and hybrid models [15]. Bottom-up models, also referred to as techno-economic models, provide detailed technical insights and are utilized for the assessment of technologies and energy flows with high precision. These models adopt a business-oriented economic approach to simulate the economic costs of the system. This techno-economic approach incorporates simulation, optimization, partial equilibrium, and multi-agent models [16]. In contrast, a top-down model employs a system-oriented economic approach, frequently used to analyze the impacts of energy policies on macroeconomic factors, such as changes in energy prices and economic growth. These models are therefore also referred to as macro-economic models. This approach incorporates input-output models, econometric models, computable general equilibrium models, and system dynamics models [16]. While top-down and bottom-up approaches were traditionally considered the only two methodologies, a third approach has recently been introduced: the hybrid model. This approach focuses on the integration of macroeconomic sectors into the highly technical bottom-up models [15]. As this study focuses on the optimization of the operation of MES, the remainder of this chapter will exclusively focus on bottom-up models.

2.3.2. Classification of Bottom-Up Energy System Models

A classification of bottom-up energy system models can be formulated based on several key aspects, which play a crucial role in the structuring of the energy model. Numerous studies have highlighted important aspects of bottom-up energy models in their research [17] [15] [18]. A comprehensive review of these studies reveals the key modeling aspects that are essential for comprehensively describing an energy system. These aspects include the time horizon, time resolution, spatial coverage, sectoral coverage, optimization purpose, programming technique, level of detail, assessment criteria, and uncertainty of data. Each of these aspects has been demonstrated to significantly impact the model's capabilities and applications. The subsequent section will discuss each of these aspects.

2.3.2.1. Time Horizon

Bottom-up models utilize either short-term or long-term time horizons, wherein the time horizon is defined as the period over which the model is applied. Short-term models emphasize operational analysis over periods ranging from one day to one year, focusing on specific system configurations and their operation. Conversely, long-term models typically extend over several decades, enabling analysis of system evolution for planning purposes.

2.3.2.2. Time Resolution

Another aspect that differentiates energy system models is time resolution. The time resolution of a model refers to the duration of a time step and can be categorized as low, medium or high resolution, depending on the number of time slices in a simulation. A time slice is defined as the number of time steps in which a simulation year is divided and is therefore determined by the relationship between the simulation horizon and the time steps or periods [15]. In the process of determining the time resolution, a trade-off must be considered between model accuracy and computational efficiency. Higher resolutions, while providing greater accuracy, necessitate increased computational effort. Conversely, lower resolutions, while reducing accuracy, enhance computational speed.

2.3.2.3. Spatial Coverage and Resolution

The spatial coverage defines the geographical range and boundaries of the system. The spatial coverage can vary in scope, ranging from local coverage, to regional or district levels, to country levels [19], to multi-country or continental levels [20]. The spatial resolution, defined as the level of detail with which a geographical area

is represented, can be a single-node or multi-node system [15]. Single-node systems generally provide simplified representations of energy systems that assume ideal transmission and distribution systems and neglect associated losses. In contrast, multi-node systems provide more detailed representations of the transmission and distribution networks, incorporating technical constraints and losses.

2.3.2.4. Sectoral Coverage

Sectoral coverage in energy system modeling encompasses two key aspects; the energy sectors addressed in the model and the demand sectors addressed [15]. The first aspect focuses on the energy carriers in the system, where models may address a single carrier, such as electricity, or multiple carriers, which can be electricity, heat, natural gas, hydrogen, and/or fuels. The second dimension concerns the addressed demand sectors, encompassing end-use sectors such as buildings, industry, and transportation [21].

2.3.2.5. Methodological Approach

Models can be classified according to their methodological approach. Simulation models enable the testing of specific system configurations to evaluate performance metrics. Dispatch optimization models focus on optimizing the operation of existing infrastructure within given constraints. Investment optimization models combine dispatch optimization with capacity expansion decisions. The categorization of these optimization-based approaches, encompassing both dispatch and investment, can be further classified as either single-objective optimization, which seeks to optimize for a primary objective, or multi-objective optimization, which considers multiple competing objectives in a simultaneous manner [15].

2.3.2.6. Level of Detail

The level of detail in energy system modeling refers to the extent to which a model incorporates the physical properties of system components, thereby differentiating between physic-based and data-driven modeling approaches. The level of detail is commonly classified in three categories; black-box, gray-box, and white-box [22]. Black-box models are entirely data-driven, utilizing statistical techniques to establish relationships between inputs and outputs, such as efficiencies and operational data. These models do not incorporate physical properties and instead depend solely on observed data patterns. In contrast, white-box models are fully physics-based, employing fundamental equations to represent the behavior of components, their interactions, and energy flows within the system. Gray-box models serve as a middle ground, combining elements of both approaches. These hybrid models integrate physical representations with statistical methods to capture system behavior, thereby offering a balance that enhances accuracy and reduces complexity relative to purely white-box models.

2.3.2.7. Assessment Criteria

Assessment criteria are the key performance indicators employed to evaluate a model. These criteria are typically categorized as economic, technical, or environmental [17]. Economic assessment focuses on minimizing the total system costs or maximizing the overall profits of the system. Technical assessment can be further divided into energetic and exergetic evaluations. Energetic assessment measures the efficiency of the system by comparing input or generated energy to output or consumed energy. The exergetic assessment evaluates the maximum share of energy within the system that can be converted into useful work. The environmental assessment examines the system's impact on the environment, often quantified through greenhouse gas emissions or air pollutant levels.

2.3.2.8. Programming Technique

A distinguishing feature of energy system modeling is the mathematical approach or programming technique employed to solve the underlying mathematical problem. The most prevalent techniques include linear programming (LP), mixed integer linear programming (MILP), non-linear programming (NLP), mixed integer non-linear programming (MINLP), dynamic programming, and heuristic programming. LP represents a fundamental optimization approach, determining the optimal solution to the objective function under a set of linear constraints. MILP extends the capabilities of LP by incorporating binary or integer decision variables. In energy system modeling, these variables can represent discrete decisions, such as the on and off states of technologies. NLP and MINLP are extensions of LP and MILP, respectively, that allow for non-linear constraints. This allows for the modeling of non-linear performance of system components or non-linear investment costs. Dynamic Programming involves the decomposition of the initial mathematical problem into a series of smaller sub-problems, leading to the identification of an optimal growth path, a method frequently employed in multi-stage planning scenarios. Heuristic techniques employ simplified rules to identify efficient solutions with high computational speed. The selection of a particular technique is dependent upon the description of the energy system, and the achievement of an optimal balance between solution accuracy and computational efficiency.

2.3.2.9. Uncertainty of data

The implementation of energy system modeling in bottom-up models is often complicated by the difficulty in obtaining accurate and reliable input data. This challenge can be attributed to several factors, including uncertainty regarding future developments, confidentiality of commercial data, lack of prior measurements, or poor data quality [17]. To address this uncertainty, various approaches can be applied. The two most common methods in energy system modeling are stochastic optimization, which incorporates probabilistic variations through scenarios analysis, and robust optimization, which focuses on solutions that perform well under varying conditions by identifying the most effective outcome for worst-case conditions [5]. However, many energy system models currently in use adopt a deterministic approach, which assumes fixed inputs and does not account for uncertainty or variability in the calculations. To address the data uncertainty within deterministic models, scenario-based analysis is frequently employed, wherein multiple scenarios are modeled to represent the various possible states of the system.

2.3.3. Aggregation Concepts

The integration and modeling of different energy carriers, each governed by distinct physical laws and relationships, within a unified optimization model is facilitated by aggregation concepts. The energy hub, a comprehensive aggregation approach, is predominantly utilized in MES optimization studies [4] [17]. An energy hub serves as an interface between different energy infrastructures and network participants. It can accommodate multiple inputs and outputs, whose relationships are typically characterized by coupling factors [23]. These coupling factors are derived from the efficiency of the converter, the internal hub topology, and the power dispatch. An example of a MES energy hub is shown in Figure 2.1, it includes the input and output flows of different energy carriers and the energy hub that represents the conversion and storage technology.

A MES can be represented by a single energy hub or by a combination of several energy hubs. Other aggregation concepts that are mentioned by Mancarella et al. [4] and Kriechbaum [17] are the virtual power plant concept, the microgrid concept, and power nodes modeling. However, these concepts have a primary focus on the electrical system with consideration of multi-energy integration, while energy hub modeling encompasses a holistic approach to multi-energy integration.

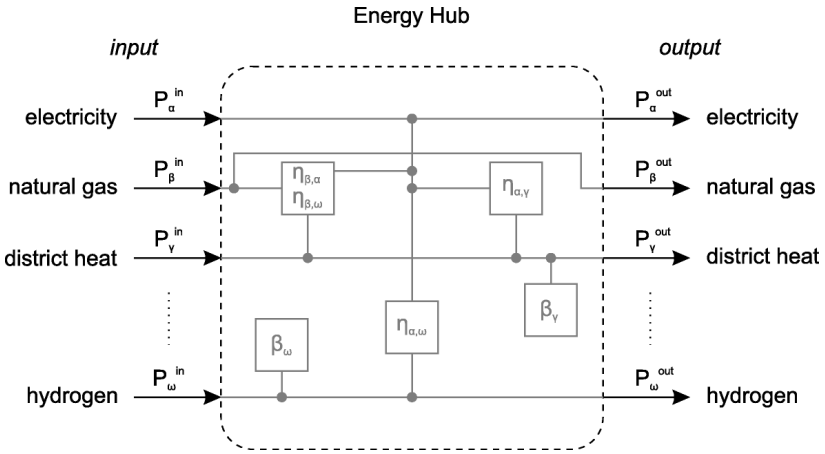

Figure 2.1: A representation of a MES Energy Hub [17].

2.3.4. Optimization Models

This study focuses on optimizing the operation of a MES. Before exploring state-of-the-art of these optimization models, it is of importance to first understand the basic principle and formulation of optimization models. An optimization model consists of three main components: the objective function, a set of decision variables, and a set of constraints. The objective function is the mathematical expression that the model aims to optimize, either by minimizing or maximizing its value, depending on the objective of the optimization. The decision variables are the parameters that can be set or varied to achieve the desired optimization result. The set of values for which the decision variables give an optimal result for the objective function, is the solution to the optimization problem. The constraints impose limits on the decision variables, restricting their possible values to those applicable to the system being modeled. A general representation of an optimization problem is shown in Figure 2.2.

$$
\begin{aligned}
&\text{Minimize or Maximize} && f_{\text{obj}}(x)\\
&\text{With respect to decision variables} && x\\
&\text{Subject to constraints} && g_{\text{lb}} \leq g(x) \leq g_{\text{ub}}\\
& && h(x) = h_{\text{eq}}
\end{aligned}
$$

Figure 2.2: General representation of an optimization problem [24].

2.3.5. Key findings from MES literature

The classification of bottom-up energy system models, in conjunction with the presentation of energy carrier integration through aggregation concepts, addresses how MES modeling is approached in the existing literature. This section will build on this by reviewing studies that apply MES models, thereby further investigating how MES modeling is currently represented in literature.

A review of the current literature on MES modeling has been conducted to establish the state of knowledge in the field and to inform the modeling approach developed in this thesis. Several authors have published comprehensive review studies on MESs, offering valuable insights into their structure, modeling approaches, and applications. One of the foundational contributions is the 2014 study by Mancarella, titled ”MES (multi-energy systems): An overview of concepts and evaluation models” [4]. This work serves as a foundation for understanding the theoretical basis of MES modeling. It outlines the fundamental aspects of MESs, introduces key aggregation concepts (as discussed in Section 2.3.3), and evaluates four different MES modeling tools. While this tool comparison was helpful in identifying general capabilities and limitations of MES tools, none were deemed suitable for the purposes of this thesis, as they lacked the ability to perform operational optimization with detailed power system representation. The review also examines the main assessment criteria used in MES modeling—economic, technical, and environmental—as discussed in Section 2.3.2.7. In 2016, Mancarella published a follow-up review study that expanded on the earlier work by emphasizing the growing importance of MES modeling and discussing its associated benefits and challenges [14]. This second review reinforces the need for integrated modeling approaches, particularly in the context of increasing system complexity and the transition to low-carbon energy systems.

A review by Mancò et al. [18] provides a structured methodology for analyzing the MES modeling literature and serves as a practical guideline for the development of MES optimization models. This study goes beyond conceptual understanding and offers concrete modeling structures, identifying key discriminating elements of MES models, which form the basis of Section 2.3.2. It presents a comprehensive reference framework for the construction of MES optimization models, supported by detailed mathematical formulations derived from six case studies. Through these formulations, the study illustrates how MESs can be translated into mathematical models, including the general structure of the objective function, technical constraints, and non-linear relationships. It also explains how flexibility measures and uncertainties can be incorporated into the model. In contrast to the conceptual focus of the reviews by Mancarella, which primarily introduce the fundamental ideas behind MES, the work by Mancò et al. focuses on the practical implementation and operationalization of MES models.

A complementary perspective is provided by Kriechbaum’s review [17], which outlines the current state, key challenges, and future directions of grid-based MES modeling. This study contributes—alongside Mancò et al.—to the formulation of the classification of bottom-up models presented in Section 2.3.2. Furthermore, it presents multiple open-source modeling frameworks used in MES modeling, with focus on Calliope, oemof, and urbs, and evaluates the extent to which various modeling aspects are supported within these tools. This evaluation highlights that most tools adopt a simplified energy hub approach, lacking physics-based network formulations.

The key findings from these literature reviews are as follows:

- Identification of critical modeling aspects that are necessary for properly describing and formulating MES models, as outlined in Section 2.3.2.
- Identification of various approaches to aggregate and coordinate multiple energy carriers in MES models. The energy hub model, described in Section 2.3.2.6, emerged as the most commonly used framework, with microgrids (MG), virtual power plant (VPP), and power nodes modeling concepts as alternative approaches.
- Assessment criteria commonly applied to MES models are predominantly environmental, economic, and

technical assessments, as seen in Section 2.3.2.7. Reliability assessment, resilience assessment, and fault issue analysis are identified but used less frequently.

- Establishment of a general understanding of MES optimization problem formulation, including objective functions, decision variables, and constraints, as outlined in Section 2.3.4. Along with different programming techniques for solving these optimizations, as described in Section 2.3.2.8.
- Most MES modelling tools adopt a simplified energy hub approach and thereby simplify physics-based network formulations.

Despite these valuable contributions, the literature reviews often stop short of offering practical implementation insights. Specifically, they rarely provide detail on the configuration and interconnection of technologies in case-specific energy systems. Moreover, these reviews do not include quantitative assessments demonstrating the operational behavior of MES systems and its benefits such as efficiency gains, cost reductions, or CO_2 emission reductions. Consequently, case-specific models that optimize the operational functionality of a MES are also consulted to bridge the gap between theoretical MES modeling and practical application. Table 2.1 provides an overview of these studies, summarizing the main aspects of the optimization model concerned, the energy sectors involved, and the demand sectors they address. The reviewed studies serve two purposes: to inform the modeling decisions in this work, and to identify the scientific gaps in the current literature.

Table 2.1: State-of-the-art literature review on operation optimization studies of Multi-Energy Systems.

Ref.	Model Scope	Programming Technique	Time Horizon	Resolution	Energy Sector							Demand Sector		
					Electricity	(Nat.) Gas	Heat	Cold	Hydrogen	Methane	Ammonia	Industry	Residential	Transport
[25]	Operation & Planning	MILP	One year	Hourly	✓	✓	✓	✗	✓	✗	✗	✗	✓	✗
[26]	Operation & Planning	MILP	One year	Hourly	✓	✓	✓	✓	✓	✗	✗	✗	✓	✗
[27]	Operation	DNLP	One day	Hourly	✓	✓	✓	✗	✓	✓	✗	✓	✗	✗
[28]	Operation	MILP	One day	Hourly	✓	✓	✓	✗	✗	✗	✗	✗	✓	✗
[29]	Operation	LP	One year	Hourly	✓	✓	✗	✗	✓	✓	✗	✓	✓	✓
[30]	Operation & Planning	LP	One year	Hourly	✓	✓	✓	✓	✗	✗	✗	✗	✓	✗
[31]	Operation & Planning	N/A	One year	Hourly	✓	✓	✓	✗	✗	✗	✗	✗	✓	✗
[32]	Operation	MILP	One day	Half-hourly	✓	✓	✓	✗	✗	✗	✗	✗	✓	✗
[33]	Operation	MILP	One day	Hourly	✓	✓	✓	✗	✗	✗	✗	✓	✗	✗
[34]	Operation	MINLP	One day	Hourly	✓	✓	✓	✓	✗	✗	✗	✓	✗	✗
[35]	Operation	MILP	One day	Hourly	✓	✓	✗	✗	✗	✗	✗	✗	✗	✗
[36]	Operation	LP	One day	Hourly	✓	✓	✓	✓	✗	✗	✗	✓	✗	✗
[37]	Operation	LP	One day	Hourly	✓	✗	✗	✗	✓	✗	✗	✗	✗	✗
[38]	Operation	MIQP	One day	Hourly	✓	✓	✓	✗	✗	✗	✗	✗	✓	✗
[39]	Operation	N/A	One year	Hourly	✓	✗	✓	✗	✓	✗	✓	✓	✗	✗
[40]	Operation & Planning	N/A	One year	Hourly	✓	✗	✗	✗	✓	✗	✓	✓	✗	✗
[41]	Operation & Planning	PSO	One year	Hourly	✓	✗	✗	✗	✓	✗	✓	✗	✗	✗
[42]	Operation & Planning	RO	One Day	Hourly	✓	✓	✓	✗	✓	✗	✓	✗	✗	✗

As illustrated in Table 2.1, MES studies span a range of energy sectors, with the specific focus varying depending on the research objective. However, the majority of existing studies concentrate on conventional energy carriers—electricity, natural gas, and heat. In contrast, alternative carriers—including hydrogen, methane, and ammonia—are considerably less represented. Most studies aim to optimize MES operation within the context of present-day energy systems, typically incorporating electricity from wind and solar as renewable sources. This trend is reflected in several studies—[28, 30, 35, 34, 38]—which apply the MES framework to assess how a holistic energy system design and operation affects system costs, emissions, and efficiency in present-day configurations. For instance, Garmabdari et al. [38] demonstrate that in conventional systems—based on natural gas, electricity, and heat—the integration of storage and conversion technologies within a MES context significantly enhances efficiency, reduces operational costs, and improves supply reliability. While such studies do include renewable electricity to reduce greenhouse gas emissions, they primarily focus on systems that mitigate variability, rather than eliminate carbon emissions. Consequently, they do not capture the potential roles of alternative energy carriers in future energy systems and fail to represent carbon-neutral or fully zero-emission future configurations.

This research gap is also recognized in a study by Alabi et al. [26], which also points out that although substantial work has been devoted to the development of low-emission energy systems, few studies have explored the realization of fully zero-carbon multi-energy systems (ZC-MES). In response, the study proposes a mathematical model for the optimal operation of a ZC-MES by replacing natural gas with hydrogen. However, the role of hydrogen in that model is limited to power generation, and the broader potential of this alternative

carrier—such as its use for energy storage, direct consumption, fuel for heat generation, or feedstock for other alternative carriers—remains unexplored.

Across various studies that do integrate hydrogen as an energy carrier, its role is often restricted to just one or a few of its potential applications. For instance, in two reviewed studies—[25, 36]—hydrogen is used solely as an energy storage medium. One study—[27]—integrates hydrogen with the sole purpose of using it as feedstock for syngas, while other studies— [40, 41, 42]—model hydrogen exclusively as feedstock for the synthesis of green ammonia. In the study by Wen and Aziz [39], hydrogen is applied for both short-term storage and electricity generation. Although this study acknowledges its potential as industrial feedstock or alternative for industrial consumption, these functions are not explicitly modeled. These examples indicate that while hydrogen is included in a growing number of MES studies, it is typically assigned a single, narrowly defined function—primarily related to system flexibility or emission reduction. An exception is found in a study by Koirola et al. [29], where hydrogen is modeled both as a storage medium, as a fuel for electricity generation, an a feedstock for methanation. However, even in this case, hydrogen is not considered for direct consumption, and remains framed solely as a flexibility provider. Direct consumption of hydrogen, particularly by industrial end-users, is thus systematically excluded.

The same pattern is observed for ammonia. As shown in Table 2.1, ammonia is addressed far less frequently than hydrogen in the MES literature. Among the few studies that do consider ammonia as an energy carrier, none examine its potential multifunctional role within future MESs. Instead, its application is typically restricted to a single function. For example, two studies—[40, 39]—model ammonia as a medium for electricity storage, while another study—[42]—considers it as a fuel for power and/or heat generation. In a study by Zho et al. [41], ammonia is included only from the perspective of the end-product, focusing solely on ammonia synthesis without modeling its subsequent use or integration into the broader energy system.

Another common pattern across the reviewed studies is the widespread use of the energy hub approach to integrate multiple energy carrier networks into a unified operational and mathematical framework. A study by Martínez Ceseña et al [32], is the only identified study that deviates from this approach by adopting the microgrid concept instead. However, this study primarily focuses on the provision of reliability services and is therefore more concerned with evaluating the resilience of MES systems than with optimizing their operation. This indicates that, when considering operational optimization, the energy hub indeed proves to be the most commonly used method, as also stated in Section 2.3.3.

By relying on the energy hub approach, most MES studies make broad assumptions about the underlying physics of energy flows and component operation. Physical constraints such as electrodynamics, fluid dynamics, thermodynamics, reaction kinetics, network losses, and operational inter dependencies are often abstracted away in favor of simplified, aggregated representations. Among the studied literature, only one study—[35]—stands out as the only study that incorporates physics-based modeling of both electricity and gas flows, using the Newton-Raphson method for modeling power flows and the Weymouth equation for gas flows in pipelines. This proves complex, non-linear flows can be accurately represented beyond simplified energy hub models. However, the model fails to include the flexibility potential of alternative energy carriers such as hydrogen and ammonia, which are expected to play a central role in future energy systems. Although the study represents a meaningful advancement in the modeling of conventional energy carriers, the exclusion of alternative energy carriers limits its relevance for future MESs.

Moreover, this study underscores a fundamental challenge of physics-based modeling in future energy system contexts: such detailed physic-based approaches require extensive knowledge of the underlying energy networks, including specific technological parameters and precise network topologies. This data is typically available for existing infrastructure but remains speculative or uncertain for future energy systems. Consequently, the application of highly detailed physics-based approaches to prospective systems is challenging, causing the persistent reliance on energy hub models for future-oriented MES studies.

A simplified representation of system dynamics is also particularly evident in the current state-of-the-art modeling of heat networks. Of the 13 reviewed studies that include heat, only three—[30, 31, 39]—distinguish between heat flows based on temperature levels. While the temperature of heat flows, in addition to their energy quantity, is a crucial indicator of their usability in specific applications, most studies treat heat solely as an absolute energy quantity. As a result, the functional value of different heat flows is not fully captured, leading to an oversimplified representation of thermal integration in MES models.

A further observation across the literature is that many studies prioritize the development of robust MES modeling frameworks as their primary objective, often without explicitly examining the resulting operation or design implications. While this development contributes to methodological advancement, it restricts practical insights

into how these models might translate to real-world system design and implementation. Despite the advancement of sophisticated modeling approaches, many studies neglect to address the actual integration or practical implementation of multi-energy systems. Only a few studies—[29, 39, 40, 41]—analyze operation strategies as part of the research objective. Each of these studies highlights the dynamic and context-dependent nature of MES operation, which varies considerably based on the selected energy carriers and their designated roles within the system.

Summary of key findings from the case-specific operational MES optimization modeling is as follows:

- Most MES studies focus on conventional energy carriers (electricity, natural gas, heat) and aim to improve system performance using renewable electricity, but they fall short of modeling potential future energy system configurations with alternative energy carriers that aim for carbon-neutral or fully zero-carbon systems.
- In most MES studies that integrate hydrogen as an energy carrier, the carrier only has one specific function, such as storage, feedstock for syngas production, or feedstock for ammonia synthesis, while its multipurpose roles are not explored.
- Direct hydrogen consumption, especially in industry, is consistently excluded; hydrogen is mainly treated as a tool for flexibility and emission mitigation for the energy system.
- Ammonia is rarely addressed in MES studies, and when it is, its role is limited to a single function such as storage, fuel for power generation, or as end-product.
- Most studies apply the energy hub framework to unify energy carriers into a single model.
- The widespread use of the energy hub model leads to simplified representations of energy flows, often overlooking the physical characteristics of energy flows and system components.
- Many studies prioritize the development of the MES model itself, without explicitly analyzing the operational or design implications.

2.3.6. Critical Gaps and Research Contribution

The literature on operational MES modeling shows several key limitations. These limitations are especially relevant when aiming to model realistic, carbon-neutral multi-energy systems in complex industrial environments. The critical gaps in found from the literature analysis together with this study's research contributions are presented in this section.

A first and critical gap is the underrepresentation of ammonia as an energy carrier. Despite its anticipated importance in future energy systems, ammonia is rarely considered in MES models, and when it is, its role is limited to a single function. Its potential to serve as a hydrogen carrier, a storage medium, a combustion fuel, and an export product is not yet explored in an integrated energy system. This study addresses that gap by modeling ammonia as a multifunctional energy carrier, linked to multiple energy sectors.

A second gap concerns the limited operational roles assigned to hydrogen. Although widely recognized as an important alternative energy carrier, hydrogen is often modeled with a singular purpose—such as storage or power generation—while its broader applications, including direct industrial use and feedstock integration, remain unexplored. This study expands the scope by including multiple roles of hydrogen in energy systems, allowing its deployment to vary dynamically depending on system needs.

Furthermore, many existing models rely on conceptual frameworks that abstract away from the physical characteristics of energy flows. As a result, network constraints are often neglected, which poses a significant limitation—particularly in the electricity system, where issues such as grid congestion are increasingly critical. The simplifications inherent in energy hub modeling reduce operational realism and limit the model's ability to reflect spatial and infrastructural bottlenecks. This study includes a higher level of operational detail for the electricity network by extending the energy hub framework with power flow equations.

In addition, heat is typically represented as a single energy quantity without consideration of temperature levels, despite temperature being a key determinant of heat usability, especially in large industrial complexes which integrate high-temperature and low-temperature heat flows. This leads to an oversimplified integration of thermal systems and reduces the model's ability to reflect the usability and applicability of heat flows. This study represents the heat system by accounting for its temperatures and usability.

Finally, operation strategies are rarely examined in depth. While many studies concentrate on the structural design of MES models, few investigate the actual integration or practical implementation of MESs. To date,

no study has explored the operational strategy of a MES that integrates natural gas, electricity, hydrogen, ammonia, and heat. This research addresses that gap by explicitly analyzing the dynamic behavior of such a system under different conditions and deriving the corresponding operational strategy that enables cost-effective and flexible system operation.

Contributions of this study to the existing literature:

- Establishing ammonia as a fully integrated, multifunctional energy carrier by modeling its roles as a hydrogen carrier, energy storage medium, combustion fuel, and export product, demonstrating its cross-sector value in industrial MESs.
- Expanding the operational scope of hydrogen by incorporating its use as storage, fuel for power generation, industrial feedstock, and direct industrial consumption, highlighting the multiple roles of hydrogen in industrial MESs.
- Bridging conceptual and physical modeling approaches by extending the energy hub approach with power flow equations, capturing power flow constraints in the electricity network—essential for addressing technical feasibility in the power network.
- Enhancing thermal system modeling through the inclusion of temperature-differentiated heat flows, allowing for more accurate assessment of heat usability and integration within industrial processes.
- Deriving and evaluating operation strategies for a system-integrating the energy carriers natural gas, electricity, hydrogen, ammonia, and heat-under variable weather conditions, offering actionable insights for real-world MES operation and operational planning.

2.4. Summary

This chapter established the theoretical foundation for developing an optimization model for MES and identified critical research gaps in the current literature on MES modeling. It demonstrated that the growing share of VRES increases the need for system flexibility—which MESs can provide more effectively than traditional power systems through energy conversion, cross-sectoral storage, and cross-sector demand-side flexibility. These insights contribute to addressing research question 3 by demonstrating how MESs can improve system flexibility. The chapter also outlined how MES models are approached and classified in literature. Critical gaps in MES modeling were identified through a literature review, particularly regarding the integration of alternative energy carriers, physic-based network modeling, and operational strategy development. In response to these gaps—and directly contributing to research question 1—this research advances the field of MES modeling by integrating the multi-functional roles of hydrogen and ammonia, incorporating a detailed description of power flow modeling in the electrical network, incorporating temperature-differentiated heat flows in thermal system modeling, and developing a cost-effective operation strategy applicable to industrial clusters.

3
Methodology

3.1. Methodological Structure

For the objective of this study, a model-based optimization approach is applied to examine the operation of a synthetic future MES, which is inspired by the Maasvlakte area in the Port of Rotterdam and therefore serves as the test case. The methodology of this thesis involves the development of the model and the design of scenarios, forming a critical part of the overall research framework presented in Figure 3.1. The methodology comprises four parts, which are detailed in this chapter. The first part involves the development of the conceptual model (Section 3.3). In the second part, this conceptual model is translated into the optimization model (Section 3.4 and Section 3.5). The third part entails the formulation of scenarios for testing the model under different weather conditions (Section 3.6). The fourth and final part consists of verification and validation steps to ensure an accurate representation of the modeled system (Section 3.7). This structured approach ensures a comprehensive understanding of how the model is developed and how the system performance is evaluated. Prior to elaborating on the model setup, a detailed description of the Port of Rotterdam and the Maasvlakte area is provided in Section 3.2 to establish contextual clarity.

Figure 3.1: Research Framework

3.2. Case Study; The Maasvlakte Area in the Port of Rotterdam

The Port of Rotterdam is the largest industrial cluster in the Netherlands and the largest port in Europe. It plays a significant role in achieving its national climate targets, given that the CO_2 emissions in the port area account for 16.8% of the nation's aggregate CO_2 emissions [43][44]. These emissions primarily originate from chemical industries, oil refineries, and power plants (both coal and gas-fired) operating within the port area. In acknowledgment of its responsibility to reduce its CO_2 emissions, the Port Authority has committed to becoming carbon-neutral by 2050, using intermediate targets of reducing CO_2 emission from its own operations by 90 per cent by 2030 compared to 2019 levels [45]. Given its important position as industrial and energy hub for both the Netherlands and Europe and its ambitious climate objectives, the Port of Rotterdam presents a highly relevant case for investigating the application and potential benefits of MESs.

Within the Port of Rotterdam, this study focuses specifically on the Maasvlakte area—the most recently developed extension of the port with direct access to the North Sea. Compared to other regions of the port, the relatively recent development of the Maasvlakte has resulted in the availability of significant space for planning purposes. In recent years, substantial investments have been directed toward the development of sustainable energy infrastructure on the Maasvlakte area. These investments aim to support the energy transition and facilitate the establishment of a carbon-neutral port. Key investments include the establishment of new connections to offshore wind farms, the construction of a hydrogen conversion park accompanied by associated infrastructure, and infrastructure for Carbon Capture and Storage (CCUS). Furthermore, the area's positioning makes it well-suited for the development of import terminals for alternative energy carriers. Given these strategic advantages and ongoing energy transition initiatives, the Maasvlakte forms an ideal case for testing the MES developed in this research.

The hypothetical future MES for this research integrates existing energy infrastructure, planned investments, and potential future developments on the Maasvlakte. Rather than focusing on a specific target year, this research will incorporate multiple potential infrastructure developments to assess their influence on system performance. By doing so, emphasis will be placed on the integration of future developments rather than simulating a specific point in time. To inform the MES design, it is necessary to understand potential developments and infrastructure plans for this area. Beyond existing investment plans, the Port of Rotterdam's "Connected Deep Green" scenario is used as the foundation to understand these developments. The Connected Deep Green scenario is one of four global future scenarios developed by the Port of Rotterdam (others being Regional Well-being, Protective Markets, and Wake-up Call) that analyze how changes in geopolitics, economics, society, and technology might impact the port and its industrial complex. This scenario was selected due to its focus on achieving climate goals and carbon neutrality by 2050, aligning with the objective of this research. Building on this scenario, while incorporating the Port Authority's investment plans for the Maasvlakte and insights from direct consultation with port officials, a synthetic MES for the Maasvlakte is designed to support the transition to carbon neutrality. The following sections provide a detailed overview of this proposed system and how it is translated into an optimization model.

3.3. Conceptual Model

In order to construct the optimization model for the Maasvlakte's MES (MMES), it is necessary to establish the conceptual model, the computational model, and the model formulation. The conceptual model, in the context of computer simulation, is defined as an abstract representation of a real-world system, wherein the abstraction process is designed to prioritize the most relevant aspects of the system, thereby defining the content of the optimization model [46]. The conceptual model delineates the scope, content (model aspects and components), inputs, outputs, assumptions, and simplifications, thus providing a clear framework for its development and application [47].

3.3.1. Modeling Scope

The model is designed to determine the most cost-effective system operation and configuration of the modeled MES, while ensuring sufficient energy supply to both industrial consumers and export requirements. It will simulate the operational dynamics of the MES incorporating electricity, hydrogen, ammonia, natural gas, and heat as energy carriers, thereby providing insights on optimal operation strategies. The MES model will represent a synthetic future-oriented system for the Maasvlakte by incorporating its existing energy infrastructure, planned projects, and potential future developments. By optimizing system behavior and projecting operational dynamics, the model serves as a predictive tool that supports the development of operation strategies and planning efforts to facilitate the transition toward carbon neutrality in industrial clusters.

3.3.2. Model Aspects

The construction of the model content will be initiated through the description of the model in accordance with the model-specific aspects outlined in Chapter 2. The model-specific aspects are summarized and presented in Table 3.1. The development of the conceptual model will be facilitated by these aspects.

Table 3.1: Overview of modeling aspects used in the MMES.

Aspect	Details
Time horizon	Short-term horizon with a one-year simulation
Time resolution	Hourly intervals for operational accuracy and reasonable computational efficiency
Spatial coverage and resolution	Multi-node system covering the Maasvlakte area in the Port of Rotterdam
Sectoral coverage	Energy sectors: electricity, natural gas, hydrogen, ammonia, and heat Demand sectors: industry (consumers located on the Maasvlakte)
Methodological approach	Single-objective dispatch optimization with capacity optimization for storages
Level of detail	Gray-box; energy-hub approach with physic-based description of the electrical network
Assessment criteria	Economic
Programming technique	Mixed-Integer Linear Programming (MILP)
Uncertainty of data	Deterministic approach with scenario analysis

3.3.3. Model Components

This section presents the components that form the MMES. The MMES is designed as an integrated network that connects various energy carriers and technologies. The components are grouped into the following categories: generation and import, demand, storage, conversion, transmission and distribution, and external network connections and exports. A schematic overview of the MMES is shown in Figure 3.2, while Table 3.8 lists the individual components and their key technical and economic characteristics. These characteristics are further detailed in the following subsections.

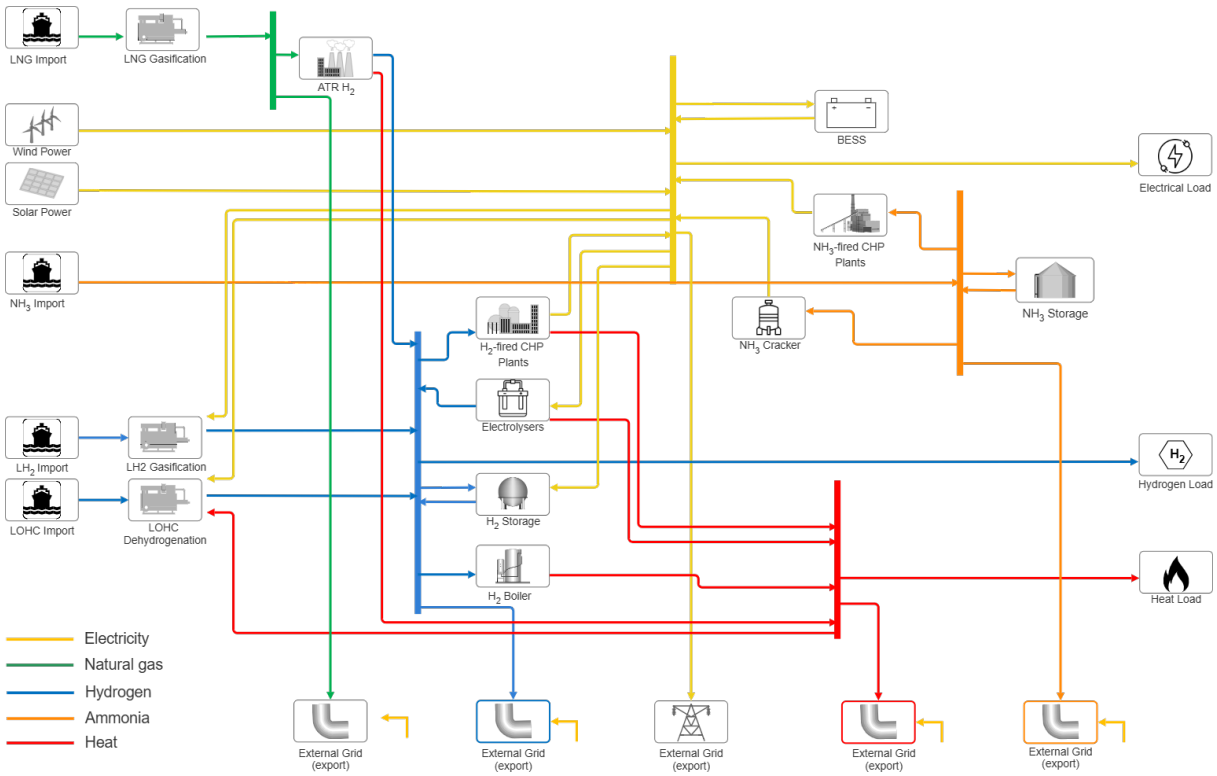

Figure 3.2: Schematic Representation of the MMES.

It is important to emphasize that the system accounts for the inclusion of CCUS technologies. This enables the assumption that all CO_2 emissions—particularly those arising from natural gas-based autothermal reforming (ATR) for hydrogen production—are effectively captured and stored. As a result, the system is regarded as carbon-neutral, and emissions are not further considered in the analysis.

3.3.3.1. Energy Carriers

The modeled MES includes five energy carriers: electricity, natural gas, hydrogen, ammonia and heat. To ensure consistency and enable unification of the system, all carriers are expressed in the same units, i.e. energy and power. Each energy carrier is characterized by a specific energy form-electrical, chemical, or thermal- which determines how its energy content is calculated.

Electrical energy carriers Electricity carries energy in the form of electrical energy, which is quantified as the product of power and time. Power, in turn, is defined as the product of voltage (V) and current (I), where voltage represents the potential difference driving the flow of electric charge, and current represents the rate at which electric charge flows. This relationship is expressed as:

$$E_{\text{elec}} = V \cdot I \cdot t = P \cdot t \tag{3.1}$$

Chemical energy carriers Natural gas, hydrogen, and ammonia store energy in the form of chemical energy. This energy content is calculated based on their lower heating value (LHV)—the amount of energy released during combustion after accounting for condensation losses—and their respective mass or volume. The LHV is used instead of the higher heating value (HHV) because it more accurately represents the amount of usable

energy, aligns with industry standards, and is more relevant when considering waste heat utilization. The relationship between chemical energy and the LHV is given by:

$$E_{\text{chem}} = LHV_m \cdot m = LHV_V \cdot V \tag{3.2}$$

Thermal energy carriers Heat carries energy in the form of thermal energy and represents the transfer of energy driven by temperature differences. Unlike electrical or chemical energy, it is not stored as an absolute quantity. Instead, the thermal energy transferred as heat depends on the mass of the medium, its specific heat capacity, and the temperature difference. This relationship is expressed as:

$$Q = m \cdot c \cdot \Delta T \tag{3.3}$$

Because thermal energy is relative to a reference temperature, heat flows must be evaluated with respects to reference state in the heat network. In contrast, electrical and chemical energy can be directly compared to each other and added within energy balances, because of their absolute energy quantities. How this fundamental difference is integrated into the model is further explained in Section 3.3.3.4, which addresses energy conversion, and in Section 3.3.3.6, which discusses the representation of transmission and distribution networks.

3.3.3.2. Generation and Import

In conventional power systems, generation refers to the production of electricity from primary energy sources, such as fossil fuels in traditional power plants or renewable sources like wind and solar. However, in a MES, some generation units function as conversion units by linking different networks. For example, a gas-fired power plant—classified as a generation unit in conventional power systems—becomes a conversion unit in a MES by connecting the natural gas and electricity networks. This shift means the conventional definition of generation no longer applies in a MES where energy flows are interconnected rather than isolated and unidirectional. In a MES framework, only energy from renewable sources is thus classified as generation. In addition, imported energy flows are also modeled as generation units, as they represent external energy input into the system.

Renewable Energy Generation In the MMES, the majority of the generation units are wind farms, as can also be seen in Table 3.8. Two wind farms, ”Hollandse Kust Zuid” (off-shore) and ”Maasvlakte 2” (onshore), are currently operational. The MMES also includes two additional off-shore wind parks, ”IJmuiden Ver” and ”Nederwiek”, which are scheduled to become operational in 2029 and 2030, respectively. The MMES also incorporates a solar farm, ”De Slufter,” which is currently in the planning phase. Many industries on the Maasvlakte have small-scale generation units on their terrain for self-consumption and net billing; however, these are not taken into account in the MMES due to their relatively small scale and lack of data.

Import Furthermore, the MMES has incoming energy flows from imports through shipments, as the Maasvlakte serves, or will serve, as a major hub for the import of various energy carriers. The model includes imports of liquefied natural gas (LNG), liquid hydrogen (LH_2), liquid organic hydrogen carriers (LOHC)(H18-DBT) and ammonia (NH_3). Of these, the LNG terminal is the only facility currently in operation. These import flows are represented in the model as continuous generation sources.

3.3.3.3. Demand

In the Maasvlakte, industrial facilities are and will continue to be the predominant energy consumers. The area is home to a number of large industries, in addition to numerous smaller customers. To simplify the energy demand in the MMES, the industrial demand has been categorized into five groups: Bio-refineries, chemical industry, terminals, CCUS, and shore power. Of these, CCUS and shore power are not yet operational. In addition to these five groups, there are some smaller customers and distribution centers on the Maasvlakte. However, these are disregarded due to their relatively small energy demand and lack of available data. At present, industrial demand is limited to electricity, natural gas, and heat. However, the MMES will also take the direct use of hydrogen into consideration as a future source of heat. The consuming groups, categorized by sector, are outlined in Table 3.2.

3.3.3.4. Conversion

Conversion technologies facilitate the transfer of energy between different energy carrier networks by transforming one form of carrier into another, and thus play a critical role in MESs. This section will discuss three

Table 3.2: Consumer groups and their consumption. *LyondellBasell has announced the closure of its plant at the Maasvlakte. However, it is still included in the system model due to the recent nature of the announcement.

Consumer group	Industry at the Maasvlakte	Current consumption	Expected to consume H_2
Bio-refineries	Neste Netherlands B.V.	Electricity, Natural Gas, Heat	Yes
Chemical industry	Lyondell Chemie Netherlands B.V. *	Electricity, Natural Gas, Heat	Yes
Terminals	Multiple Industries	Electricity	No
CCUS	Porthos	Electricity, Heat	No
Shore Power	Multiple Industries	Electricity	No

types of conversion technologies included in the MMES; combined heat and power plants, hydrogen production plants, and import conversion plants. All conversion units are conceptualized within the framework of the energy hub model, as detailed in Section 2.3.3, thus characterized by energy conversion efficiencies, using the general form:

$$P_{\text{out}} = \eta_{\text{conversion}} \cdot P_{\text{in}} \tag{3.4}$$

Combined Heat and Power Plants The Maasvlakte is home to several operational combined heat and power (CHP) plants, which are currently fired by either coal or gas. The Enecogen CHP plant, located in the Europort area, is electrically connected to the grid on the Maasvlakte and is therefore included in the MMES. CHP plants simultaneously generate electricity and heat from chemical energy carriers, i.e. combustion fuels. The input chemical energy is converted to electrical and thermal energy, each characterized by a specific conversion efficiency:

$$P_{\text{electrical, out}} = \eta_{\text{conversion, electrical}} \cdot P_{\text{chemical, in}} \tag{3.5}$$

$$Q_{\text{thermal, out}} = \eta_{\text{conversion, thermal}} \cdot P_{\text{chemical, in}} \tag{3.6}$$

Coal-fired CHP plants are scheduled to cease operations by 2030. Ammonia is identified as a promising substitute for coal, as highlighted by the ISPT's 'Clean Ammonia Roadmap' and IRENA's 'Renewable Ammonia Innovation Outlook' [48] [49]. The potential of co-firing coal and ammonia offers a transitional pathway, facilitating a gradual phase-out of coal and gradual repurposing of the existing infrastructure. In parallel, gas-fired power plants are projected by the Port of Rotterdam to transition to hydrogen as a fuel source, for which co-firing is also a possibility. This transition is supported in literature, as demonstrated in the TNO and PBL study 'Trajectory exploration Climate neutral Netherlands 2050' [50]. Accordingly, in the MMES model, coal-fired power plants are retrofitted to operate on ammonia and gas-fired power plants are retrofitted to operate on hydrogen. This approach aligns with the Port of Rotterdam's Deep Green Scenario, which envisions both ammonia and hydrogen as fuels for low/zero-carbon power and heat generation.

Hydrogen Production The MMES includes several hydrogen production technologies: electrolyzers, autothermal reforming (ATR) plants, and ammonia cracker plants. These conversion units are not yet operational, but are in the planning or developing stages as outlined by the Port of Rotterdam.

Electrolyzers use electricity to split water into hydrogen and oxygen, thereby converting electricity into hydrogen. In the MMES, electrolyzers are directly linked to wind power to ensure that all hydrogen production qualifies as green hydrogen. The operation of the electrolyzers is therefore synchronized to the generation profile of the offshore windfarm IJmuiden Ver, with one hour delay to account for the adjustment time. Alkaline electrolyzers are selected, as they represent the first confirmed technology for deployment in the Port of Rotterdam and are currently the most mature and technologically advanced option available. Low-temperature heat is produced alongside hydrogen production, which is also accounted for in the model. The conversion processes are represented as follows:

$$P_{\text{hydrogen, out}} = \eta_{\text{conversion}} \cdot P_{\text{electrical, in}} \tag{3.7}$$

$$Q_{\text{thermal, out}} = \eta_{\text{thermal}} \cdot P_{\text{electrical, in}} \tag{3.8}$$

ATR reactors convert natural gas into hydrogen by partial oxidation and steam reforming. During this process, CO_2 can be effectively captured with capture rates reaching up to 95% through carbon capture technologies, while the remaining 5% is vented back as stack gas in ATR-CSS-R systems [51]. ATR plants require a small

amount of electricity for its operation and are capable of generating and recycling their own heat. The operation of ATR units is represented by the following relationships:

$$P_{\text{hydrogen, out}} = \eta_{\text{conversion}} \cdot P_{\text{natural gas, in}} \tag{3.9}$$

$$Q_{\text{electrical, in}} = \eta_{\text{electrical}} \cdot P_{\text{natural gas, in}} \tag{3.10}$$

Ammonia cracking enables the conversion of ammonia into hydrogen and nitrogen through high-temperature endothermic processes. The necessary heat is provided by a hydrogen burner, and is accounted for in the efficiency. Waste heat is recycled during the process, and thus not used for waste heat utilization. This results that the ammonia cracker is represented by a single conversion relationship:

$$P_{\text{hydrogen, out}} = \eta_{\text{conversion}} \cdot P_{\text{ammonia, in}} \tag{3.11}$$

Import Conversion Import conversion units, including LNG gasification, LH_2 gasification, and LOHC hydrogenation, convert the imported energy carriers to the form that meets the network specifications of the MMES. While in reality, these operations involve intermediate tank storage to buffer the variability of vessel-based deliveries, this is simplified in the model by assuming a constant import flow with immediate conversion and injection into the respective networks. At present, only the LNG gasification plant is operational on the Maasvlakte; the LH_2 and LOHC facilities are still under development.

LNG gasification converts liquefied natural gas into its gaseous form using heat from seawater and requires electricity for its operation. Which is presented as:

$$P_{\text{natural gas, out}} = \eta_{\text{conversion}} \cdot P_{\text{LNG, in}} \tag{3.12}$$

$$Q_{\text{electrical, in}} = \eta_{\text{electrical}} \cdot P_{\text{LNG, in}} \tag{3.13}$$

LH_2 gasification similarly uses heat from seawater to vaporize the liquefied hydrogen, and requires electricity for its operation:

$$P_{\text{hydrogen, out}} = \eta_{\text{conversion}} \cdot P_{\text{LH}_2\text{, in}} \tag{3.14}$$

$$Q_{\text{electrical, in}} = \eta_{\text{electrical}} \cdot P_{\text{LH}_2\text{, in}} \tag{3.15}$$

In contrast, LOHC dehydrogenation requires high-temperature heat input, approximately 300°C, which is provided by hydrogen burners [52]. The LOHC compound DBT-H18 is selected in the model due to its high hydrogen storage density and commercial availability [52].

$$P_{\text{hydrogen, out}} = \eta_{\text{conversion}} \cdot P_{\text{LOHC, in}} \tag{3.16}$$

3.3.3.5. Storage

The current energy system at the Maasvlakte does not yet include storage technologies specifically designed to regulate the supply and demand of the energy system. However, a range of storage solutions for electricity, hydrogen, and ammonia are currently under consideration to improve system flexibility, cost-effectiveness, and operational independence. In line with the energy hub approach, storage systems are modeled based on their energy conversion efficiencies. The storage technologies included are: a Li-ion battery for electrical storage, underground hydrogen storage in caverns, hydrogen storage in pressurized tanks, and ammonia storage in refrigerated ammonia tanks. Although hydrogen storage in the Port of Rotterdam would likely be in depleted gas fields, this technology is less mature and less studied compared to salt cavern storage. Salt caverns are therefore used in the model, as they are a proven technology with available data and are already planned for implementation in Groningen, which may eventually connect to the Rotterdam region. Each storage technology is characterized by a charging efficiency, a storage efficiency, a discharging efficiency, and standing losses. These are represented by the following energy balance:

$$P_{\text{out}} = (P_{\text{in}} \cdot \eta_{\text{charge}} - P_{\text{loss}}) \cdot \eta_{\text{store}} \cdot \eta_{\text{discharge}} \tag{3.17}$$

The term P_{loss} reflects standing losses, which are defined as:

$$P_{\text{loss}} = \lambda \cdot E_{\text{store}} \tag{3.18}$$

Here, λ represents the standing loss coefficient.

Hydrogen and ammonia storage systems require electricity during the storage process, specifically for hydrogen compression and ammonia refrigeration. These electrical demands are modeled additional power consumption associated with the storage process. To represent this, an electrical efficiency term is used, linking the power input into the storage medium (during charging) with the electricity consumed for its operation:

$$P_{\text{electrical, in}} = \eta_{\text{electrical}} \cdot P_{\text{storage medium, in}} \tag{3.19}$$

3.3.3.6. Transmission & Distribution

Energy carriers move through transmission and distribution networks, each driven by different physical principles. This section details the transmission and distribution of each energy carrier network and also explains how electricity, gas, hydrogen, ammonia, and heat networks—despite their fundamental physical differences—are represented in the model within a unified modeling framework. Notably, the section describes that electricity networks require physics-based power flow equations to capture their complex electromagnetic behavior, while other carrier networks can be effectively represented using the more systematic energy hub approach based on energy- and mass conservation principles.

Electrical Network The electrical network on the Maasvlakte is characterized by a layered structure that spans multiple voltage levels. The physical infrastructure includes high voltage (380kV and 150kV) transmission through alternating current (AC) overhead lines and medium-voltage (66kV, 25kV, 23kV) distribution via underground AC cables. Transformers connect the different voltage levels. The network model is based on existing infrastructure supplemented by the new 380kV Amaliahaven high-voltage substation currently under construction, scheduled to become operational in 2026. The complete network topology is illustrated in the single-line diagram presented in Appendix A.

From a conceptual perspective, electrical power transmission follows principles of AC power flow rather than simple energy balances. This distinction is often neglected in current MES modeling, as outlined in Section 2.3.5, yet is critical for assessing technical feasibility and operational limits in power systems, particularly when examining existing infrastructure with high renewable energy penetration and grid congestion issues. AC power systems exhibit complex behaviors including voltage-dependent characteristics, reactive power flows, and physical network constraints, necessitating a more sophisticated modeling approach to realistically evaluate system behavior, capacity limitations, and operational constraints that determine actual power flows. While the detailed mathematical implementation of these power flow equations will be presented in Section 3.4.2, the conceptual model incorporates two primary loss mechanisms at the component level: line losses and transformer losses. These losses are represented using fixed efficiency parameters:

$$P_{\text{electrical, out}} = (1 - \eta_{\text{line losses}}) \cdot P_{\text{electrical, in}} \tag{3.20}$$

$$P_{\text{electrical, out}} = (1 - \eta_{\text{transformer losses}}) \cdot P_{\text{electrical, in}} \tag{3.21}$$

Natural gas, Hydrogen, and Ammonia networks The transmission and distribution systems for natural gas, hydrogen, and ammonia rely on pipeline networks that transport these chemical energy carriers using pressure gradients. Although actual flows in these systems are governed by complex fluid dynamics equations, this research employs a simplified modeling approach aligned with the energy hub concept. In this abstraction, energy flows are determined by energy balance equations, without explicitly modeling pressure dynamics or flow velocities. The network topologies are also provided in Appendix A.

The Port of Rotterdam already features an extensive natural gas pipeline infrastructure that interconnects various industries with the natural gas grid. Since the MMES model only considers connections to import facilities and the ATR plant, the natural gas network is simplified to just a few nodes. This simplification assumes sufficient capacity exists to accommodate the modeled flows. Transmission of natural gas includes compression-related losses, which are driven by natural gas fueled pumps:

$$P_{\text{natural gas, out}} = \eta_{\text{comp}} \cdot P_{\text{natural gas, in}} \tag{3.22}$$

Hydrogen transmission and distributions systems represent new energy infrastructure in the system. For this, the model assumes that industries on the Maasvlakte area will be served by a network of retrofitted natural gas pipelines, while export is centralized at the electrolyzer's location through the Hynetwork network that

transports hydrogen to industries in the hinterland, for which the export pipeline is currently under construction. Hydrogen transmission considers both leakage losses and electricity consumption for pumping:

$$P_{\text{hydrogen, out}} = (1 - \eta_{\text{leakage}}) \cdot P_{\text{hydrogen, in}} \tag{3.23}$$

$$P_{\text{electrical, in}} = \eta_{\text{comp}} \cdot P_{\text{hydrogen, in}} \tag{3.24}$$

Ammonia transmission and distributions systems also represent new energy infrastructure in the system. The model assumes that a new dedicated pipeline network will be constructed to serve industries using ammonia, with a centralized export point close to the ammonia facilities. Transmission of ammonia considers the electrical demand for pumping and refrigeration, with zero leakage assumed due to safety risks associated with ammonia:

$$P_{\text{ammonia, out}} = P_{\text{ammonia, in}} \tag{3.25}$$

$$P_{\text{electrical, in}} = \eta_{\text{comp}} \cdot \eta_{\text{cooling}} \cdot P_{\text{ammonia, in}} \tag{3.26}$$

The natural gas, hydrogen, and ammonia networks are modeled under the assumption that transport capacity will be sufficient to meet system requirements. This supports the use of a simplified energy hub approach to model these networks, while detailed physics-based modeling is applied only to the electricity network. This distinction is based on differing expectations regarding future transmission constraints. The electricity grid is facing significant stress due to increasing demand, VRES integration, and its mostly fixed infrastructure. This poses limitations on its operation, necessitating a detailed analysis of power flows. In contrast, the natural gas network is considered mature and is not expected to experience significant additional stress. The development of the hydrogen and ammonia networks remains to be completed, and it can be assumed that they are designed with sufficient capacity to avoid bottlenecks. Furthermore, the development of detailed physics-based models necessitates the availability of extensive data regarding network topologies and technical parameters, as stated in Section 2.3.6. This information is mostly absent for hydrogen en ammonia networks, hindering the ability to accurately model and predict network behavior. The energy hub approach, therefore, offers a computationally efficient and technically sound alternative for modeling non-electrical networks.

Heat Network The heat network represents a district heating system that is connected to the WarmtelinQ district heating network that is currently under development in the Port of Rotterdam, a project jointly initiated by the Port of Rotterdam and Gasunie. The network operates at a supply temperature of 110-120°C and a return temperature of approximately 50°C lower (60-70°C). As previously stated in section 3.3.3.1, the evaluation of heat flows in heat networks must be conducted with respect to a reference state. The supply and return temperatures serve as this reference state. The complete network topology is provided in Appendix A and further analysis of all temperature flows in the Maasvlakte is provided in appendix C. This network leverages industrial waste heat to provide thermal energy to industrial, residential and horticultural applications in the region [53]. The model represents the heat network with a centralized connection point to the Warmtelinqs network for the entire Maasvlakte, to which various industries are connected through decentralized heat pipelines. Depending on the temperature requirements, industrial entities can establish connections with either the high-temperature network (120°C) or the low-temperature network (70°C), thereby facilitating the optimal utilization of the available heat.

In the MMES, it is assumed that high-temperature industrial processes deliver heat at 120°C to the district heating network. This medium-temperature heat exchange is thus included in the system model. In practice, heat integration involves trade-offs between supplying the district heating network (ca. 120°C), generating electricity through further cooling, and delivering high-pressure steam (ca. 400°C). However, a separate high-temperature steam network is excluded from the scope of this system, as interactions in such a high-temperature steam network are based on inter-industry agreements, confidential information and contractual terms that are exclusive, making them unsuitable for inclusion in the current integrated energy system model.

Similar to the natural gas, hydrogen, and ammonia networks, the heat network is modeled under of sufficient transport capacity at all times, assuming that the new Warmtelinqs infrastructure is able to handle all the anticipated heat flows. This allows the transmission and distribution to be modeled according to the energy hub approach, i.e. expressed by efficiency parameters.

Usable waste heat is injected into the heat network at the supply side (120°C or 70°C) with a heat exchanger. The amount of heat that is injected into the network is determined by the temperature differences (determine the theoretical maximum of the heat exchanger), and the operational efficiency of the heat exchanger:

$$Q_{\text{DH, in}} = \eta_{\text{heat exchanger, practical}} \cdot \eta_{\text{heat exchanger, theoretical}} \cdot Q_{\text{waste heat}} \tag{3.27}$$

$$\eta_{\text{heat exchanger, theoretical}} = \frac{T_{\text{waste heat}} - T_{\text{DH return}}}{T_{\text{waste heat}} - T_{\text{ambient}}} \tag{3.28}$$

The heat delivered to end-users is withdrawn from the district heating network by a heat exchanger. So the amount of heat that is delivered to end-users is reduced by both network thermal losses and heat exchanger efficiency:

$$Q_{\text{DH, out}} = \eta_{\text{heat exchanger, practical}} \cdot \eta_{\text{heat exchanger, theoretical}} \cdot (1 - \eta_{\text{thermal losses}}) \cdot Q_{\text{DH, in}} \tag{3.29}$$

The electrical energy required for pumping water through the district heating network is modeled as proportional to the thermal input flow:

$$P_{\text{electrical, in}} = \eta_{\text{pump}} \cdot Q_{\text{DH, in}} \tag{3.30}$$

When necessary, heat pumps are used to bridge the temperature gaps between available heat sources and the district heating network. These devices require electricity to elevate the temperature of the heat source. The basic energy balance of a heat pump is:

$$Q_{\text{HP, out}} = Q_{\text{HP, in}} + W_{\text{HP, in}} \tag{3.31}$$

The coefficient of performance (COP) expresses heat pump efficiency, and thus determines the electrical input:

$$COP = \frac{Q_{\text{HP, out}}}{W_{\text{in}}} \tag{3.32}$$

Rewriting this expression gives the total heat output in terms of the input heat and COP:

$$Q_{\text{out}} = Q_{\text{in}} \times \frac{COP}{COP - 1} \tag{3.33}$$

The COP is determined by the Carnot limit and system efficiency:

$$COP = \eta_{HP} \times COP_{\text{max}} = \eta_{HP} \times \frac{T_{\text{hot}}}{T_{\text{hot}} - T_{\text{cold}}} \tag{3.34}$$

Accordingly, the electrical energy required to drive the heat pump is:

$$P_{\text{electrical, in}} = W_{\text{in}} = \frac{Q_{\text{in}}}{COP - 1} \tag{3.35}$$

These formulations enable accurate representations of heat exchangers and heat pumps within the MMES and supports the integration of low-temperature industrial heat into the district heating network.

3.3.3.7. External Networks

In the MMES, multiple energy carrier networks are connected to (inter)national networks. The electricity network is connected to both the national high voltage (HV) network operated by TenneT and the medium voltage (MV) network operated by Stedin. The natural gas network is connected to the national gas network operated by GasUnie. A hydrogen pipeline will be constructed for hydrogen export to industry clusters in the hinterland by Hynetwork. The ammonia network facilitates exports to external industrial applications beyond the Maasvlakte, while the heat network is linked to the external Warmtelinqs district heating infrastructure.

The MMES models both electricity and hydrogen exports using dedicated demand profiles to reflect their role in supplying electricity to the Netherlands or hydrogen to industries in the hinterland. Given the uncertainty surrounding the amount of natural gas, ammonia, and heat that will be exported, this export to the external grids is regarded as variable.

3.3.4. Inputs

The model inputs define the experimental factors of the MMES and are critical for ensuring an accurate and representative simulation of the system [47]. These inputs are organized into five primary categories: generation profiles, load profiles, technology parameters, carrier parameters and prices.

3.3.4.1. Generation Profiles

Actual generation profiles from renewable energy sources are not available due to the confidentiality of data. Consequently, the generation profiles for wind and solar energy are constructed using open-source weather data from the KNMI (Royal Netherlands Meteorological Institute) database [54]. This database contains hourly meteorological measurements for all KNMI weather stations within the Netherlands. The wind and solar generation profiles were derived from meteorological measurements collected at the KNMI weather station in Hoek van Holland in 2024, which was selected due to its proximity to the Maasvlakte.

Wind generation profiles Wind generation profiles for specific wind farm locations were generated by scaling the mean wind speed at the location of the KNMI station in Hoek van Holland, derived from the Global Wind Atlas database [55], with the mean wind speed at the location of the respective wind farm. For currently operational wind farms, the turbine types are specified, while for new wind farms, the most advanced wind turbine currently available on the market is selected. Knowing the turbine specifications, the availability profiles are generated incorporating the scaled wind speeds, cut-in speeds, cut-out speeds and rated speeds. Generation profiles are then obtained by multiplying the availability profile by the rated capacity of the wind farm. All calculations are provided in Appendix D.

Solar generation profiles The generation profile for the solar farm 'De Slufter' is created by generating an availability profile using hourly solar irradiance data from the weather station in Hoek van Holland, a scaling factor based on the GHI on the site, [56], the maximum solar irradiance, and the efficiency of the solar panels. Detailed calculations can be found in the Appendix E.

Import profiles The import capacities of import flows are derived from the Connected Deep Green scenario executed by the Port of Rotterdam, based on the scenario's forecast for 2030. The scenario forecasts import flows of 13 Mton LNG, 11 Mton ammonia, 0.2 Mton LH_2, and 0.1 Mton H_2-equivalent LOHC [57]. Import is regarded as a continuous process, resulting in a flat generation profile. It is assumed that hydrogen and ammonia imports are solely blue or green.

3.3.4.2. Demand Profiles

Due to the confidential nature of the data, actual load profiles, i.e. demand profiles, of consumers are not available. The generation of load profiles requires two elements: the capacities of consumed energy by the industry and, if applicable, a time-varying load factor profile. DSM is not taken into account for any consumer because of the lack of predictability due to the variability of consumer behavior and the fact that it is unfavorable for energy-intensive industrial processes to adjust their processes. The demand profile per consuming group will be detailed in the subsequent sections. All load capacities are also summarized in Table 3.8.

Chemical Industry The energy demand of the chemical industry, that is Lyondell Chemie Netherlands B.V., located at the Maasvlakte, is derived from the Midden Database developed by TNO and PBL [58]. According to the report, the facility consumes 8.05 PJ steam and 0.513 PJ electricity annually, for the production of propylene oxide and styrene monomer. Currently, natural gas is used as the primary heat source. To support decarbonization, the MIDDEN report identifies several alternative heat supply options, including electrode boilers, hydrogen combustion, and biomass combustion. The MMES model assumes a full transition to H_2 boilers with a 90% efficiency due to their high capacity, retrofitting potential, and superior temperature range compared to electric alternatives [58]. This results in a projected annual energy demand of 283.67 PJ hydrogen and 0.518 PJ electricity. The industrial load is modeled using a flat load profile, reflecting constant operation at maximum capacity, as heat-intensive processes operate optimally at constant speed [59].

Bio-refineries The energy demand for bio-refineries, that is Neste Netherlands on the Maasvlakte, is also derived from the Midden Database [60], shows an annual demand of 0.686 PJ steam, 0.157 PJ electricity, and 0.0086 PJ natural gas. Again, assuming that hydrogen combustion replaces natural gas combustion to meet the heat demand, the final annual energy demand is calculated to be 0.772 PJ hydrogen and 0.157 PJ electricity. Again, a flat load profile is assumed.

Terminals For terminals located on the Maasvlakte, the energy demand profile is based on the assumption that operations occur exclusively during standard working hours (08:00–16:00). While it is acknowledged that terminal operations in industrial port areas can occur on a continuous basis, this study assumes operations based on daytime operations. A study by Budiyanto, Huzaif, Sirait, et al. provides average energy consumption per square meter of terminal [61]. Assuming full electrification of terminal operations, the annual electricity consumption was estimated by calculating the total area of container terminals on the Maasvlakte. The detailed calculation methodology and terminal surface area assumptions are provided in Appendix F.

CCUS CCUS facilities are assumed to operate continuously at maximum capacity due to a lack of data on their operating patterns. For the CCUS facility on the Maasvlakte, Porthos, electricity and heat consumption are determined by calculating the average of six potential CO_2 capture technologies, as outlined by [62], with a CO_2 capture rate of 2.5 million tons per year, calculations are presented in Appendix G.

Shore Power Shore power facilities are assumed to operate continuously at maximum capacity, due to the absence of detailed data on their actual operating patterns. The electricity demand for shore power is derived from shore power development projections provided by the Port of Rotterdam, which outline an expected capacity of 33.3 MW [63].

External networks The MMES models both electricity and hydrogen exports using dedicated demand profiles to reflect their role in supplying electricity to the Netherlands or hydrogen to industries in the hinterland. The current annual electricity demand of the Netherlands is approximately 120 TWh. With an installed adjustable generation capacity of around 2.75 GW (excluding VRES), the Maasvlakte has the theoretical capability to supply one-fifth of the Dutch electricity demand if operating continuously at full load [64][65]. However, in practice, power plants do not run at full capacity year-round. A study by CE Delft reports that average full-load hours for Dutch power plants are approximately 6,000 hours annually, corresponding to a capacity factor of about 70 percent [66]. Another study by CE Delft projects the Dutch electricity demand to reach 147 TWh by 2030 [67]. To account for this projected increase while assuming that the Maasvlakte's relative contribution remains constant, a scaled load profile is constructed using the hourly load data of the Netherlands from 2024, obtained from ENTSO-E's database [68]. The modeled Dutch electricity demand is determined using:

$$\text{Scaled Load Profile} = \min\left(\text{Load Profile}_{2024} \times S, C_{\text{max}}\right), \tag{3.36}$$

$$\text{with } S = \frac{147 \text{ TWh}}{120 \text{ TWh}} \times \frac{1}{5} \times 0.7 \tag{3.37}$$

Where C_{max} reflects the maximum capacity of the overhead AC lines that connects the electrical system of the Maasvlakte to the Dutch electricity grid (Tennet).

Similarly, hydrogen exports follow a pre-defined load profile, assuming a constant export rate. This assumption is based on the expectation that hydrogen exports to the hinterland are mainly for industrial applications and that industrial hydrogen consumption remains constant over time [69]. The export volume is derived from the Connected Deep Green scenario, which anticipates an annual export volume of 1.25 Mton H_2 (equal to 3,425 tonnes/day or 4,556 MWh/h (LHV)).

External connections for natural gas, ammonia and heat are all modeled as absorbing slack buses within the system. While the natural gas connection to Gasunie's national network is technically bi-directional, the role of Maasvlakte as a LNG import hub means that in the practical application of the model, the flow is only export-oriented. Similarly, the modeling assumes unidirectional flows for ammonia and heat to external networks. This approach reflects Maasvlakte's function as a transit port and energy cluster, where these energy carriers are primarily exported to external connections. Consequently, these external connections serve as sinks within the model, representing variable export-only flows.

3.3.4.3. Technology Parameters

Technology parameters refer to the operating characteristics of generators, converters, storage systems, and transmission infrastructure. These parameters are essential for accurately representing the performance and limitations of each component in the MMES. As summarized in Table 3.8, the parameters include nominal power or energy capacity, efficiencies, minimum and maximum load levels, ramping limits, standing losses (for storage systems), technical lifetimes, capital expenditures (Capex), and operational expenditures (Opex). For units requiring high-temperature thermal heat, a minimum power load of 0.1 is assumed, as not stated differently in literature. This value represents a hot standby mode, which allows for rapid ramping and eliminates the need to account for cold start-up times.

For some components, the nominal capacity is extendable in the optimization, which is also indicated in Table 3.8. This applies to all storage components, providing valuable insights into the storage needs for cost-effective and flexible system operation, illustrating their role in meeting energy demand. The extendable nature of storage will serve as a guideline to shape future plans around necessary storage facilities for flexibility. Additionally, heat and ammonia pipeline infrastructure capacities are extendable, as the nominal capacity of a single pipeline has been found potentially insufficient for the system purposes. This means multiple pipelines would be required for these carriers to meet the anticipated flow volumes. In contrast, natural gas and hydrogen pipelines maintain fixed capacities since they can carry more than sufficient volumes and do not require extendability in the model.

For hydrogen- and ammonia-fired CHP plants, specific techno-economic data is currently limited, as these technologies are still in the early stages of commercial deployment. According to Freitag et al. [70], the

estimated costs of retrofitting existing gas-fired power plants to full hydrogen capability is approximately 20% of the original expenses. This estimate is thus applied to determine the capital expenditure for both gas-to-hydrogen retrofitting and coal-to-ammonia retrofitting. With regard to technology-specific parameters, the same values are assumed as the conventional technologies-a common practice in literature, as demonstrated by Cesaro et al. [71].

It is important to note that, although not explicitly shown in Table 3.8, the underground hydrogen storage system is subject to an operational constraint on the hourly injection and withdrawal rate. Specifically, a maximum rate of 667 MW per cavern is assumed, based on data from HyStock's underground hydrogen storage project [72]. This limit reflects physical constraints imposed by allowable pressure fluctuations within the cavern on a daily basis, and is modeled as a hard boundary condition.

The network infrastructure cannot be fully represented by the parameters listed in Table 3.8, therefore, complete specifications for AC lines, AC cables, transformers, and pipelines are provided in Appendix H. The data for AC lines and cables are based on specifications from existing infrastructure provided by De Twentsche Kabelfabriek. These specifications are given per single conductor, while AC lines consist of three conductors. As a result, the nominal apparent power listed in Table 3.8 has been calculated using the following equation:

$$S = \sqrt{3} \cdot V \cdot I \tag{3.38}$$

The identification of the operational ratings of the system components, including capacity limits, efficiencies, and minimum/maximum operating thresholds, constitutes the initial step in answering research question 2. These technology parameters define the operational constraints that govern how each component can function within the energy system. In Section 3.5, these parameters are translated into mathematical formulations for the optimization model. Together, these steps provide answer to how operational constraints are defined and implemented in the model.

3.3.4.4. Carrier Parameters

As stated in section 3.3.3.1, energy carriers are typically expressed in different physical units (i.e., mass, volume, and energy). Standardizing these carriers into a common unit is essential for system integration and comparability. Therefore, it is crucial to consider carrier properties when developing a MES model. The specific carrier properties used for unit conversion—such as energy content per unit mass or volume—are listed in Appendix I.

3.3.4.5. Prices

Carrier prices, modeled as hourly market prices, are integrated into the model to guide dispatch and calculate total system operating costs. Nevertheless, accurately forecasting and modeling the hourly carrier prices is beyond the scope of this study, especially for hydrogen, ammonia, and heat, which currently lack established markets. In contrast, the electricity market is well-established with available hourly spot market prices. For the model's electricity price, the hourly electricity price profile of Denmark in 2024 was used, obtained from the Ember database [73]. Denmark was selected as the reference case due to its electricity mix, which consists of approximately 80% renewables, with 57% of these renewables generated from wind energy [74]. For comparison, the current electricity mix in the Netherlands comprises 50% renewables [75]. The future energy system in the Netherlands is anticipated to resemble Denmark's renewable-dominated mix, validating its use as the reference for electricity prices in this study.

For the chemical energy carriers (natural gas, hydrogen, ammonia), constant market prices are assumed. The price of natural gas, including LNG imports, is based on a combination of historical spot market data and future price projections [76][77]. The prices of hydrogen and ammonia are obtained from a spot market simulation study conducted by HyXchange, which provides indicative pricing under future market conditions [69]. The heat price is based on the 2025's tariffs and the projection that it drops with 50 percent in 2030 [78]. The carrier prices for each energy carrier are presented in Figure 3.3. It is important to note that, although these values are literature-based, they are subject to considerable uncertainty due to potential fluctuations driven by market dynamics, policy developments, and geopolitical factors [79].

3.3.5. Outputs

The outputs represent the model responses and reflect the optimized operation of the system, providing valuable insights into its technical, economic, and operational behavior [47]. The optimization process generates a range of outputs that highlight different aspects of system operation. Technical outputs include information on

Table 3.3: Carrier Price Overview

Carrier	Price [€/MWh]	Ref.
Electricity	Time dependent (average of 70)	[73]
Natural gas	30	[77] [69]
LNG import	30	[76] [69]
H_2	70.9	[69]
NH_3	79.8	[69]
LH_2 import	110	[80]
LOHC import	110	[80]
District Heat	79	[81] [78]

system efficiency, capacity utilization, optimal capacities, renewable energy curtailment, and load balancing. Economic outputs focus on the total cost of the system, encompassing both capital expenditures (Capex) and operational expenditures (Opex). Operational outputs describe the optimal dispatch of components during operation and energy flows, offering insight into the behavior of the system under varying system conditions.

An environmental assessment is not included in the model, based on the assumption that all possible CO_2 emissions are fully captured through CCUS. Consequently, the model is considered carbon-neutral by design, eliminating the need to optimize for emissions reduction. Given this assumption, the operational outputs are considered the most relevant for determining the operation strategy. They provide critical insight into how the energy system should be operated under different conditions to ensure adequate energy supply, flexibility, and cost-effectiveness. Furthermore, the technical outputs—such as optimal storage capacities, capacity utilization, and curtailed energy—serve as key indicators for identifying the required component capacities in future energy systems, thereby informing operational planning. Together, these outputs provide a comprehensive assessment of the MES across technical, economic, and operational dimensions, offering valuable insights into the broader operation of MESs within industrial cluster contexts.

3.3.6. Model Assumptions

Assumptions are incorporated into energy system models to address the uncertainties inherent in the real-world system being represented [47]. In addition to the assumptions previously mentioned in this chapter, it is necessary to highlight additional assumptions to better understand the scope of the model. These assumptions are the following;

- All stakeholders collaborate seamlessly, providing full transparency and unrestricted access to operational data while working toward a shared objective of minimizing overall costs of the energy system.
- The model's focus is exclusively on technical systems, while from a market perspective, certain generation or consumption may occur outside the geographical area of the Maasvlakte (e.g., wind power generation for electrolyzers or hydrogen imports in other parts of the Netherlands).
- The model operates under perfect foresight, which encompasses the knowledge of future demand, renewable energy production, and operational characteristics.
- All energy carriers operate in centralized and regulated markets.
- All technologies that emit CO_2 during operation are equipped with carbon capture technologies, ensuring the entire system is CO_2 neutral.

3.3.7. Model Simplifications

Simplifications differ from assumptions because they are made with the objective of simplifying established knowledge, not on the basis of limited information or presumptions. The aim is to yield more straightforward, efficient, and transparent models [47]. The simplifications are the following:

- The natural gas, hydrogen, ammonia, and heat networks are modeled using the energy hub approach. This is based on the assumption that transport capacity in these networks will be sufficient to meet system requirements.
- Only linear values for system performance and costs are considered.
- The operation of the MES is simulated with an hourly resolution, which may not fully account for short-term dynamics and response times.
- Multiple technologies performing in the same process are aggregated into a single representative component, for example in conversion units.

3.4. Computational Model

Following the development of the conceptual model, the next step involves translating it into a detailed computational model suitable for optimization. This model is implemented in Python using the PyPSA (Python Power System for Analysis) toolbox, an open-source library designed for the simulation and optimization of power and energy systems [82]. The choice of PyPSA is motivated by its ability to capture the technical details of power systems and support sector coupling, both of which are essential for this study. The HiGHS solver, an open-source optimization software package, is employed to solve the linear optimization problems that arise in the model formulation [83].

3.4.1. PyPSA Toolbox

PyPSA has been developed for the specific purpose of simulating and optimizing power and energy systems. With built-in support for VRES, storage systems, and sector coupling, PyPSA is well-suited to address the needs of modern and future (multi-) energy systems. Its selection for optimizing MESs in this research is motivated by its detailed representation of the power system, an aspect often simplified or lacking in other MES toolboxes, including widely used ones such as Calliope, oemof, and urbs [82]. This detailed power network representation is crucial for realistically capturing grid constraints and assessing system feasibility.

A potential limitation of PyPSA for the modeling of MESs is the absence of built-in functionality for detailed modeling of non-electrical networks, such as gas or liquid flows in pipelines. Such modeling would require representations of fluid dynamics and thermodynamics. Nevertheless, this limitation does not directly hinder the study's scope, as only the electricity network is modeled in physical detail using power flow calculations. The energy hub approach is adopted for the other energy carriers networks, as outlined in Section 3.3.3.6. Consequently, PyPSA provides a suitable framework for the objective of this research. Notably, there is currently no open-source toolbox available that supports integrated physics-based modeling of both electrical power flows and gas or liquid flows within a single network framework.

3.4.1.1. Components and structure

In PyPSA, the energy system is constructed by connecting the components presented in Table 3.4. This table is directly adapted from a study by Brown et al [82]. In a network, loads, generators, storage units, stores, and shunt impedances can be attached to a single bus. These buses serve as system nodes and are designed to enforce energy conservation. Buses can be connected to each other by lines, transformers, or links.

Table 3.4: Description of PyPSA model components [82].

Component	Description
Network	Container for all other network components.
Bus	Fundamental nodes to which all other components attach.
Carrier	Energy carrier (e.g., wind, solar, gas, etc.).
Load	A consumer of energy.
Generator	Generator whose feed-in can be flexible, subject to minimum loading, minimum down and up times, or variable according to a given time series of power availability.
Storage Unit	A device which can shift energy from one time to another, subject to efficiency losses.
Store	A more fundamental storage object with no restrictions on charging or discharging power.
Shunt Impedance	An impedance in shunt to a bus.
Line	A branch which connects two buses of the same voltage.
Transformer	A branch which connects two buses of different voltages.
Link	A branch with a controllable power flow between components.

3.4.1.2. Functionalities

PyPSA is capable of performing static power flow calculations, (security-constrained) linear optimal power flow analyses, and least-cost investment optimization. The toolbox includes built-in models for meshed AC-DC networks, standard line and transformer types, conventional dispatchable generators and links, generators with time-varying power availability, storage units, simple hydroelectric models, and sector coupling. Additionally, it provides models in which basic components are integrated to build more complicated energy system assets [84].

3.4.2. Power Flow Modeling

PyPSA is selected as the modeling toolbox for this study due to its ability to represent power systems with high technical detail. As discussed in Section 3.3.3.6, this level of detail is essential to assess the technical feasibility in the electrical infrastructure. In power flow analysis, the distribution of electrical power across the network is determined through an iterative process that considers nodal voltage magnitudes and phase angles, together with power injections and the overall network topology, as illustrated in Figure 3.3.

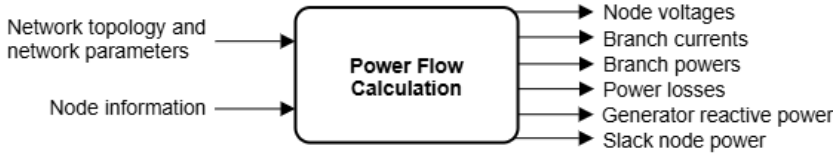

Figure 3.3: Power Flow Calculation [85].

Power injections at each bus n are modeled and calculated using the AC power flow equations. These non-linear equations, expressed below, relate complex power injections to bus voltages (V_n, V_m) and the admittance matrix (Y_{nm}) of the network:

$$S_n = P_n + jQ_n = V_n I_n^* = \sum_m V_n Y_{nm}^* V_m^* \tag{3.39}$$

Solving these equations yields the nodal voltages, from which both bus injections and physical line flows—including losses—can be computed. To enable efficient optimization, PyPSA uses a linear approximation of these equations [84]. The linearization assumes decoupling of reactive power, fixed voltage magnitudes, small voltage angle differences, and small line resistances. This approximation reduces computational complexity while maintaining essential physical behavior. This leads to a linear relationship between voltage angles and active power flows:

$$P_n = \sum_m (KBK^T)_{nm}\theta_m - \sum_l K_{n\ell} b_\ell \theta_\ell^{\text{shift}} \tag{3.40}$$

Here, K is the network's incidence matrix, B represents the series susceptances, θ_n are the voltage angles, $\theta_\ell^{\text{shift}}$ are transformer phase-shifts.

PyPSA implements the standard equivalent PI model to represent transmission lines and cables [84]. This model accounts for the internal impedances of the lines and relates the series impedance ($z = r + jx$), shunt admittance ($y = g + jb$), to the currents (I_0 and I_1) and voltages (V_0 and V_1) between to buses:

$$\begin{pmatrix} i_0 \\ i_1 \end{pmatrix} = \begin{pmatrix} \frac{1}{z} + \frac{y}{2} & -\frac{1}{z} \\ -\frac{1}{z} & \frac{1}{z} + \frac{y}{2} \end{pmatrix} \begin{pmatrix} v_0 \\ v_1 \end{pmatrix} \tag{3.41}$$

For transformers, PyPSA uses the standard equivalent T model which additionally includes the transformer tap ratio (τ), and transformer phase shift (θ^{shift}) as presented in Equation 3.42. This equation assumes the tap changer on the primary side. The transformer T model is converted to the PI model for consistency, as described in the PyPSA documentation [84].

$$\begin{pmatrix} I_0 \\ I_1 \end{pmatrix} = \begin{pmatrix} \frac{1}{z} + \frac{y}{2} & -\frac{1}{z} \cdot \frac{1}{\tau e^{-j\theta^{\text{shift}}}} \\ -\frac{1}{z} \cdot \frac{1}{\tau e^{j\theta^{\text{shift}}}} & \left(\frac{1}{z} + \frac{y}{2}\right) \cdot \frac{1}{\tau^2} \end{pmatrix} \begin{pmatrix} V_0 \\ V_1 \end{pmatrix} \tag{3.42}$$

3.4.3. Sector Coupling

PyPSA enables the integrated modeling of multiple energy sectors within a unified framework by assigning energy carriers—such as electricity, natural gas, or hydrogen—to the buses. This structure supports sector-specific networks that interact through conversion components, referred to as links, which govern energy transfers between carriers. As described in Section 3.3.3.6, non-electrical energy carrier networks—such as those for natural gas, hydrogen, ammonia, and heat—are not modeled with explicit infrastructure constraints. As a result, they are represented using the energy hub approach introduced in Section 2.3.3, where energy flows and conversions are governed by fixed efficiency values rather than detailed physical models.

The injected energy per bus and per carrier is governed by carrier-specific energy balances, formulated as constraints in Section 3.5.3.5. Energy flow through the system is thus determined by these balances, and

shaped by fixed conversion and transmission efficiencies:

$$\begin{pmatrix} P_{\alpha}^{\text{out}} \\ P_{\beta}^{\text{out}} \\ \vdots \\ P_{\omega}^{\text{out}} \end{pmatrix} = \begin{pmatrix} \eta_{\alpha,\alpha} & \eta_{\beta,\alpha} & \cdots & \eta_{\omega,\alpha} \\ \eta_{\alpha,\beta} & \eta_{\beta,\beta} & \cdots & \eta_{\omega,\beta} \\ \vdots & \vdots & \ddots & \vdots \\ \eta_{\alpha,\omega} & \eta_{\beta,\omega} & \cdots & \eta_{\omega,\omega} \end{pmatrix} \begin{pmatrix} P_{\alpha}^{\text{in}} \\ P_{\beta}^{\text{in}} \\ \vdots \\ P_{\omega}^{\text{in}} \end{pmatrix}$$

In this formulation, each matrix element $\eta_{i,j}$ represents the efficiency of converting input from carrier j into output in carrier i. This approach enables scalable and integrated modeling of sector coupling, while still capturing key transformation losses and operational constraints in the optimization process.

3.5. Model Formulation

In the optimization model, the model is described by mathematical model formulations. As previously delineated in Chapter 2, an optimization problem is comprised of three fundamental aspects: an objective function, decision variables, and constraints. The subsequent section will delve into the mathematical formulations of these aspects.

3.5.1. Decision Variables

An overview of the input variables for the optimization model is shown in Table 3.5. The decision variables, the variables that can be adjusted in the optimization, are shown in Table 3.6.

Table 3.5: Input variables

Input Variable	Description
$n \in N = \{0, \ldots, \lvert N \rvert - 1\}$	Set of network busses
$t \in T = \{0, \ldots, \lvert T \rvert - 1\}$	Set of network snapshots
$l \in L = \{0, \ldots, \lvert L \rvert - 1\}$	Set of network branches
$s \in S = \{0, \ldots, \lvert S \rvert - 1\}$	Set of generator and/or storage types at each bus
$\bar{g}_{n,s}$	Nominal power of generator, if not extendable
$\bar{e}_{n,s}$	Nominal energy of store, if not extendable
F_l	Nominal capacity of branch l (i.e. link, line, or transformer), if not extendable
$d_{n,s,t}$	Capacity of load d at time t
$\tilde{g}_{n,s}$	Minimum nominal power of generator, if nominal power is extendable
$\hat{g}_{n,s}$	Maximum nominal power of generator, if nominal power is extendable
$\tilde{e}_{n,s}$	Minimum nominal energy of store, if nominal energy is extendable
$\hat{e}_{n,s}$	Maximum nominal energy of store, if nominal energy is extendable
$\tilde{f}_l$	Minimum nominal power of branch, if nominal power is extendable
$\hat{f}_l$	Maximum nominal power of branch, if nominal power is extendable
$u_{n,s,t}$	Binary value for unit commitment
rd_{l}	Ramp-up limit up of link l
ru_{l}	Ramp-down limit of link l
$\eta_{n,s}$	Efficiency of generator g
η_l	Efficiency of branch l
$\eta_{\text{stand},n,s}$	Standing efficiency of store e
$c_{n,s}$	Capital cost of increasing nominal power by 1 MW
c_l	Capital cost of increasing branch capacity by 1 MW
$o_{n,s}$	Marginal cost of increasing dispatch by 1MWh
o_l	Marginal cost of increasing branch's (link) dispatch by 1MWh
v_n	Nominal voltage of bus
x_n	Longitude of bus
y_n	Latitude of bus
$carrier_n$	Carrier of bus
$l_{n,s}$	Lifetime of generator, storage unit, or store
l_l	Lifetime of branch
f_x	Series reactance of line or transformer
f_r	Series resistance of line or transformer
f_f	Nominal frequency of line or transformer
w_t	Weighting of time, equals 1 in hourly simulation

Table 3.6: Decision variables

Decision variable	Description
$g_{n,s,t}$	Power output of generator s at bus n at time t
$h_{n,s,t}$	Power output of store s at bus n at time t
$f_{l,t}$	Power flow in branch l (line, link, or transformers) at time t
$\bar{g}_{n,s}$	Nominal power of generator, if extendable
$\bar{h}_{n,s}$	Nominal power of store, if extendable
F_l	Capacity of branch l, if extendable

3.5.2. Objective Function

The objective function, presented in Equation 3.43, is defined as the minimization of the total system's cost, which encompasses the capital and operational expenditures of generation, stores, and network branches—where network branches refer to transmission lines, transformers, and links.

$$\min_{\substack{\bar{g}_{n,s},F_l,\bar{h}_{n,s},\\ g_{n,s,t},f_{l,t},h_{n,s,t},}} \left\{ \sum_{n,s} c_{n,s}\bar{g}_{n,s} + \sum_{l} c_l F_l + \sum_{n,s} c_{n,s}\bar{h}_{n,s} + \sum_{t} w_t \left[\sum_{n,s} o_{n,s,t} g_{n,s,t} + \sum_{l} o_{l,t} f_{l,t} + \sum_{n,s} o_{n,s,t} h_{n,s,t} \right] \right\} \tag{3.43}$$

It should be noted that the export of energy to external networks is modeled by the use of generator components. In such a model, a negative value for generation indicates an exit of energy from the system. In this configuration, the external networks effectively act as energy sinks. As these negative generation values represent exports, they are associated with revenues in the objective function. Consequently, such exports have been demonstrated to reduce the total system cost, thereby reflecting the financial benefit of delivering energy to external markets.

3.5.3. Constraints

The optimization is subject to a set of constraints that define the allowable values of the decision variables and reflect the technical and physical limitations of the system components. This section thereby addresses part of research question 2 by outlining the manner in which the system's operational constraints are mathematically implemented in the model. The subsequent description of each constraint type is made with reference to the relevant input or decision variables.

3.5.3.1. Generator Constraints

Generators with time-dependent restrictions on the dispatch obey the constraint given in Equation 3.44. This time dependent restriction originates from wind or solar availability in VRES.

$$\tilde{g}_{n,s,t} \cdot \bar{g}_{n,s} \leq g_{n,s,t} \leq \bar{g}_{n,s,t} \cdot \bar{g}_{n,s} \tag{3.44}$$

With $\tilde{g}_{n,s,t}$ and $\bar{g}_{n,s,t}$ representing the lower and upper limits, respectively, of the time-dependent generation restrictions due to its availability. For VRES, the lower limit is equal to zero and the upper limit equals the maximum possible generation at that moment, taking into wind and solar availability. This makes renewable curtailment possible when necessary.

For generators that allow curtailment of their energy output, unit commitment can be enabled or disabled. The generator's dispatch is thus constrained by the following condition:

$$u_{n,s,t} \cdot \tilde{g}_{n,s,t} \cdot \bar{g}_{n,s} \leq g_{n,s,t} \leq u_{n,s,t} \cdot \bar{g}_{n,s,t} \cdot \bar{g}_{n,s} \quad \forall n, s, t \tag{3.45}$$

Here, $u_{n,s,t} \in 0, 1$ which indicates if the generator is on (1) or off (0) in period t.

For generators whose rated power can be extended in the optimization can be constrained to set minimum and maximum values for the nominal capacity, as shown in Equation 3.46:

$$\tilde{g}_{n,s} \leq \bar{g}_{n,s} \leq \hat{g}_{n,s} \tag{3.46}$$

Because the generators in this model consist entirely of renewable generation units and import flows, they are not subject ramping limits.

3.5.3.2. Link Constraints

Controllable links are restricted by the nominal capacity of the branch as shown in Equation 3.47:

$$|f_{l,t}| \leq F_l \tag{3.47}$$

If $f_{l,t} > 0$, it means that it withdraws $f_{l,t}$ from bus 0 and feeds $\eta_l f_{l,t}$ into bus 1.

Links that are restricted by a minimum and maximum output for each snapshot per unit, are also constrained by time-dependent restrictions due to their availability, as given by constraint:

$$\tilde{f}_{l,t} \cdot F_l \leq f_{l,t} \leq \bar{f}_{l,t} \cdot F_l \tag{3.48}$$

With $\tilde{f}_{l,t}$ and $\bar{f}_{l,t}$ representing the lower and upper limits, respectively, of the time-dependent generation restrictions due to its availability.

If the nominal power of the links is extendable in the optimization, and if applicable, the links are constrained by their minimum and maximum nominal power, as shown in equation 3.49:

$$\tilde{f}_l \leq \bar{f}_l \leq \hat{f}_l \tag{3.49}$$

Links with ramping limits obey constraints for ramping up and/or ramping down as shown in Equation 3.50:

$$-rd_l \cdot F_l \leq (f_{l,t} - f_{l,t-1}) \leq ru_l \cdot F_l \quad \text{for } t \in \{1, \ldots, |T| - 1\}. \tag{3.50}$$

3.5.3.3. Store Constraints

Store units have two time-dependent variables; the energy stored ($e_{n,s,t}$) and the store power dispatch ($h_{n,s,t}$).

The store dispatch is not constrained within the store unit itself, as the store is connected to the network through links, which determine the dispatch limits when applicable. So the constraint is therefore given by Equation 3.51:

$$-\infty \leq h_{n,s,t} \leq +\infty \tag{3.51}$$

If the nominal power of the store is extendable in the optimization, and constrained by a minimum and/or maximum nominal power, this is given by Equation 3.52:

$$\tilde{e}_{n,s} \leq \bar{e}_{n,s} \leq \hat{e}_{n,s} \tag{3.52}$$

The dispatch of the store and the energy stored in the store unit are related by Equation 3.53:

$$e_{n,s,t} = \eta_{\text{stand},n,s} \cdot e_{n,s,t-1} - h_{n,s,t} \tag{3.53}$$

With $\eta_{\text{stand},n,s}$ representing the standing losses in the store. The energy that is stored is subject to minimum and maximum fill levels of the store, as provided by Equation 3.54:

$$\tilde{e}_{n,s,t} \cdot \bar{e}_{n,s} \leq e_{n,s,t} \leq \bar{e}_{n,s,t} \cdot \bar{e}_{n,s} \tag{3.54}$$

With $\tilde{e}_{n,s,t}$ and $\bar{e}_{n,s,t}$ representing the lower and upper limits, respectively, of the time-dependent generation restrictions due to its availability.

3.5.3.4. Line and Transformer Constraints

Similar to the links, the lines and the transformer are constrained to their nominal capacity of the branch, for which the constraint was also given in Equation 3.47:

$$|f_{l,t}| \leq F_l \tag{3.55}$$

Furthermore, power flows in lines and transformers must comply to Kirchhoff's circuit laws; Kirchhoff's current law (KCL) and Kirchhoff's voltage law (KVL). KCL states that the sum of current entering a node in an electrical circuit equals the sums of currents leaving the node, ensuring electric charge conservation:

$$\sum_{k=1}^{n} I_k = 0 \tag{3.56}$$

KVL states that the sum of all voltages in a closed loop in an electrical circuit equals zero, ensuring energy conservation:

$$\sum_{k=1}^{n} V_k = 0 \tag{3.57}$$

Solving Kirchhoff's equations for all loops in the entire network can be computationally intensive, so PyPSA uses the cycle-based formulation of KVL (Equation 3.58), which has proven to be much faster than other formulations because it reduces the number of equations to satisfy KVL [86]. All power flows in lines and transformers are thus constrained to comply with this equation.

$$\sum_{l} C_{l,c} x_l f_{l,t} = 0 \quad \forall c \tag{3.58}$$

Where the cycle-based matrix C is constructed from the network graph, and x_l represents the series reactance.

3.5.3.5. Energy flow balances

The energy flow balance ensures that the energy flow is balanced at each bus n for each time t, and is given in Equation 3.59.

$$\sum_{s} g_{n,s,t} + \sum_{s} h_{n,s,t} - \sum_{l} K_{nl} f_{l,t} = \sum_{s} d_{n,s,t} \tag{3.59}$$

Where $d_{n,s,t}$ is the exogenous load at each node and K_{nl} is the incidence matrix for the network graph which indicates if a branch starts or ends at that node.

3.5.3.6. Custom Constraints

In addition to the model's technical constraints, certain operational constraints are manually incorporated to capture specific system behavior. These constraints are described in detail below.

Electrolyzers constraint The first constraint ensures that the electrolyzers operate based on the power output of the IJmuiden Ver wind farm to produce green hydrogen. When the generated wind power exceeds the rated capacity of the electrolyzers, the electrolyzers operate at maximum capacity. When the generated wind power falls below the minimum operational power of the electrolyzers, they operate at the minimum level. Between these limits, the electrolyzers dynamically follow the wind power generation profile with an one hour delay. This constraint is represented in Equation 3.60.

$$f_{l,t}^{\text{min,pu,electrolyzer}} = f_{l,t}^{\text{max,pu,electrolyzer}} = \begin{cases} 1.0, & \text{if } g_{n,s,t-1}^{\text{windfarm IJV}} \geq f_l^{\text{max,pu,electrolyzer}} \cdot \bar{F}_l^{\text{electrolyzer}}, \\ f_{\text{l}}^{\text{min,pu,electrolyzer}}, & \text{if } g_{n,s,t-1}^{\text{windfarm IJV}} \leq f_l^{\text{min,pu,electrolyzer}} \cdot \bar{F}_l^{\text{electrolyzer}}, \\ \frac{g_{n,s,t-1}^{\text{windfarm IJV}}}{\bar{F}_l^{\text{electrolyzer}}}, & \text{otherwise.} \end{cases} \tag{3.60}$$

Electricity load shedding constraint The second constraint activates a load shedding generator when the available electricity in the system cannot meet the electricity consumption and export requirements. As a result, the export volume can be reduced by activating the load shedding generator. Load shedding carries a high marginal cost (100 EUR/kWh, default by PyPSA) to ensure it's used only as a last resort balancing mechanism. The constraint prioritizes the system's local electricity demand over external network demands, assuming shortfalls in the broader systems can be covered by power suppliers outside the modeled system.

$$-g_{n,s,t}^{\text{shed}} = \max\left(0, d_{n,s,t}^{\text{AC export}} - \left[\sum_{s' \in S^{\text{elec}}} g_{n,s',t} + \sum_{s' \in S^{\text{elec}}} h_{n,s',t} + \sum_{l' \in L^{\text{elec}}} K_{nl} f_{l',t} - \sum_{s' \in S^{\text{elec}}} d_{n,s',t}^{\text{Maasvlakte}}\right]\right) \quad \forall\, s \in S^{\text{elec}} \tag{3.61}$$

$$S^{\text{elec}} = \{s \in S \mid \text{carrier}_{n,s} = \text{electricity}\} \tag{3.62}$$

$$L^{\text{elec}} = \{l \in L \mid \text{carrier}_{\text{bus0}} = \text{electricity} \vee \text{carrier}_{\text{bus1}} = \text{electricity} \vee \text{carrier}_{\text{bus2}} = \text{electricity}\} \tag{3.63}$$

Hydrogen load shedding constraint The third constraint is similar to the second, but focuses on load shedding of the hydrogen export volume, if the hydrogen supply is insufficient to meet consumption and export demands. Load shedding incurs a penalty cost (100 EUR/kWh, default by PyPSA).

$$-g^{\text{shed}}_{n,s,t} = \max\left(0, d^{\text{H2 export}}_{n,s,t} - \left[\sum_{s' \in S^{\text{H2}}} g_{n,s',t} + \sum_{s' \in S^{\text{H2}}} h_{n,s',t} + \sum_{l' \in L^{\text{H2}}} K_{nl} f_{l',t} - \sum_{s' \in S^{\text{H2}}} d^{\text{Maasvlakte}}_{n,s',t}\right]\right) \quad \forall\, s \in S^{\text{H2}} \tag{3.64}$$

$$S^{\text{H2}} = \{s \in S \mid \text{carrier}_{n,s} = \text{hydrogen}\} \tag{3.65}$$

$$L^{\text{H2}} = \{l \in L \mid \text{carrier}_{\text{bus0}} = \text{hydrogen} \vee \text{carrier}_{\text{bus1}} = \text{hydrogen} \vee \text{carrier}_{\text{bus2}} = \text{hydrogen}\} \tag{3.66}$$

Cyclicity of charge constraint In order to ensure that storage systems do not accumulate or deplete energy over the modelled time horizon, a cyclicity constraint is applied. This constraint enforces the condition that the state of charge at the conclusion of the simulation period is equivalent to that at the beginning, thereby preserving energy neutrality in long-term operation.

$$e_{\text{n,s,t=-1}} = e_{\text{n,s,t = |T|-1}} \quad \text{for } t \in \{-1, \ldots, |T| - 1\} \tag{3.67}$$

3.6. Scenarios for Meteorological Uncertainty

In order to evaluate the impact of meteorological variability on energy system operation, and thereby addressing research question 2, a scenario-based analysis is conducted. This method systematically assesses system performance under different meteorological conditions by simulating three distinct scenarios: a normal case, a worst-case, and a best-case scenario. These scenarios are constructed using historical hourly meteorological data from the Hoek van Holland KNMI station over the period 1970–2025 to ensure realistic weather conditions [54]. Wind measurements have been available since 1970, while solar measurements have been recorded since 2000.

The normal case serves as a baseline scenario and is represented by the most recent historical weather data from 2024, as outlined in Section 3.3.4.1. This scenario represents typical system operation under current conditions, with an average wind speed of 6.81 m/s and an average solar irradiance of 123 W/m². Appendix J.1 presents frequency distributions of the yearly averages for wind speed and solar irradiance, showing that these values occur all within the most commonly observed range of the analyzed historical data. This confirms that the 2024 weather conditions provide a representative basis for the normal-case scenario.

As wind energy represents the predominant renewable energy source in the MMES, the worst-case scenario is characterized by minimal wind resource availability. Consequently, this scenario is defined by the historical year exhibiting the lowest mean wind speed (1971, 5.49 m/s). For scenario construction, the hourly wind speed time series from 1971 is utilized. However, as solar irradiance data is unavailable for 1971, an alternative approach was required. To address this limitation, an analysis of all available meteorological datasets was conducted, revealing an inverse correlation between wind speed and solar irradiance, as graphically shown in Appendix J.2. Utilizing this empirical relationship, the worst-case scenario was completed by incorporating data from the year characterized by the highest average solar irradiance (2022, 143.77 W/m²). The hourly solar irradiance time series was implemented to complete the scenario formulation.

Conversely, the best-case scenario is characterized by high wind availability throughout the year. To construct this scenario, the year with the highest average wind speed (1992, 9.10 m/s) and the year with the lowest solar irradiance (2000, 114.83 W/m²) were selected, again using the hourly time series for the respective years.

A summary of the key meteorological characteristics for each scenario is provided in Table 3.7. accompanied by a visual comparison of the average monthly wind speed and the average monthly solar irradiance for each scenario in Figure 3.4. The frequency distributions in the before-mentioned Appendix J.1, provide further insight into the likelihood of the different weather scenarios. The incorporation of a normal-case scenario, a worst-case scenario (defined by minimal wind availability), and a best-case scenario (defined by maximum wind availability) enables the analysis to capture a representative spectrum of meteorological variability. Consequently, it facilitates the evaluation of system operation across a full range of conditions, from highly unfavorable to highly favorable, thereby offering insight into the operational behavior of the MMES under both typical and extreme weather conditions.

Table 3.7: Key meteorological characteristics of scenarios.

Scenario	Average Annual Wind Speed	Average Annual Solar Irradiance
Worst-Case: Minimal Wind Scenario	5.49 m/s (1971)	143.77 W/m^2 (2022)
Normal-Case: Current Conditions Scenario	6.81 m/s (2024)	123.00 W/m^2 (2024)
Best-Case: Maximal Wind Scenario	9.10 m/s (1992)	114.83 W/m^2 (2000)

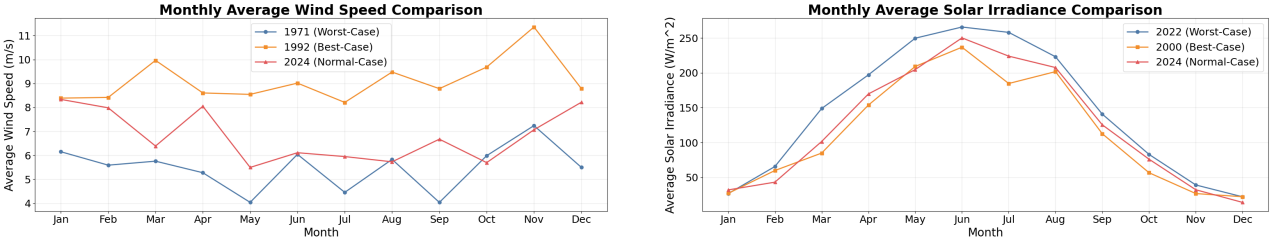

(a) Wind speed comparison.

(b) Solar irradiance comparison.

Figure 3.4: Comparison of monthly average wind speed and solar irradiance for the scenarios.

3.7. Verification and Validation

In order to ensure that the model is technically correct, of qualitative accuracy and useful in achieving its goal, it is imperative that verification and validation steps are completed [87]. Validation ensures that the model replicates the underlying system, thereby verifying that the model built is the 'right' model for the intended purpose. Verification ensures that the model and model implementations are correct, thereby verifying that the model is built in the 'right' way. Multiple verification and validation steps are taken, including software verification, model validation, model verification, and a sensitivity analysis. The sensitivity analysis is presented in the following chapter, Section 4.4, as part of the overall results analysis.

3.7.1. Software Verification

To verify PyPSA's capability to accurately model power flows, and thus generate reliable results, the toolbox was tested against the verified IEEE 9-bus model in PandaPower, which is a widely-adopted test case model. This was done by reconstructing the IEEE 9-bus model in PyPSA with identical topology and parameters as the reference PandaPower system. Power flow simulations were performed in both tools, and the resulting outputs were compared by evaluating the voltage magnitudes at all nine buses—an accepted comparison method as demonstrated by Fernández-Guillamón et al. [88]. As shown in Figure 3.5, the results from PyPSA closely matched those from PandaPower, confirming that PyPSA can accurately simulate power systems and is therefore suitable and reliable tool for the purposes of this research.

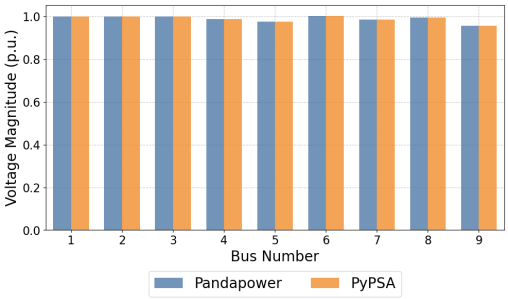

Bus	Voltage Difference (%)
1	0.000000e+00
2	0.000000e+00
3	0.000000e+00
4	1.272811e-09
5	1.108263e-09
6	-2.880189e-10
7	-5.702475e-10
8	-2.238645e-10
9	2.503721e-09

Figure 3.5: Comparison of bus voltage magnitudes in the IEEE 9-bus system between Pandapower and PyPSA power flow simulations (left figure), and the percentual differences in voltage magnitudes between the two simulations (right table).

3.7.2. Model Verification

To ensure that the model implementation in Python is consistent with the conceptual model, several validation steps were performed. PyPSA stores all component-specific technology parameters in data frames, which were systematically checked to verify the correct integration of values for each network component. In addition, a geographic map of the Maasvlakte was created using the Cartopy toolbox to visualize spatial relationships. This map was regularly checked to confirm that all components were included and correctly connected via

their respective branches. Power flow results were also plotted at each bus to validate that all flows were properly integrated and behaved as expected. Finally, PyPSA's built-in network consistency checks were used to ensure that all components were connected to valid buses and that the system contained no singular impedances, i.e. all branches were correctly connected.

3.7.3. Model Validation

The qualitative accuracy of the representation of each of the energy carrier networks, its components, and the interaction between the networks, has been validated by subject matter experts. Specifically, the electrical system was reviewed by an asset management expert at Stedin. The hydrogen system was reviewed by the Program Manager of Electrification and Hydrogen and the Business Manager of Energy & Infrastructure, both from the Port of Rotterdam. The ammonia system was evaluated by the Manager of Energy & Infrastructure at the Port of Rotterdam. Finally, the heat system and energy system as a whole were reviewed by the Business Development Manager at Port of Rotterdam. The validation was achieved by validating the single-line diagram of the respective network, as presented in Appendix A, the technical network and component characteristics outlined in Table 3.8, and the network interactions illustrated in Figure 3.2.

3.8. Summary

This chapter outlined the methodology used to develop a model-based optimization approach for analyzing the operation of MESs. The methodology was structured into four key components: the development of a conceptual model, its translation into an optimization model, the formulation of scenarios to evaluate system performance under varying weather conditions, and verification and validation procedures to ensure both technical soundness and qualitative accuracy. The modeled system is a synthetic, future-oriented MES inspired by the Maasvlakte area in the Port of Rotterdam, which served as the case study. The model integrates five energy carriers—electricity, hydrogen, ammonia, natural gas, and heat—through a network of components including generation and import facilities, storage technologies, conversion units, transmission and distribution networks, end-use consumers, and connections to external networks. The computational model was implemented in PyPSA, incorporating physics-based power flow modeling for the electricity network and applying the energy hub approach for the integration of other carrier networks. The optimization problem was formulated as a cost-minimization problem, subject to a range of operational constraints that ensure technical feasibility and realistic system behavior.

Table 3.8: Dataframe of the MMES components and the respective technology parameters.

Network Component	Component	Nominal Power / Energy (MW(h))	Pnom / Enom Extendable (y/n)	Efficiency (-)	Efficiency 2 (-)	Efficiency 3 (-)	Minimal Power Load (p.u.)	Max Power Load (p.u.)	Ramping Limit Up (p.u.)	Ramping Limit Down (p.u.)	Standing Loss (h^{-1})	Lifetime (y)	Capital Costs (Euro/MW(h))	Fixed Opex (- / Capex)	Variable Opex (Euro / MWh)	Ref.
Import	LNG import	19416	no	1.00	-	-	-	-	-	-	-	30	-	-	$\sum(MWh_{carrier} \times price_{carrier})$	[57]
Import	LH2 import	761	no	1.00	-	-	-	-	-	-	-	30	-	-	$\sum(MWh_{carrier} \times price_{carrier})$	[57]
Import	LOHC import	381	no	1.00	-	-	-	-	-	-	-	30	-	-	$\sum(MWh_{carrier} \times price_{carrier})$	[57]
Import	NH_3 import	6488	no	1.00	-	-	-	-	-	-	-	30	-	-	$\sum(MWh_{carrier} \times price_{carrier})$	[57]
Generation	Windfarm 'Hollandse Kust Zuid'	1529.00	no	1.00	-	-	0.00	1.00	-	-	-	30	2621000	0.03	0.00	[89]
Generation	Windfarm 'Maasvlakte 2'	116.70	no	1.00	-	-	0.00	1.00	-	-	-	26	1240000	0.028	0.00	[89] [90]
Generation	Windfarm 'IJmuiden Ver'	4000.00	no	1.00	-	-	0.00	1.00	-	-	-	30	2621000	0.03	0.00	[89]
Generation	Windfarm 'Nederwiek'	2000.00	no	1.00	-	-	0.00	1.00	-	-	-	30	2621000	0.03	0.00	[89]
Generation	Solarfarm 'De Slufter'	128.00	no	0.166	-	-	0.00	1.00	-	-	-	27	1290000	0.017	0.00	[90]
Conversion	MPP3 NH_3-fired CHP	1070 (MWe)	no	0.4 (elec)	0.4 (heat)	-	0.30	1.00	0.5	0.5	-	40	2448000.00	0.03	$\sum(MWh_{carrier} \times price_{carrier})$	[89] [91] [92] [93] [94]
Conversion	Onyx NH_3-fired CHP	870 (MWe)	no	0.4 (elec)	0.4 (heat)	-	0.30	1.00	0.5	0.5	-	40	2448000.00	0.03	$\sum(MWh_{carrier} \times price_{carrier})$	[89] [91] [92] [93] [94]
Conversion	UCML H_2 -fired CHP	80 (MWe)	no	0.3345 (elec)	0.4259 (heat)	-	0.45	1.00	-	-	-	25	720000	0.10	$\sum(MWh_{carrier} \times price_{carrier})$	[95] [89]
Conversion	Enecogen H_2-fired CHP	731 (MWe)	no	0.3345 (elec)	0.4259 (heat)	-	0.45	1.00	-	-	-	25	720000	0.10	$\sum(MWh_{carrier} \times price_{carrier})$	[95] [89]
Conversion	Electrolyzers	2000	no	0.62 (H_2)	0.12 (heat)	-	0.2	1.00	-	-	-	15	900000	0.035	$\sum(MWh_{carrier} \times price_{carrier})$	[96] [89] [97]
Conversion	Autothermal Reforming Hydrogen	1522	no	0.75 (H_2)	-0.0625 (elec)	-	0.20	1.00	-	-	-	30	339480	0.02	$\sum(MWh_{carrier} \times price_{carrier})$	[98] [99] [51]
Conversion	NH_3 cracker	4815	no	0.90	-	-	0.10	1.00	-	-	-	20	756794	0.025	$\sum(MWh_{carrier} \times price_{carrier})$	[100] [101] [102]
Conversion	H_2 boiler	300	yes	0.90	-	-	-	-	-	-	-	25	120000	0.03	-	[58] [103]
Conversion	LNG gasification	19416	no	0.99919 (LNG)	-0.00081 (elec)	-	1.00	1.00	-	-	-	30	489250	0.025	$\sum(MWh_{carrier} \times price_{carrier})$	[57] [104]
Conversion	LH_2 gasification	761	no	0.8326 (H_2)	-0.1674 (elec)	-	1.00	1.00	-	-	-	30	489250	0.025	$\sum(MWh_{carrier} \times price_{carrier})$	[57] [105]
Conversion	LOHC dehydrogenation	381	no	0.72 (H_2)	0 (elec)	-	1.00	1.00	-	-	-	30	53000	0.025	$\sum(MWh_{carrier} \times price_{carrier})$	[57] [106] [52]
Storage	H_2 underground storage	200000	yes	0.995 (H_2)	-0.03(elec)	-	0.50	1.00	-	-	-	40	6041	0.02	$\sum(MWh_{carrier} \times price_{carrier})$	[72] [107] [108] [109]
Storage	H_2 pressurized tank storage	1000	yes	1.00 (H_2)	-0,20 (elec)	-	-	1.00	-	-	0.001	23	10000	0.02	$\sum(MWh_{carrier} \times price_{carrier})$	[90] [110] [111]
Storage	NH_3 storage	4500	yes	1.00 (NH_3)	-0,06 (elec)	-	0.035	0.0965	-	-	0.001	20	120	0.022	$\sum(MWh_{carrier} \times price_{carrier})$	[106] [112] [113]
Storage	BESS	5	yes	0.91 (elec)	-	-	0.035	0.0965	-	-	0.002	13	285000	0.022	$\sum(MWh_{carrier} \times price_{carrier})$	[89] [114]
Transmission	HVAC - 380kV	2635	no	0.0989	-	-	-	-	-	-	-	30	190000 / km / GW	0.00	-	[115] [116]
Transmission	HVAC - 150kV	566.25 (MVA)	no	0.0989	-	-	-	-	-	-	-	30	190000 / km / GW	0.00	-	[116] [117]
Transmission	MVAC - 66kV	82.5 (MVA)	no	0.0989	-	-	-	-	-	-	-	30	190000 / km / GW	0.00	-	[116] [117]
Transmission	MVAC - 25kV	13 (MVA)	no	0.0989	-	-	-	-	-	-	-	30	190000 / km / GW	0.00	-	[116] [117]
Transmission	Transformers: 380/150, 150/66, 150/25, 66/25	590, 128, 35.74, 32.85 (MVA)	no	0.0989	-	-	-	-	-	-	-	30	-	-	-	[116]
Transmission	H_2 pipelines	13000	no	0.98	-	-	-	-	-	-	-	40	2750000 Euro / km	0.01	-	[116]
Transmission	H_2 pipelines & compressor station	13000	no	0.98	-0.0006 (elec)	-	-	-	-	-	-	40	6150000 Euro / km	0.01	-	[116]
Transmission	NG pipelines	16900	no	0.99	-	-	-	-	-	-	-	40	1830000 Euro / km	0.01	-	[116]
Transmission	NG pipelines & compressor station	16900	no	0.99	-0.0006 (elec)	-	-	-	-	-	-	40	3720000 Euro / km	0.01	-	[116]
Transmission	NH_3 pipelines	260	yes	0.99	-0.000006 (elec)	-	-	-	-	-	-	40	1429000 Euro / km	0.03	-	[118] [119]
Transmission	NH_3 pipelines & booster station	260	yes	0.99	-0.000006 (elec)	-	-	-	-	-	-	40	3649000 Euro / km	0.03	-	[118] [119]
Transmission	Heat pipelines	300	yes	0.95 (heat)	-0.05 (elec)	-	-	-	-	-	-	50	1416000 Euro/km	0.018	-	[120] [121] [122] [123]
Transmission	Heat exchangers	300	yes	0.95	-	-	-	-	-	-	-	50	133000	0.018	-	[120] [121] [122]
Transmission	Heat pumps	90	yes	COP dependent	-	-	-	-	-	-	-	30	547500	0.018	-	[120] [121] [124]
Consumption	Chemical industry: electricity	4.98	no	-	-	-	-	-	-	-	-	-	-	-	-	[58]
Consumption	Chemical industry: hydrogen	24.60	no	-	-	-	-	-	-	-	-	-	-	-	-	[58]
Consumption	Refineries: electricity	18.43	no	-	-	-	-	-	-	-	-	-	-	-	-	[60]
Consumption	Refineries: hydrogen	283.67	no	-	-	-	-	-	-	-	-	-	-	-	-	[60]
Consumption	Terminals : electricity	0.52 / 0	no	-	-	-	-	-	-	-	-	-	-	-	-	[61]
Consumption	CCUS : electricity	81.65	no	-	-	-	-	-	-	-	-	-	-	-	-	[62]
Consumption	CCUS : heat	66.59	no	-	-	-	-	-	-	-	-	-	-	-	-	[62]
Consumption	Shore Power	33.33	no	-	-	-	-	-	-	-	-	-	-	-	-	[63]

4

Results & Discussion

4.1. Introduction to Result Analysis

The result analysis starts with a detailed analysis of the optimized operation of the MMES in the normal case—characterized by average wind and solar availability—in Section 4.2, examining the dynamic interactions between electricity, natural gas, hydrogen, ammonia, and heat networks. Subsequently, the findings from the normal-scenario are compared with the other scenarios in Section 4.3, revealing how the system adapts to varying levels of renewable energy availability. Following, the sensitivity analysis on export volumes and carrier prices is presented and discussed in Section 4.4. From the executed analyses emerges the new operation strategy for the operation of MESs, that is further detailed in Section 4.5. While grounded in the MMES case, this strategy provides generalizable principles for the cost-effective operation of MESs in industrial clusters. Finally, Section 4.6 discusses the implications for operational planning, followed by a reflection on the results and the model limitations in Section 4.7.

4.2. Systems Analysis of the Normal-Case Scenario

The normal scenario results will be examined network by network, allowing for a focused analysis of each energy carrier network. However, given the high degree of integration among all networks in the MMES, other carriers will be referenced to describe cross-sector interactions and interdependencies. Each section begins with a high-level annual system analysis, before delving into more detailed operational patterns.

4.2.1. Electricity Network Operation

The annual operation of the electricity network is shown in Figure 4.1. This figure comprises two plots: a simplified representation of the annual generation dispatch and consumption of electricity, and a more detailed plot of the electricity generation mix.

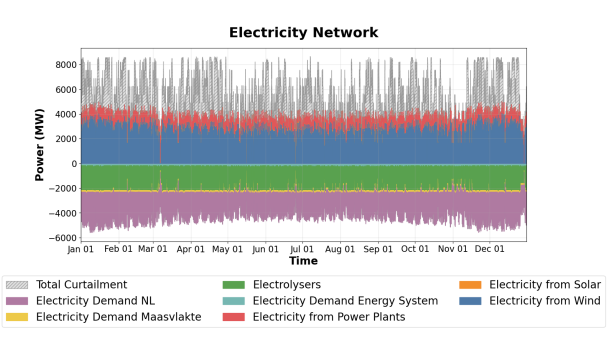

(a) Dispatch and Demand Balance*

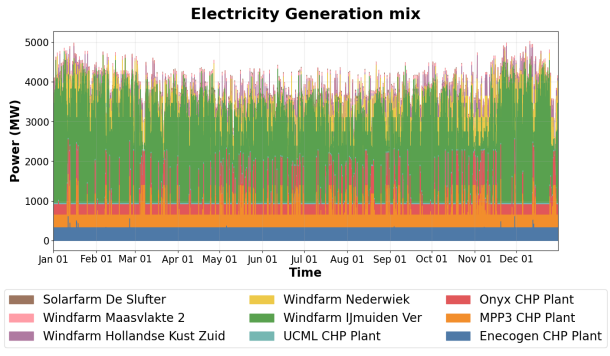

(b) Electricity Generation Mix

Figure 4.1: Annual power dispatch and demand (electricity network). (* Electricity Demand Energy System refers to electricity consumed by components within the electricity system itself, including conversion units and pipeline compressors).

As demonstrated in Figure 4.1a and 4.1b, the electricity system demonstrates a very strong reliance on offshore wind power generation, while solar power generation has such a small capacity that it appears negligible compared to wind power generation. Power plants generally operate at their minimum operating level (30% for

ammonia-fired power plants and 45% for hydrogen-fired power plants), only increasing their output when wind power generation falls short of meeting demand. As shown in Figure 4.1a, the Dutch electricity demand and electrolyzers' electricity demand account for the majority of electricity demand in the system. On an annual basis, Dutch electricity demand constitutes 50.55% of total electricity demand, while electrolyzers represent 43.67%. The remaining consumption is divided between industrial facilities at the Maasvlakte (3.12%) and the energy system itself (2.67%). Furthermore, an analysis of the data reveals that a considerable proportion of wind power is curtailed on an annual basis, as evidenced by the gray areas in the figure. Specifically, the amount is 44.82% per year. This finding indicates a potential for increased electricity use, particularly for hydrogen production via electrolysis—the only P2X technology in the system and thus best suited to absorb surplus electricity. However, any supplementary demand must remain flexible to avoid bottlenecks during low wind periods. Consequently, in scenarios where additional electrolyzers would be operational to benefit from the surplus renewable generation, it would be recommended to install them in conjunction with a battery system to ensure that the electrolyzers do not draw electricity from the grid during periods of low wind availability, as they require a minimum operational limit of 20% to maintain operational stability. From a system design perspective, expanding electrolysis capacity could replace the need of the ATR plant, moving the system toward zero-carbon configurations. In systems that incorporate other P2X technologies, these could also be considered for absorbing access renewable electricity that would otherwise be curtailed.

As evident in 4.1b, ammonia-fired power plants are preferred over hydrogen-fired power plants to generate power during periods of low wind power generation. This preference exists despite the higher inherent fuel cost of ammonia compared to hydrogen, suggesting that other economic factors influence this operational decision. A number of factors contribute to the economic advantage of ammonia as a fuel for power generation in this system:

1. First, ammonia is less resource-constraint than hydrogen due to high import volumes, independency of wind power generation, no competition with consumption, and variable export volumes.
2. Secondly, ammonia can be utilized directly as a fuel, whereas hydrogen (which is not inherently abundant in the system) requires cracking from ammonia, incurring additional costs.
3. Finally, the fixed operational costs of ammonia-fired plants are lower than those of hydrogen-fired power plants, as shown in Table 3.8.

Consequently, despite the higher fuel cost of ammonia, the total system cost is minimized by prioritizing ammonia-fired generation during periods of low renewable power generation.

4.2.1.1. Battery Storage; Dual Purpose Operation

The significance of battery storage, sized at 467 MWh, becomes particularly evident when examining a single month of operation. Figure 4.2 illustrates the dispatch and demand dynamics of the electricity network in January, demonstrating that the battery typically charges during nighttime hours (when electricity prices are lower) and discharges during daytime hours (when prices peak). This pattern corresponds directly to the volatility of electricity prices which is due to the inherent variability of solar and wind power generation combined with fluctuating demand patterns.

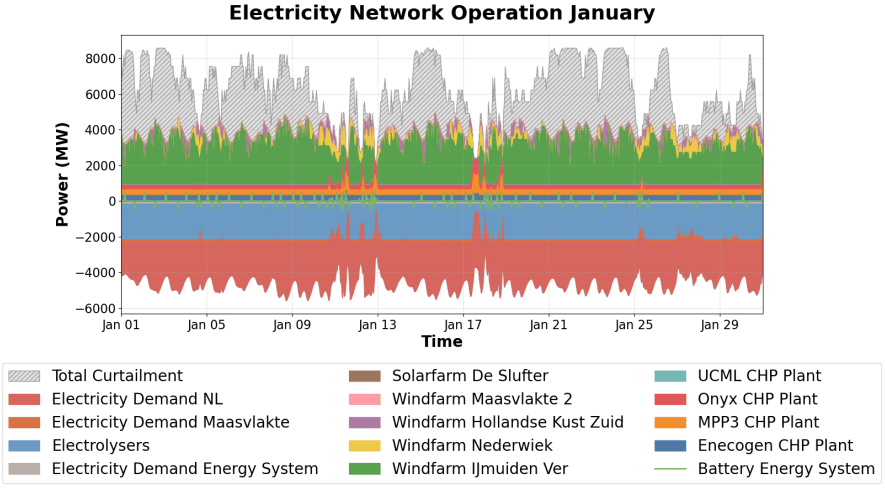

Figure 4.2: January's power dispatch and demand (electricity network)

A comprehensive analysis of yearly electricity prices reveals an average of 70 Euro/MWh, with significant extremes, reaching a maximum of 936.29 Euro/MWh during periods of minimal renewable generation and dropping to a minimum of -59.96 Euro/MWh during substantial electricity curtailment events. The price profile displays distinct diurnal patterns, with peak prices occurring twice daily: morning peaks (03:00-06:00, averaging 77.33 Eur/MWh) and afternoon peaks (15:00-18:00, averaging 103.54 Eur/MWh). These temporal price variations fundamentally shape the battery storage operation. As demonstrated in 4.3, a strong correlation exists between fluctuations in electricity prices and the cycle of battery charge and discharge. The battery strategically accumulates energy during periods of price drops and subsequently releases this stored energy during high-price intervals. This mechanism allows the system to utilize cheaper electricity during high-price periods, creating a financial advantage by exploiting price differences between different time periods.

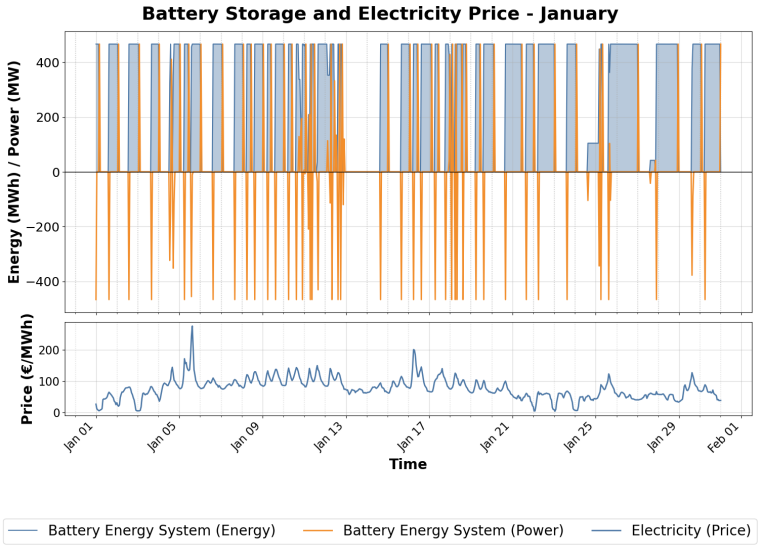

Figure 4.3: Correlation between battery storage and electricity price.

An important consideration is that the model employs fixed electricity prices without feedback mechanisms. In actual market conditions, this battery discharge behavior during high-price periods could reduce electricity market prices, creating a dampening effect on price volatility that isn't captured in the current model. Nevertheless, for batteries to significantly influence Dutch market prices, they would need to be large in capacity, likely significantly larger than the sized 467 MWh. This suggests that while batteries are indeed effective at balancing price fluctuations, they might be more advantageous within this context as components of consumer systems that directly benefit from low-cost electricity, rather than as elements of the electricity grid where prices are determined by the entire national system operation.

Another note is that Denmark's electricity mix reflects a significant dependence on wind power generation and the electricity modeled price profile is therefore related to the wind availability in Denmark for 2024. While Denmark and the Netherlands are geographically proximate, increasing the probability of similarities in wind patterns (especially in extreme cases), a direct hourly correlation between wind availability and electricity price is not fully captured in this study. To obtain more accurate insights into the interactions between wind availability, electricity price fluctuations, and battery operation, future research should examine electricity price data and wind speed measurements from the same geographical location and time period.

Besides functioning as a price-balancing mechanism, the network's operation in January also reveals that the storage system contributes to maintaining continuous power supply during periods of low renewable power generation. In these instances, the storage discharges in the absence of electricity curtailment and in the simultaneous increase of power generation from power plants, indicating that the battery supports continuous system operation during times of limited wind power generation. For example, this occurs on January 11 at 12:00.

Network operation: January 11, 12:00 On January 11 at 12:00, presented in Figure 4.4a, the combined output of the power plants reaches one of the highest levels recorded throughout the entire year, second only to November 29 at 19:00, which exceeds it by 0.5 MWh.

During this hour:

- Electricity generation from wind is 0 MWh.
- Despite the absence of wind power generation, electrolyzers continue to operate at 72% due to the hour-delay reaction time.
- The battery discharges its full energy capacity of 467 MWh.
- Ammonia-fired power plants operate at nominal capacity (1070 + 870 MWh(e)).
- Hydrogen-fired power plants operate below nominal capacity (36 + 610 MWh(e), which is 80% of rated capacity).
- The ATR plant's operations are reduced (897.6 MWh hydrogen output, which is 78% of nominal capacity) to decrease electricity consumption during periods of heightened electricity scarcity.
- The ammonia cracker operates at its maximum hydrogen delivery capacity (3803.85 MWh (H_2 LHV) output).
- The hydrogen storage tank discharges its full energy capacity of 467 MWh ((H_2 LHV)).
- The hydrogen underground storage doesn't supply any hydrogen to the system.

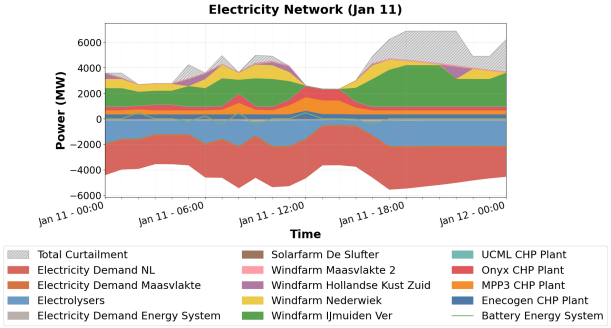

(a) Electricity network.

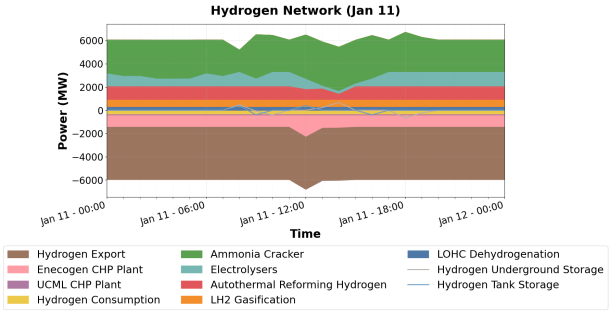

(b) Hydrogen network.

Figure 4.4: Daily power dispatch and demand for Januray 11.

It can be deduced from this hour's data that when wind power generation drops to zero, both batteries and power plants activate to address the electricity shortage. This shortage is further intensified by the one-hour delay in the operation of the electrolyzers, which means that they continue to consume significant amounts of electricity despite the absence of wind power. The function of both power plants and batteries is to ensure sufficient electricity supply to meet electricity consumption and export demand. The dispatch of ammonia power plants are prioritized before hydrogen-power plants and are operating at maximum capacity. When the batteries are fully discharged at their sized capacity, hydrogen only needs to operate at 80% of its capacity. The hydrogen deficits caused by reduced electrolysis and increased flow to hydrogen plants are compensated by hydrogen from storage and maximizing ammonia cracker operations. It is remarkable that the ATR is also subject to down scaling, despite the overall increasing hydrogen production demand and the plant's ability to supply hydrogen at the lowest marginal cost. This down scaling is presumably aimed at conserving electricity, given the ATR's electricity requirements in the production process. This demonstrates a strategic preference for down scaling this component, despite the increased demand for hydrogen production due to low electrolyzer output. Thus, in circumstances where electricity is in extreme shortage, there appears to be a preference for sourcing hydrogen from alternative sources (ammonia and storage), so that non-essential components that consume electricity can be reduced.

Network operation: January 29 19:00 It is interesting to compare this situation with the operational scenario observed on November 29 at 19:00, shown in Figure 4.5, which is almost similar to the observed situation on January 11th.

The only differences are that:

- Hydrogen power plants have a joint output of +0.5MWh more.
- The ATR plant operates at minimum operational capacity (228.3 MWh hydrogen output, which is 20% of nominal capacity).

- Hydrogen underground storage supplies hydrogen to the network at maximum supply rate (663 MWh (H_2 LHV)).

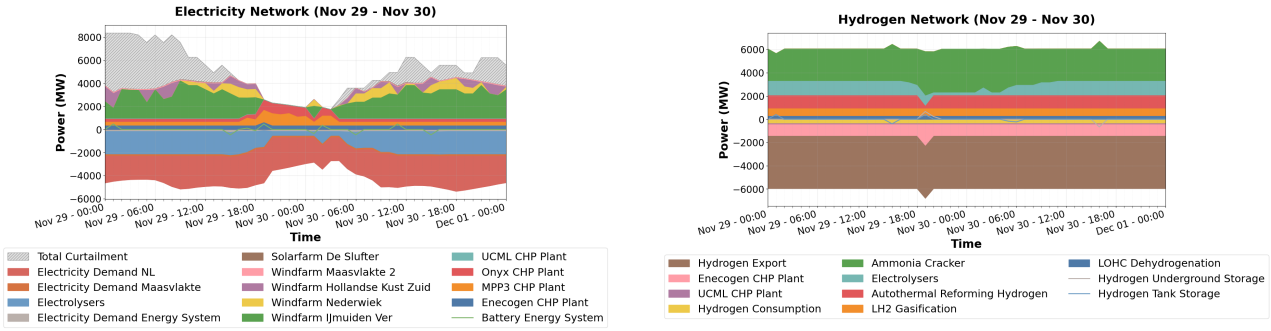

(a) Electricity network.

(b) Hydrogen network.

Figure 4.5: Daily power dispatch and demand for November 29-30.

Despite the operational similarities for these two situations, the system responds with distinct dispatch decisions. In this instance, the system opts for the complete shutdown of the ATR, extracting the maximum amount of hydrogen from the underground storage. This strategy is to maximise electricity savings while still meeting the hydrogen demand. The explanation for this difference lies the optimization method that uses perfect foresight. Rather than optimizing for each individual hour, the model delivers the most cost-effective solution across the entire annual simulation period. For example, on January 11 at 12:00, hydrogen extraction from underground storage was delayed until the following two hours when it was more cost-optimal, contrasting with the situation observed on November 29 at 19:00, when the underground hydrogen storage was almost completely emptied immediately.

Battery vs. hydrogen-fired power generation The analyzed scenarios reveal a trade-off between the battery's investment costs and its economical value to the system. The optimization process determines a battery capacity that maximizes cost-effectiveness by leveraging price differentials and providing power during critical shortage periods. It's noteworthy that the hydrogen-fired power plants consistently operate below their maximum capacity throughout the entire simulation period, meaning that they could operate more frequently to allow for a smaller battery capacity. However, this approach appears not cost-optimal for the system as a whole as it would reduce price balancing profits. This further illustrates the cost balance between battery investment costs and the benefits of price balancing.

It is important to note, however, that the model's hourly time resolution assumes uniform response times across all networks (except for those with specific ramp rate constraints, which few technologies maintain over a full hour). In reality, chemical processes like combustion for power generation typically respond more slowly than batteries, making them less flexible than the model suggests. During brief periods of rapid electricity shortage, batteries would likely need to bridge the gap until CHP plants could fully ramp up. This temporal mismatch means that real-world battery capacity requirements would probably exceed model predictions to account for the varying reaction speeds of different technologies, particularly when conversion components involving chemical reactions cannot immediately adjust their output to changing conditions.

4.2.1.2. Effect of Perfect Foresight

The comparison between the two situations on January 11 and January 29 demonstrates how perfect foresight enables strategic storage management based on anticipated future conditions. In real-life systems without perfect foresight, storages would likely be emptied when demand for it occurs. Such operation could lead to shortages in subsequent periods, as demonstrated in the January 11 scenario, where the ATR would be constrained to minimum capacity while the ammonia cracker would already be at maximum capacity in the following two hours. Systems operating without perfect foresight would therefore require additional hydrogen and battery storage capacity. This underscores the importance of incorporating reserve margins for storage systems to account for the perfect foresight assumption in the modeling approach.

4.2.1.3. Effect of Non-Essential Loads

The availability of flexible, non-essential loads could play a beneficial role in enhancing the cost-effectiveness and flexibility of the energy system during periods of electricity scarcity. This conclusion emerges from observations that the ATR is ramped down during periods of electricity scarcity. In these periods, when hydrogen is

available in storage systems while electricity becomes scarce (particularly due to significantly reduced wind power generation), it appears more cost-effective to fully ramp down non-essential electrical loads (in this case, the ATR plant) and withdraw the necessary hydrogen from storage. This approach conserves electricity directly by reducing consumption rather than increasing production through hydrogen-fired power plants or investing in additional battery capacity, proving it more economical to preserve electricity by deactivating the ATR plant and utilizing stored hydrogen than to expand electricity generation capabilities. This suggests that DSM in the power network represents a valuable additional integration option, as it enables the strategic reduction of non-essential loads precisely when needed to maintain system balance without disrupting other network operations.

4.2.2. Hydrogen Network: Key Enabler to Decarbonize Industrial Consumption

The hydrogen network operation, Figure 4.6, reveals the constant import and export capacities, the near-constant hydrogen production from the ATR plant, and the baseline hydrogen supply to the hydrogen-fired power plants for their minimum operation requirement. During system equilibrium (i.e. no storage activity) with maximum electrolyzer and ATR operation, the base hydrogen demand (i.e. fixed minimum requirement for hydrogen-fired power plants, fixed hydrogen consumption at Maasvlakte and fixed hydrogen export volumes) is met through multiple sources: 14% from imports (10% LH_2 and 4% LOHC), 19% from natural gas autothermal reforming, 21% from electrolyzers, and 46% from ammonia cracking.

Fluctuations in electrolyzers' hydrogen production—following the IJmuiden Ver wind farm's power generation profile—create variable production patterns throughout the system. The ammonia cracker operates with flexibility while maintaining a near-constant minimum capacity of 2774 MW (72% of rated capacity) to meet the base hydrogen demand. Its production increases to fill hydrogen storages, support additional hydrogen-fired power generation, or compensate during periods of reduced hydrogen output from electrolyzers and/or the ATR plant.

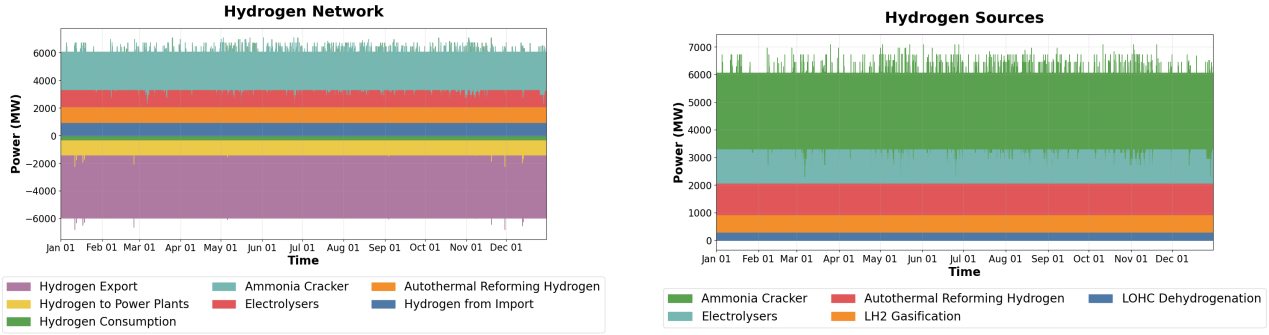

(a) Dispatch and demand balance.

(b) Hydrogen production mix.

Figure 4.6: Annual power dispatch and demand (hydrogen network).

4.2.2.1. Hydrogen Storage; Critical Balancing Role

The hydrogen storage systems are of critical importance in ensuring the balance of supply and demand during periods of reduced hydrogen production. This is achieved by ensuring that both industrial consumption and export requirements are reliably met, while also generating electricity when necessary. This function assumes particular importance during periods of low wind, when the ammonia cracker's capacity is inadequate to compensate for production shortfalls, necessitating alternative hydrogen sources. A notable paradox exists where hydrogen shortages often coincide with electricity deficits that reduce electrolysis output, yet hydrogen is precisely what's needed to address these electricity shortages by fueling power plants. This is due to the dependence of both processes on wind availability. This creates a challenging dynamic where hydrogen production decreases while its demand increases, highlighting the essential role of storage facilities in maintaining continuous operation under fluctuating conditions.

Again, the storage operation becomes more apparent when examining system operation at a monthly scale. Looking at January's operation, it can be seen that the hydrogen storage systems charge itself when ammonia crackers increase their hydrogen production. Conversely, during periods of low hydrogen production (i.e. low electrolyzer output and/or low ATR output), the storage is discharged to ensure that the demand for hydrogen is still met and that hydrogen demand does not have to be shedded.

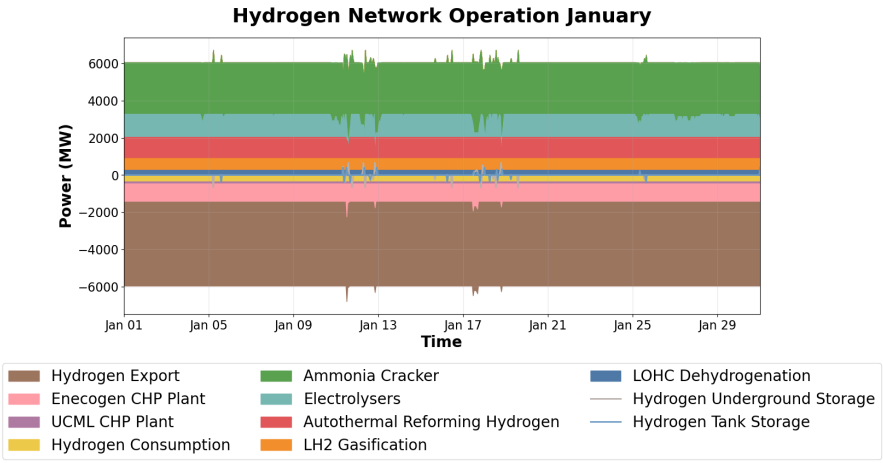

Figure 4.7: January's power dispatch and demand (hydrogen network).

The underground storage has gained a higher nominal capacity of 898 MWh in the optimization compared to the tank storage with an optimized capacity of 397 MWh. This is due to the higher costs of tank storages. Nevertheless, the tank storage still has a significant nominal capacity, as the underground storage is limited by injection and production rates. Once this limit is reached, the tank storage is used to meet the remaining demand for hydrogen. The utilization and capacity of tank storage is thus dependent on the operating limits of the underground storage. The model incorporates average hourly injection and production limits based on daily parameters—meaning the hourly rates used in the model are derived by dividing daily maximum rates by 24 hours. In reality, underground storage facilities typically have the flexibility to exceed these average hourly rates for short periods, as long as the total daily limit isn't exceeded. The model shows these hourly limits are typically reached for only a few consecutive hours at a time. This observation suggests that, in practical applications, the utilization of tank storage may be unnecessary, as the actual underground storage system could temporarily exceed the modeled hourly rates to handle short-term peaks, while still remaining within daily operational constraints. It is also necessary to note that the model assumes a maximum storage capacity of 200 GWh per underground cavern. When considering multiple caverns, the injection/production rate of hydrogen in these storage systems would also multiply accordingly.

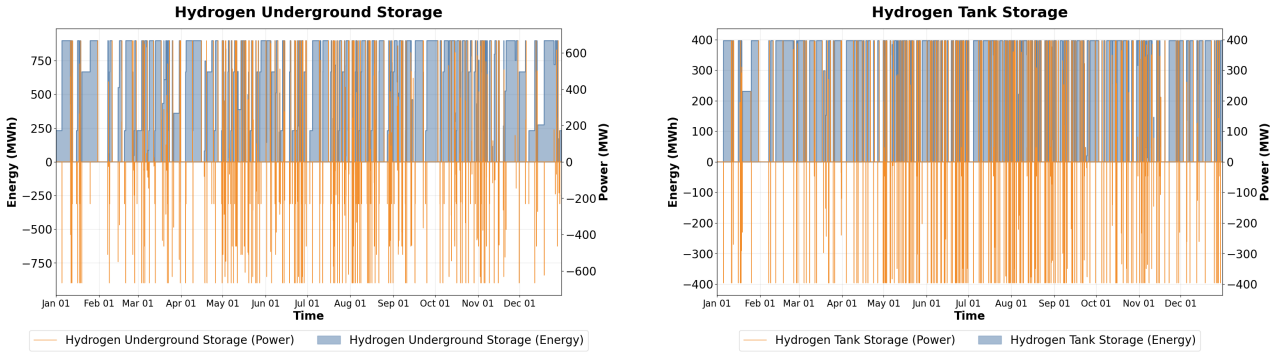

(a) Underground storage.

(b) Tank storage.

Figure 4.8: Power dispatch and energy storage of hydrogen storages.

4.2.2.2. Dynamic Operation of Hydrogen Production

The hydrogen network demonstrates a continuous dynamic operation by balancing between multiple sources of hydrogen production (fixed and variable) and storage systems. With the goal of continuously meeting the fixed hydrogen demand (consumption, export and minimum operation supply to power plants) and meeting the variable hydrogen demand for increasing electricity generation. The operation is characterized as follows;

1. **Base hydrogen supply establishment:** The base hydrogen demand consists of the fixed hydrogen consumption at the Maasvlakte, fixed export volume, and fuel supply for the minimal operation of hydrogen-fired power plants. When the system is in equilibrium (no storage charging or discharging), this baseline

demand is met by the full capacity of fixed hydrogen imports, the variable output of electrolyzers (following the IJmuiden Ver wind farm profile), continuous operation of the ATR plant, and the ammonia cracker (operating at a minimum threshold of approximately 72% when electrolyzers and ATR output is both 100%) to supply any remaining hydrogen needs.

2. **Dynamic scarcity response:** During periods of reduced hydrogen availability (typically coinciding with low wind conditions), multiple factors contribute to the hydrogen deficit:
   - Reduced hydrogen production from electrolyzers due to low wind power generation.
   - Potential reduction in ATR hydrogen production to conserve electricity during grid scarcity.
   - Elevated hydrogen demand from hydrogen-fired power plants responding to electricity shortages.

   The system's response to these conditions is not hierarchical but rather dynamic, with dispatch decisions based on system conditions and resource availability. The range of available responses encompasses the augmentation of ammonia cracker operation and the strategic discharge from both underground and tank storage systems. The specific deployment of these responses is determined by overall system optimization.
3. **Strategic storage management** hydrogen storage systems function strategically rather than in a fixed hierarchy. The primary storage medium is underground storage due to its cost efficiency. The capacity of tank storage is sized to accommodate hydrogen demand when the limits on underground storage injection/production are reached. Both storage systems are capable of independent charging and discharging, based on system-wide optimization. Storage primarily functions as a means of charging during periods of hydrogen surplus, which is typically the result of increased ammonia cracking.

Effect of fixed carrier prices The integration of multiple hydrogen production pathways introduces significant operational flexibility, thereby enabling the energy system to adapt dynamically to varying conditions. However, this analysis has not accounted for the feedback effects between production pathway selection and hydrogen pricing mechanisms. HyXchange research indicates substantial price variations in hydrogen for the different production pathways: for example, hydrogen cracked from blue ammonia (55.5 Eur/MWh H2 (LHV)), hydrogen cracked from green ammonia (88.0 Eur/MWh H2 (LHV)) and the electrolyzer following the market-based dispatch price [69]. The current modeling approach uses fixed hydrogen market prices throughout the year, which does not capture the price variation that would occur when switching between production pathways. This limitation assumes particular relevance during periods when the decision is taken to reduce the output of the ATR plant in order to minimize electricity consumption. In real-world conditions, the reduction of blue hydrogen production during periods of electricity and hydrogen scarcity would likely trigger significant price increases in the hydrogen market. Consequently, such increases would result in elevated costs of hydrogen-based power generation and hydrogen consumption. Consequently, the continuation of blue hydrogen production during periods of scarcity may prove to be a more economically viable strategy compared to the model's projections.

As mentioned in the previous section, the system prefers, and thus finds it more economical, to scale down electricity supply to non-essential loads during electricity shortages, rather than further increasing battery storage or hydrogen-based power generation. In this model, the system considers the ATR plant as a non-essential load. However, as previously argued, the model's projections do not account for how scaling down the ATR plant affects hydrogen prices, suggesting that it might be more economically beneficial to maintain operations than the model predicts. To ensure the ATR plant can continue operating—thereby providing affordable hydrogen and maintaining relatively stable and low hydrogen prices—while still benefiting from the relatively cost-effective electricity savings achieved through scaling down non-essential loads, a potential solution would be to focus on loads where this has been explicitly agreed upon, essentially loads operating under DR or DSM arrangements, a viable solution which is also presented in section 4.2.1. This approach would enable targeted load reductions without disrupting low-cost hydrogen supply. By incorporating contractual flexibility into load prioritization, the system can better navigate the interplay between electricity conservation and hydrogen market dynamics, ultimately resulting in a more economically optimized energy system that accounts for cross-sectoral price dynamics.

4.2.3. Ammonia Network; Key Flexibility Provider

As can be seen from Figure 4.9, the operations within the ammonia network are centered around a single source of inflow, which is ammonia import with an import capacity of 6489 MW (NH_3 (LHV)). The imported

ammonia is then either directed to the ammonia tank storage, utilized for hydrogen production through ammonia cracking, sent to ammonia-fired power plants for electricity generation, or exported. The export volumes are variable and appear to be adjusted according to the availability of surplus ammonia.

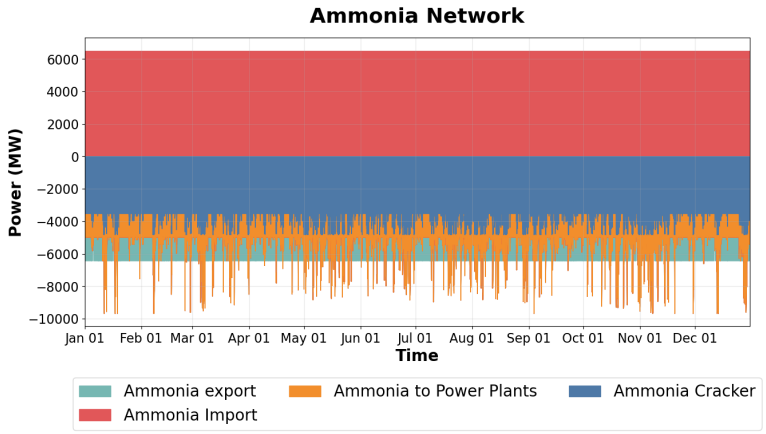

Figure 4.9: Annual power dispatch and demand (ammonia network).

The ammonia cracker maintains a near-constant minimum operation at 72% of its rated capacity. At this operational level, the cracker provides precisely enough hydrogen to meet system demand when electrolyzers and ATR operate at 100%, hydrogen storages are balanced (neither consuming nor supplying), and the hydrogen-fired power plants run at minimum load. The cracker functions below this 72% threshold in only 2% of instances, specifically during periods when ammonia is prioritized for power plant electricity generation and the system draws hydrogen from the hydrogen storages instead. Conversely, the cracker can always increase output to 100% by utilizing ammonia that would otherwise be exported, indicating that ammonia storage is exclusively reserved for supplying ammonia to power plants when required. This operational pattern underscores the role of ammonia storage in maintaining sufficient ammonia supply for power generation during periods of low electricity availability.

4.2.3.1. Ammonia Storage

A monthly examination of the ammonia system (Figure 4.10) reveals that ammonia storage, optimized at a nominal capacity of 83 GWh, functions to supply large volumes of ammonia to power plants during periods of low wind power generation when electricity must be produced through power plants. This is evident from the pattern where ammonia charges during periods without elevated cracker and/or power plant consumption, then fully discharges when power plants require ammonia. Figure 4.11 illustrates that the ammonia storages gradually charge over time, followed by periods of rapid, full discharge. These discharges coincide with electricity shortages, during which large amounts of ammonia are required for power generation. Occasional partial discharges also occur meanwhile.

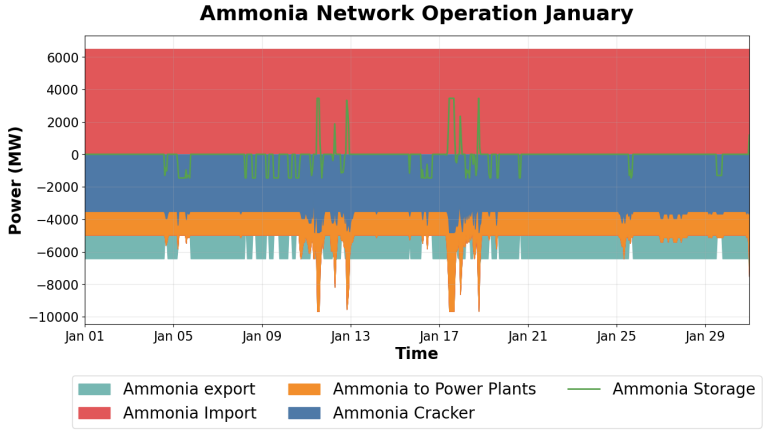

Figure 4.10: January's power dispatch and demand (ammonia network).

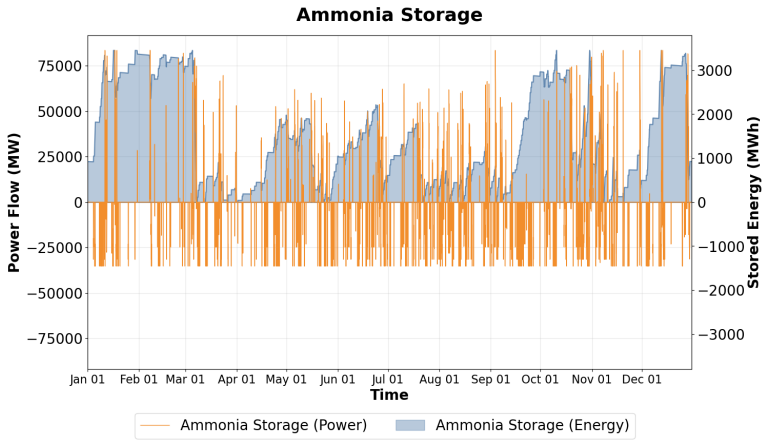

Figure 4.11: Power dispatch and energy storage of ammonia storage.

While the storage capacity of 83 GWh may appear substantial compared to the other storage sizes, it falls within technically feasible ranges, as evidenced by the largest ammonia storage tank currently under construction in the Port of Rotterdam with a 60,000-tonne capacity (equivalent to approximately 310 GWh in NH_3 LHV) and a 72-meter diameter [125]. However, the Maasvlakte's spatial constraints may limit such expansive above-ground storage solutions. Underground storage of ammonia, increasingly explored in literature, offers a potential alternative. Research conducted by Geostock [126], for instance, demonstrates that underground ammonia storage, specifically in lined rock caverns, presents a significant opportunity for commercialization.

4.2.3.2. Flexibility Roles of Ammonia

The ammonia network represents a critical flexibility mechanism within the MMES. With a constant import rate at large volumes, the system distributes ammonia four pathways based on system conditions:

1. **Hydrogen production with dynamic adjustment:** The ammonia cracker maintains a minimum 72% capacity operation to provide baseline hydrogen supply, complementing electrolyzers and ATR production. This operating level is reduced only during the 2% of periods when electricity generation fueled by ammonia takes priority. Conversely, the cracker increases to 100% capacity when additional hydrogen is required—whether to fill hydrogen storage reserves, compensate for reduced electrolyzer/ATR output during electricity scarcity, or supply hydrogen power plants during peak electricity demand. This flexibility ensures hydrogen availability even when primary production methods are constrained.
2. **Electricity production with dynamic adjustment:** Ammonia is continuously supplied to CHP plants to maintain their minimum operational requirements, thereby providing a base load electricity and heat supply. During periods of low wind, additional ammonia is directed to ammonia-fired CHP plants to balance the power system, taking precedence over ammonia export. The system prioritizes meeting electricity demand over maximizing export revenue.
3. **Strategic storage management:** Ammonia storage accumulates during periods of surplus ammonia, taking precedence over export, and (fully) discharges when power plants require ammonia for electricity generation.
4. **Variable export as balancing mechanism:** Export volumes function as the system's flexible variable, adjusting based on internal system requirements rather than fixed export commitments.

What significantly contributes to ammonia's flexibility is that, in contrast to electricity and hydrogen, its availability is not dependent on wind conditions as it is fully imported. This import-based and thus non-intermittent supply enables continuous energy provision and essential flexibility when electricity production and hydrogen generation decreases due to reduced power generation from wind farms and the resulting diminished electrolyzer production. This characteristic enables ammonia to serve as a dependable energy carrier during periods of renewable intermittency, effectively bridging supply gaps and maintaining continuous system operation when weather-dependent resources under perform. However, it is important to note that if the cost structures of the imported hydrogen carriers—LOHC or LH_2—become more favorable in the future, these import pathways could also play a similar stabilizing role. As such, ongoing evaluation of carrier economics is essential for operational planning.

4.2.3.3. Comparison Alternative Non-Intermittent Energy Carriers

Other possible alternative energy carriers not examined in this study, yet also independent of wind availability, include biomass and nuclear energy. As with ammonia, biomass has the ability for balancing intermittency across both electricity and hydrogen networks through biomass-fueled power generation and gasification. Whilst these processes do emit CO_2, biomass is generally considered to be carbon-neutral, given that the CO_2 released during combustion is counterbalanced by carbon sequestration during plant growth. Nevertheless, the question of the environmental acceptability of biomass remains a subject of debate when placed in contrast with carbon-free ammonia. Carbon capture technologies could potentially mitigate the emissions in these processes, however, this results in increased costs and system complexity. In addition, biomass is a scarce resource and its large-scale use is frequently constrained by negative impacts on ecosystems, such as deforestation, soil degradation, and loss of biodiversity. Moreover, biomass production often competes with other land uses, including food production and nature conservation.

Nuclear energy is widely recognized for its ability to deliver continuous baseload power; however, it can be considered less suitable for directly addressing intermittency, as most nuclear plants are engineered for constant rather than flexible output. Small Modular Reactors (SMRs), which are currently under development, offer greater potential for flexible operation and could contribute to balancing variable electricity supply. Still, the high capital costs associated with nuclear power renders it less advantageous for variable operation. This limitation assumes even greater significance when nuclear electricity is utilized for the variable production of hydrogen via electrolysis. While this is a technically feasible pathway, it is economically challenging due to the substantial investment required for both nuclear infrastructure and electrolyzer systems. Additionally, although nuclear electricity is not associated with CO_2 emissions, it produces nuclear waste, which remains a significant disadvantage compared to green fuels that produce neither emissions nor long-lived waste streams.

Both ammonia and biomass could have the technical and economical potential to contribute to the integrated stabilization of electricity and hydrogen networks, thereby providing flexibility to MESs. Ammonia offers a significant advantage due to its established use as a feedstock. This results in the already established presence of large-scale production chains and commercial technologies. Furthermore, ammonia provides a substantial benefit as a zero-carbon solution and is not subject to additional constraints on ecosystems or competition with land use. A notable benefit of biomass is its non-hazardous nature, which significantly reduces safety concerns in comparison to ammonia. Given the considerable risks associated with large-scale storage and transportation of ammonia, as it is considered highly toxic. It is thus recommended that subsequent research undertake in-depth comparative analyses of ammonia and biomass. These analyses should evaluate economic parameters, technological maturity, safety profiles, environmental assessment, and policy frameworks.

4.2.4. Natural Gas Network; Import Hub Function

The operation of the natural gas network is shown in Figure 4.12. Natural gas is imported at a constant rate from the Maasvlakte LNG hub, where it serves two primary purposes: hydrogen production through autothermal reforming (ATR) and export to the national gas grid. The majority of imported LNG is directed to the national grid, with only a small portion allocated to the ATR process. This distribution pattern establishes Maasvlakte primarily as a gateway facility to the wider national gas infrastructure, ensuring that natural gas availability remains guaranteed throughout the year regardless of local energy system operations.

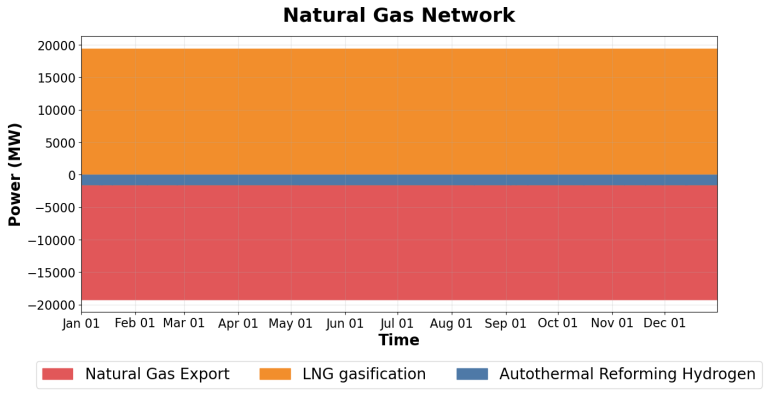

Figure 4.12: Annual power dispatch and demand (natural gas network).

The ATR plant generally operates at or near its maximum capacity due to the low marginal cost of hydrogen

production from natural gas. However, it sporadically reduces output during periods of low wind availability (3% of the instances within the whole year), when electricity becomes scarce in the system. This operational pattern aligns with the technical characteristics of the ATR process, which requires both natural gas and electricity as inputs. So in response to electricity shortages, the system prioritizes the use of previously stored hydrogen over continued production via ATR. This could possibly also have an economical cause, as electricity prices during electricity scarcity, and thus ATR ramp-down periods, typically increase significantly—ranging from 0.8 to 13 times the average price, with a mean approximately three times higher than baseline. So when electricity prices become high, it is better to ramp down the more expensive operation of the ATR, thereby conserving electricity and improving system costs under conditions of high electricity prices compared to operating the ATR under constrained power conditions.

However, as previously noted in Section 4.2.1, the model does not account for the potential impacts that ramping down the ATR plant could have on hydrogen prices, so also not when taking into account what effect spikes in electricity prices have on the production costs of hydrogen. However, this requires a more nuanced perspective, as often in industrial power agreements, plants operate under fixed-price contracts, which is common for large industrial consumers. Under that consideration, continuous operation would likely be more economical. Conversely, with significant electricity price fluctuations, particularly during extreme price spikes, and under dynamic pricing contracts, the ATR plant would likely reduce hydrogen production as increased power costs would indirectly lead to elevated hydrogen prices. Unfortunately, this cannot be captured by the current model as it does not include the influence that prices and production pathways have on the real-time market price, since the market price is already predetermined.

4.2.5. Heat network Operation; Baseline Supply Potential

As illustrated in the Figure 4.13, the heat system demonstrates a predominantly linear operating pattern. Residual heat from industries at the Maasvlakte is fed into the Warmtelinq district heating network and delivered to potential consumers, which include residential, commercial, and agricultural buildings. The results provide an approximate quantification of the thermal energy that can be delivered from the Maasvlakte to this network.

As can be seen from the figure, the MMES provides a relatively constant heat generation, which could effectively serve as a baseline thermal input to the Warmtelinq heat network. However, it should be noted that the Maasvlakte industrial sector itself derives limited benefit from the 120°C heat network, with the exception of the relatively small heat requirement for CCUS systems. This is because industrial processes in the Maasvlakte predominantly require high-temperature heat of approximately 400°C. The district heating network therefore primarily enhances energy efficiency through waste heat utilization rather than providing significant integration or flexibility options for the overall energy system operation.

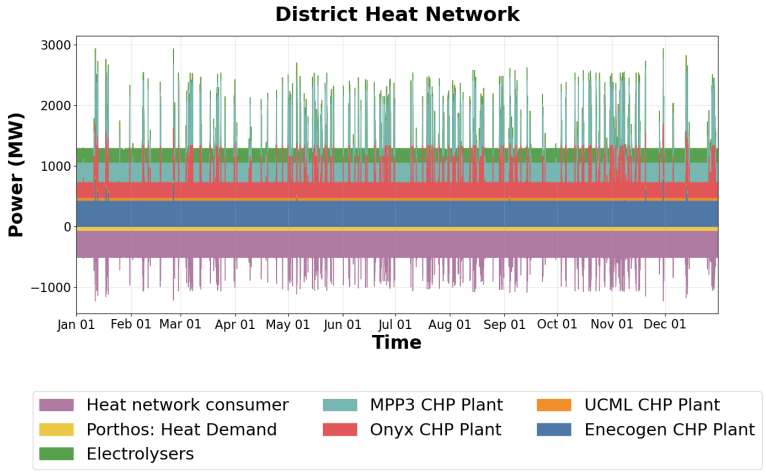

Figure 4.13: Annual power dispatch and demand (heat network).

To develop a more integrated heat system with greater flexibility potential, future research should focus on high-temperature heat networks that better align with actual industrial heat requirements at the Maasvlakte. Additionally, these high-temperature heat systems could incorporate technologies such as electric boilers coupled with thermal storage and steam turbines to introduce valuable electricity grid flexibility on system level. Such configurations would enable electricity-to-heat-to-electricity conversion pathways, creating bidirectional

flexibility that the current low-temperature district heating network cannot provide. A comprehensive analysis of high-temperature heat interactions could thus also provide valuable insights into potential synergies between industrial steam requirements, high-temperature waste heat utilization, and integration with other networks at the Maasvlakte. Nevertheless, interactions within high-temperature heat network are generally based on cooperation among industries that is regulated by confidential contracts and private data. This complicates the development of integrated system modeling and open data analysis for these networks.

For the studied district heating network, thermal storage systems could further optimize this infrastructure by mitigating the peaks in heat supply that typically occur when CHP plants increase production for electricity generation purposes. Additionally, given that heat demand in buildings is largely seasonal, seasonal thermal storage solutions could facilitate the matching of baseline supply and seasonal demand consumption patterns. Therefore, further research into this heat network could comprehensively analyze the waste heat potential and external demand patterns, specifically assessing the storage requirements to balance seasonal variations.

4.3. Scenario Comparison

To assess the operation of the system under different weather conditions, three scenarios were developed: the normal-case, the worst-case, and the best-case scenario. These scenarios vary in wind and solar availability, which directly affects renewable power generation. All other model parameters are held constant and storage capacities remained to be treated as optimization variables, allowing the system to adjust its storage needs in response to fluctuating renewable energy supply.

In order to draw comparisons between system operation under varying weather conditions, a set of key indicators was selected to reflect technical, operational, and economic performance. The analysis of windless period frequency and duration is indicative of discrepancies in the availability of renewable power generation. Optimized storage capacities illustrate the system's reliance on the flexibility provided by storages in each scenario, while the dispatch of ammonia- and hydrogen-fired power plants signifies the importance of flexible generation in balancing power supply. The evaluation of curtailment and load shedding provides insight into the renewable energy utilization potential and energy supply reliability of the system. The analysis of total system cost facilitates a comparative assessment of system costs.

Table 4.1: Scenario result comparison.

	Worst-Case	**Normal-Case**	**Best-Case**
Wind Resource Availability	Low	Medium	High
Average Annual Wind Speed [m/s]	5.5	6.8	9.1
Average Annual Solar Irradiance [W/m^2]	143.8	123.0	114.8
Frequency of Windless Hours [%]	20.5	7.6	0.5
Average Duration of a Windless Period [h]	5.2	4.0	2.4
Hydrogen Underground Storage Capacity [GWh]	1.5	0.9	0.7
Hydrogen Tank Storage Capacity [GWh]	0.2	0.4	0.9
Ammonia Storage Capacity [GWh]	311.2	83.5	11.4
Battery Storage Capacity [GWh]	0.9	0.5	0.2
Operation above min. Load - Ammonia CHP Plants [%]	28.7	14.0	2.9
Operation above min. Load - Hydrogen CHP Plants [%]	0.3	0.2	0.1
Renewable Electricity Curtailment [%]	38.8	44.8	53.0
Load Schedding - Electricity [MWh]	0	0	0
Load Schedding - Hydrogen [MWh]	0	0	0
Total System Cost [bln Euro]	34.1	34.0	33.4

Wind intermittency persists as a fundamental challenge across all scenarios despite the favorable wind conditions in the best-case scenario. The frequency and duration of windless periods decrease significantly as conditions improve—from over 20% of all hours with an average duration of 5.2 hours in the worst-case scenario to less than 1% with an average duration of 2.4 hours in the best-case scenario. This reduction translates to fewer instances requiring supplementary generation from power plants or energy discharge from batteries. Nevertheless, the energy system must still be designed with sufficient capacity to manage these inevitable periods of low wind availability, necessitating the integration of conversion and storage technologies even under the best wind conditions.

4.3.1. Storage Requirements

The results in Table 4.1 demonstrate that increasing wind availability leads to substantial shifts in system operation, with the most notable changes observed in the sizing, and thus requirement, of storage components. The diminishing need for batteries in improved wind scenarios directly results from less frequent and shorter periods of low wind power generation, rendering battery storage increasingly redundant as a balancing mechanism. Similarly, the reduced requirement for ammonia storage in better wind scenarios reflects the decreasing role of ammonia-fired power plants as dispatchable resources. Since ammonia is predominantly stored to meet electricity demand during low-wind events, the storage volume requirements decrease corresponding as these events become shorter and less frequent. This scaling aligns closely with the corresponding reduction in ammonia-fired CHP plant utilization observed across the scenarios.

A similar trend is observed for underground hydrogen storage. In the best-case scenario, the optimized storage capacity is equal to its maximum injection and production rate, rather than large volumetric storage. This indicates that hydrogen is primarily needed during short periods—often only one hour at a time—when power production from renewables temporarily drops. As a result, the system prioritizes rapid charge and discharge capability over long-duration hydrogen backup. This pattern reflects a shift from long-term backup capacity to short-term responsiveness as wind availability improves.

Interestingly, while both ammonia, batteries and underground hydrogen storage capacities decrease, hydrogen tank storage capacity increases with better wind conditions. This counterintuitive trend can be explained by the economic trade-off between power-efficient battery storage and more cost-efficient hydrogen tanks. In scenarios with frequent wind shortages, battery storage is favored due to its high power efficiency and no competition with hydrogen demands. However, in scenarios where wind deficits are rare but still occur, investing in underutilized battery capacity becomes economically inefficient. Instead, the model shifts towards hydrogen tanks, which offer lower-cost storage solutions suitable for infrequent shortages. This trade-off is exemplified in the best-case scenario, where hydrogen-fired power plants are briefly ramped up to full capacity during a single two-hour windless period (22 November, 10:00). This level of hydrogen CHP plant utilization is never reached in the other scenarios, reinforcing that hydrogen tank storage accompanied with hydrogen-fired power generation is preferred over battery storage for infrequent short-term backup purposes. Notably, ammonia-fired plants see a dramatic reduction in utilization from worst- to best-case (−89.9%), while hydrogen-fired plants decline more modestly (−60.7%), underscoring hydrogen's increasing role as a infrequent short-term balancing mechanism, in contrast to expanding battery capacity for this purpose. This indicates a storage shifting preference from worst- to best-case, from battery utilization toward hydrogen storage combined with hydrogen-fired power generation when additional electricity is needed. Nevertheless, across all scenarios, the system maintains a clear operational hierarchy regarding CHP plant utilization where hydrogen-fired power plants are only ramped up when ammonia-fired capacity reaches its maximum, demonstrating a consistent preference for ammonia-based generation as the primary dispatchable power source.

Need for reserve margins The scenario analysis demonstrates that the optimal system operation—particularly with respect to storage deployment—varies under different weather conditions. This variation is a direct consequence of the model's cost-minimizing optimization, which adjusts storage capacities in response to renewable availability. The increased storage capacity observed in the worst-case scenario suggests that reserve storage capacities should be considered to maintain continuous system operation under unfavorable conditions. Such additional capacity enables the system's operation to maintain continuous across a broad range of weather scenarios. Importantly, no load shedding occurred in any of the scenarios, underscoring that—when appropriately dimensioned—flexible storages can ensure continuous supply even under extreme weather conditions.

These findings directly address research question 2, as they show that the MMES responds to changing wind conditions by adjusting both the sizing and utilization of storage and power generation components. As electricity scarcity becomes less frequent in favorable scenarios, the system shifts away from battery storage and increasingly relies on hydrogen storage in combination with hydrogen-fired power plants for infrequent short-term power balancing. This analysis suggests that battery systems should be sized based on their frequency of use rather than maximum theoretical capacity needs, as dimensioning battery storage to handle regular, high-frequency balancing operations rather than rare extreme events maintains cost-optimal functionality. Despite the overall decrease in dispatchable generation, ammonia remains the dominant carrier for energy storage and power generation, highlighting the important role of ammonia as flexibility provider in all scenarios.

4.4. Sensitivity Analysis

As demonstrated in the preceding sections, the operation is primarily driven by two factors: marginal costs and resource availability. The scenario analysis has demonstrated how variations in weather conditions affect system operation through changes in renewable generation. However, in addition to meteorological uncertainty, there are several other variables whose future values are highly uncertain, yet may significantly impact both system costs and the availability of energy carriers. As such, the energy carrier (market) price is highly volatile and inherently difficult to predict, particularly over the long time horizons. This uncertainty is further compounded by the absence of mature, transparent market mechanisms for hydrogen and ammonia, which are yet to be established. Consequently, it is essential to understand how fluctuations in these prices affect system operation in order to develop a strategy that can adapt effectively to changing economic conditions.

In addition to market price uncertainty, export volumes of electricity and hydrogen also are subject to considerable uncertainty. For instance, CE Delft projected a total electricity demand of 143 TWh by 2030, yet reported a broad range between 122 and 173 TWh, reflecting significant variation across scenarios [67]. TenneT, in its high-ambition scenario, projected an even higher national electricity demand of up to 180 TWh in 2030 [65]. The hydrogen export volume used in this model is derived from the Connected Deep Green scenario developed by the Port of Rotterdam. While this estimate provides a plausible future outlook, it remains highly uncertain given the rapidly evolving role of hydrogen. The export volumes in question have a direct impact on the availability of electricity or hydrogen within the MMES, influencing both supply-side flexibility and infrastructure requirements. Consequently, this sensitivity analysis also investigates how variations in these export volumes affect overall system operation and the requirements for storage technologies.

The sensitivity analysis conducted in this study employs stepwise deterministic sensitivity analysis (DSA), whereby the effect of a model input is evaluated independently across multiple points throughout a plausible range, while all other input parameters are held constant at normal-case levels. This approach enables a precise evaluation and systematic comparison of the relative importance of different inputs. In contrast to conventional DSA, which tests only the extremes of parameter ranges, the stepwise approach examines multiple intermediate values with uniform steps to capture non-linear relationships and marginal effects [127]. The sensitivity analysis conducted varies over a range from -50% to +50%, with steps of 10%. Appendix K provides a visual representation of all sensitivity analyses in the form of heatmaps. In order to indicate the resulting impact on system outputs, the results are expressed as the percentual change relative to the normal-case scenario. However, an exception has been made with regard to the load shedding output, given that its value is zero in the normal-case, thereby precluding the calculation of a percentual change. Instead, load shedding is shown as a percentage of the total export demand.

4.4.1. Export Volume Sensitivity

Changes in the export volumes of hydrogen and electricity have the most significant impact on storage capacity and CHP plant operations. This direct impact of export volumes on storage capacity is understandable, as they affect the overall energy balance, which must remain in constant equilibrium. Interestingly, these changes in export volumes lead to relatively smaller adjustments in total system costs compared to changes in carrier price. This can be attributed to the fact that variations in storage system capacities represent a relatively small portion of the total energy system costs in the system, compared to carrier prices which affect marginal costs of operations.

In addition to the aforementioned observation, several clear, mostly linear relationships emerge between the changes in export volumes and the system outputs. For instance, all storage requirements increase with rising export demand, both for electricity and hydrogen. The specific storage technology that experiences the greatest effect of this depends on the export variable being adjusted. To reduce overall storage needs in the MMES, further investigation should therefore focus on potentially reducing export volumes. This could be accomplished by analyzing actual electricity export data to the Dutch grid rather than using scaled estimates, and by refining the expected hydrogen export to industry in the hinterland. Such adjustments could significantly decrease required storage capacities across all carriers, thereby reducing both investment costs and spatial constraints while maintaining system functionality.

4.4.2. Price Sensitivity

In contrast to the sensitivity analysis on export volumes, variations in carrier prices—hydrogen, electricity, or ammonia—exhibit a comparatively limited effect on storage capacity and CHP operation. However, they exert a more significant influence on total system costs, which remain comparatively stable under volume sensitivities. This is due to the fact that carrier prices have a significant impact on the marginal costs of many

components throughout the system, resulting in a more substantial cost impact than that of isolated changes in storage investment. It is important to note that this relationship is only observed in the absence of load shedding. When load shedding occurs—particularly under high hydrogen export volumes—system costs rise sharply due to the high penalties associated with unmet demand.

Additionally, the finding that price variability exerts limited influence on storage capacities and dispatch decisions of CHP plants, while export volume variations lead to significant changes, reinforces the notion that resource availability serves as one of the primary drivers of system operation, as discussed earlier in this section.

Clear relationships emerge between carrier price variations and system behavior. In particular, changes in the electricity prices affect the relative distribution between different storage capacities, rather than causing a uniform scaling effect across all storage types. For example, at lower electricity prices, underground hydrogen storage is preferred over tank storage. As electricity prices rise, underground hydrogen storage remains relatively stable, while battery storage increases and hydrogen tank storage decreases. This illustrates a non-linear behavior of the hydrogen tank storage, which declines with both lower and higher electricity prices compared to the normal case. These dynamics clearly demonstrate that the preferred type of storage is sensitive to electricity price variations. Ammonia price variations influence the balance between hydrogen tank storage and battery storage, with lower ammonia prices favoring power generation via hydrogen-fired power plants instead of batteries. This occurs because lower ammonia prices make hydrogen production from ammonia cheaper, which in turn reduces the cost of hydrogen-based power generation, creating a preference shift relative to battery usage—though ammonia for power generation still remains preferred over hydrogen for power generation. Similarly, hydrogen price differences alter the ratio between battery and hydrogen tank storage (though to a lesser extent than ammonia price effects), with low hydrogen prices favoring generation through hydrogen-fired power plants and high hydrogen prices increasing the preference for battery storage.

4.5. System Operation Strategy

This section outlines the new system operation strategy for the operation of industrial MESs, derived from the MMES's optimal operation under perfect foresight and seamless collaboration among all stakeholders. While such conditions are unattainable in reality, the resulting operation strategy serves as a strategic blueprint for how industrial clusters can organize system operation in a cost-optimal and flexibility-oriented manner. The section begins by introducing the core principles that underpin the strategy in Section 4.5.1. It then details the structure and logic of the operation strategy itself in Section 4.5.2, including explanation on how the strategy is derived from the model's optimal operation results. Section 4.5.3, discusses the broader implications of the strategy and highlights how it fundamentally differs from conventional system operation strategies. Finally, Section 4.5.4 outlines how the proposed operation strategy addresses the barriers to industrial cluster decarbonization, which were introduced in Section 1.2.

4.5.1. Core Operational Principles

The new operation strategy developed in this research redefines conventional single-carrier operation by implementing four core principles. First, it emphasizes cross-sector economic optimization, wherein intersectoral synergies are exploited between energy carrier networks, rather than optimizing each network in isolation. Second, the dispatch strategy is dynamically responsive, moving away from static and decoupled control structures. Instead, it adapts in real-time to fluctuations in system states—such as renewable availability, storage levels, and carrier prices—thereby enhancing cost-effective and continuous operation and operational flexibility. Third, the approach enhances cross-sectoral flexibility which is enabled by conversion, the multifunctional roles of hydrogen and ammonia, and storage technologies. The flexibility provided by this ensures energy availability even during extended periods of low renewable energy generation, thus protecting system's continuity under stress. Finally, the strategy prioritizes industrial energy consumption by ensuring an uninterrupted energy supply to local industrial consumers under all dispatch conditions. In doing so, the strategy explicitly recognizes energy reliability as a prerequisite for maintaining industrial competitiveness in industrial clusters. Together, these principles establish the basis for industrial MES operation in which cost-effectiveness, dynamic dispatch decisions, operational flexibility, and continuous energy supply to industrial consumers are treated as pillars of the optimal system operation.

4.5.2. Operation Logic

The new system operation strategy for MES in industrial clusters, involving the five energy carriers—electricity, hydrogen, ammonia, natural gas, and heat—is presented using decision trees that illustrate the operation or

dispatch logic in each network. These decision structures form the foundation of the system's operational decisions and reflect how the system responds to varying demand and supply conditions across all energy carriers networks.

The electricity and hydrogen networks are shown together in a single, integrated decision tree in Figure 4.14, while the ammonia, natural gas, and heat networks are represented individually in separate decision trees in Figures 4.15, 4.16, 4.17, respectively. This structure reflects the distinct roles and levels of interdependence among the networks in the MES. The integrated representation of the electricity and hydrogen network reflects their strong interdependence in technical operation. They are the only carriers subject to fixed consumption and export profiles in the MES, which imposes strict demand constraints that must be balanced in every time step. In addition, they are both subject to wind intermittency and their operations are directly interlinked through electrolyzers and hydrogen-fired CHP plants. As a result, their dispatch decisions must be coordinated, and a shared decision logic is required to capture their mutual influence. In contrast, natural gas, ammonia, and heat are not subject to rigid demand constraints and are also not bound to intermittent or variable import, and thus do not typically act as limiting factors in the system's operation. Therefore, while the natural gas, ammonia, and heat networks are fully integrated into the overall MES operation, they are represented in separate decision structures, as function to support the operation logic for balancing supply and demand in the electrical and hydrogen network.

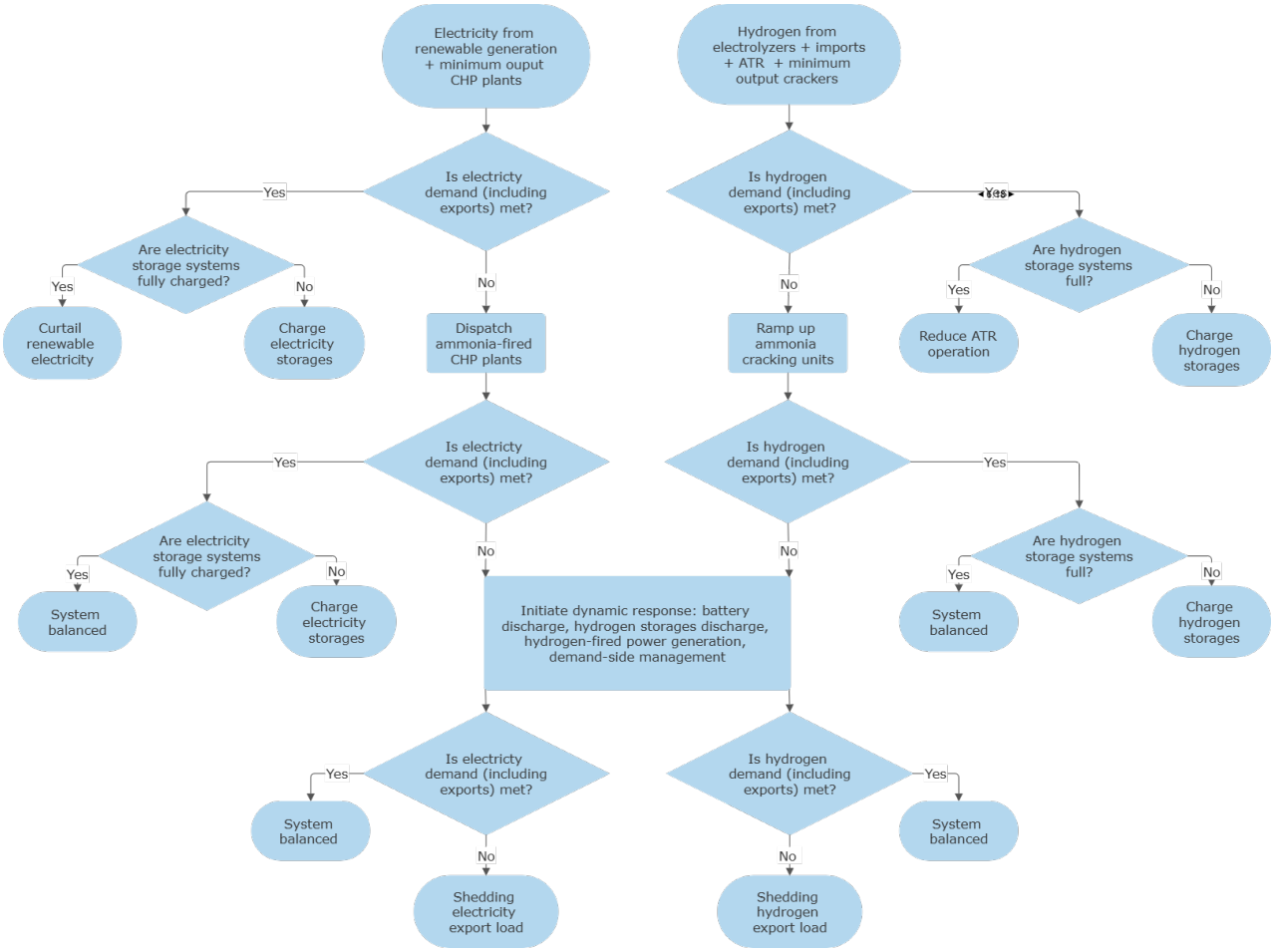

Figure 4.14: Operation logic in electricity and hydrogen networks.

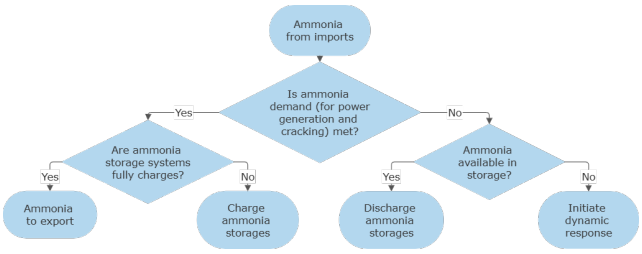

Figure 4.15: Operation logic in ammonia network.

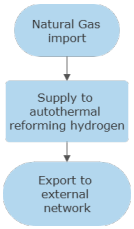

Figure 4.16: Operation logic in nat. gas network.

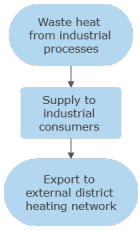

Figure 4.17: Operation logic in heat network.

4.5.2.1. Derivation of Operation Logic from Modeling Results

The operation strategy is derived directly from the optimization results of the modeled MMES. This section explains how the observed results are translated into the presented operation strategy and its underlying operation logic.

The observed modeling results demonstrate a clear prioritization of renewable power generation from wind and solar, due to their zero marginal costs. The electrolyzer operation is tightly coupled to wind power generation to ensure the generation of renewable (green) hydrogen. As a result, renewable generation forms the first layer in the dispatch logic for both the electricity and hydrogen networks, alongside fixed contributions from import streams and the technical minimum outputs of system components.

Ammonia plays a key balancing role in both the electricity and hydrogen networks. From the modeling results and scenario analysis appears that ammonia-fired power plants are consistently dispatched as the first backup when renewable power generation fall short for meeting demand. For hydrogen balancing, ammonia cracking precedes the use of hydrogen storage in 97% of cases observed in the modeling results of the normal scenario. Based on this, the strategy incorporates the decision that ammonia is always dispatched before hydrogen storage to maintain operational simplicity while ensuring cost-effectiveness. Ammonia forms the first flexibility response, and thus the second decision layer, in both the electricity and hydrogen networks when renewable and fixed generation is insufficient to meet demand, bridging supply gaps via ammonia-fired power generation and ammonia cracking.

The modeling results show occasional reductions of the ATR operation as a cost-effective way of conserving electricity during periods of low renewable power generation. However it is also discussed that reducing hydrogen production from ATR potentially increases hydrogen prices in real-world systems, which was not accounted for in this optimization. Therefore, the ATR operation is integrated in the operation strategy as a continuous hydrogen production source in order to ensure hydrogen supply to industry at a competitive price. It only scales down when hydrogen demand can already be fully met by electrolyzers, imports, and minimal ammonia cracking.

While ATR is assumed to operate continuously, the occasional ramp-downs seen in the modeling results indicate potential cost savings through load flexibility. To account for this, DSM is included in the dynamic response layer of the strategy—applicable to both electricity and hydrogen systems—allowing non-essential loads to be curtailed under stressed conditions.

Dynamic response is initiated when the ammonia-based flexibility layer cannot meet system demands, i.e. when operation of ammonia-fired power generation and/or ammonia cracking reach their maximum capacities and demand is still not met. In this dynamic response, the system evaluates the real-time state of all networks, including carrier availability, conversion capacity, storage levels, marginal costs, technical constraints, and demand and selects from the best operational decision. From the modeling results, the need for this dynamic response became evident through the observed varying dispatch patterns of storages, hydrogen-fired power generation, and demand reduction over time. This third decision layer reflects the continuous trade-off observed between electricity and hydrogen and their dependencies on resource availability in storages. This dynamic response allows the MES to adapt to varying system conditions in a cost-effective manner.

The final decision layer incorporates load shedding of electricity or hydrogen export demands. This operational strategy is incorporated to ensure continuous energy supply to industrial consumers and is based on the assumption that shortfalls in the broader external networks can be covered by suppliers operating outside the industrial clusters.

For the natural gas network, modeling results show that natural gas in the modeled system primarily serves as a broad import hub for supply to external networks. This same structure applies to industrial clusters that

do not necessarily function as this import hub, under the assumption that natural gas supply from the national network is continuously available. Thus, the operation strategy of natural gas is linear assuming constant natural gas availability for ATR operation.

The heat network operating under the studied temperatures in industrial systems primarily functions as waste heat utilization instead of flexibility measure, given the limited potential industrial consumptions at these temperatures. It thus follows a linear operation sequence in which waste heat is first directed to the share of industry that could benefit from it, and then directed towards external district heating networks.

In this operation strategy, battery storage is exclusively utilized for balancing electricity supply and demand, rather than for regulating electricity prices. This operational choice reflects the observation that local grid-scale batteries are expected to have limited direct influence on electricity market prices, whereas price-related benefits are more effectively achieved through on-site battery systems at industrial facilities (see Section 4.6.4 for operational planning recommendations regarding on-site batteries). Consequently, price regulation is not considered a primary function of grid-scale batteries in this operation strategy. However, when batteries are integrated into the MES, they may offer a secondary benefit by contributing to price stabilization during periods of electricity peak prices.

4.5.3. Strategic Implications

This section details the distinguishing elements of the proposed operation strategy in relation to conventional approaches, illustrating how these features facilitate a more flexible and cost-effective energy system operation. In contrast to conventional, uni-sectoral operation strategies that function in isolation and depend on static price-based hierarchies that assume continuous resource availability—particularly from dispatchable fossil-fueled generation, the strategy developed in this study aims to dynamically coordinate multiple energy carriers across interconnected networks. By implementing these measures, the system's ability to respond to fluctuations in renewable energy supply, varying demand, and infrastructure constraints will be significantly enhanced.

4.5.3.1. Dynamic System Operation

An important function of the new operation strategy is the integrated dynamic response in events of electricity and hydrogen scarcity. This dynamic, cross-sectoral, real-time operation marks a fundamental shift from conventional energy system operations. Traditional approaches optimize each energy carrier independently, based on static hierarchies and limited cross-network interaction. In contrast, the proposed strategy treats the energy system as an integrated and interdependent whole. This enables a more coordinated, flexible, and efficient operation compared to static, price-driven, uni-sectoral methods. Dynamic operation is particularly essential in a system increasingly reliant on VRES, where continuous adaptation to resource availability is critical for maintaining continuous system operation and minimizing costs.

4.5.3.2. Ammonia as Key Flexibility Provider

The strategy positions ammonia as a critical flexibility provider within integrated energy systems. By strategically connecting hydrogen and electricity networks, ammonia delivers cross-sectoral balancing that decouples both sectors from wind power generation dependency. Four fundamental properties substantiate ammonia's central role in system flexibility. First, ammonia can be imported in large volumes regardless of wind power generation, creating crucial decoupling from renewable intermittency. Second, ammonia's export capacity remains variable, serving as an adjustable balancing mechanism based on internal system needs rather than rigid external constraints. Third, ammonia's connections to both electricity and hydrogen networks enable flexibility through multiple pathways. Fourth, ammonia represents the most cost-effective solution for large-scale energy storage. These properties make ammonia a key enabler of continuous operation during extended periods of low renewable power generation. This positions ammonia as a cornerstone for maintaining continuous system operation in renewable-dominated energy landscapes.

4.5.3.3. Flexibility through Multifunctional Carriers

The operation strategy incorporates the multiple roles that energy carriers can fulfill within an integrated industrial MES, thereby significantly enhancing adaptability to changing system states. Energy carriers with multifunctional capabilities—as storage media, dispatchable fuels for power generation, industrial feedstock, and direct consumption sources—expand the decision space for dynamic response. This enables dynamic resource allocation based on real-time conditions, providing substantially greater flexibility than conventional single-purpose approaches that treat carriers as having fixed, predetermined functions.

4.5.3.4. Strategic Roles of Storage Technologies

The operation strategy incorporates a combination of complementary storage technologies to enable cost-effective balancing of energy supply and demand. Each technology serves a specific function based on its technical characteristics and economic viability. Ammonia storage provides cost-effective long-duration capacity, particularly crucial for ensuring dispatchable power generation during extended periods of low renewable power generation. While underground hydrogen storage offers substantial volumetric capacity, its operational constraints—injection and production limits—reduce its effectiveness for rapid high-capacity balancing, necessitating supplementary hydrogen tank storages. Battery storage remains essential for managing high-frequency fluctuations in the electricity network. Beyond grid stabilization during renewable variability, batteries could help mitigate electricity price volatility when installed on industrial sites, thereby fostering a more attractive economic environment for industrial consumers and investors.

4.5.4. Addressing Energy Transition Challenges

The new operation strategy directly addresses the challenges faced in the transition toward carbon-neutral industrial energy systems, as stated in the introduction—Section 1.2. These challenges include the threat to the reliability of energy supply by VRES intermittency and grid congestion, delayed initiation of new energy infrastructure developments due to limited access to new grid connections, investment uncertainty for new infrastructure developments, and the need to maintain industrial competitiveness and an attractive investment climate, while reducing the reliance on continuously available and considerably cheaper fossil fuels. This section elaborates on how the proposed system operation strategy responds to and mitigates these challenges.

4.5.4.1. VRES Integration and Grid Congestion

The operation strategy enables large-scale integration of VRES within the existing electricity infrastructure and infrastructure developments. This is achieved by dynamically deploying a diverse range of flexibility options, including storage and conversion technologies. By dynamically managing storage systems and conversion technologies that respond in real-time to changing system conditions, networks are able to respond effectively to fluctuations in renewable power generation. This enables systems to accommodate higher shares of VRES without requiring extensive grid expansions, making the integration of renewables both technically practical and economically efficient.

In addition to balancing VRES fluctuations with storage and conversion, the strategy also addresses grid congestion through two mechanisms. Firstly, a substantial share of offshore wind electricity is directed to hydrogen production via electrolyzers, thereby relieving strain from a large part of the electricity grid during periods of high renewable power generation. Secondly, rather than pursuing high electrification of industrial processes, the strategy focuses on decarbonizing industrial energy demand primarily through hydrogen consumption, thus avoiding a significant increase in electricity consumption.

4.5.4.2. Development of New Energy Infrastructure

The proposed operation strategy leverages cross-sectoral synergies to maximize the utility of existing infrastructure, particularly the electricity grid, while providing clear direction for future system development. By distributing flexibility across multiple energy carriers that enables continuous load balancing, this integrated approach shows that large-scale offshore wind deployment can be absorbed within current grid development pathways, without the need for extensive additional grid reinforcement.

This cross-sectoral integration also yields considerable economic benefits by minimizing system costs across all sectors simultaneously. In contrast to conventional siloed approaches, the proposed strategy avoids redundant infrastructure investments—especially in storage technologies—that would otherwise be necessary if each sector were optimized independently. This significantly reduces overall system costs and addresses issues of affordability and investment uncertainty. The operational findings not only reduce the scale and thus overall cost of required investments but also provide essential clarity on investment prioritization. This supports system planning and lowers investment uncertainty, making the transition to carbon-neutral energy systems more actionable and financially viable.

4.5.4.3. Industrial Competitiveness and Investment Climate

Maintaining industrial competitiveness and an attractive investment climate during decarbonization was identified as a key challenge in Section 1.2. Both are closely linked to energy reliability and affordability. Energy costs directly influence industrial operating expenses, while energy reliability provides the certainty required for process optimization and long-term growth. The presence of favorable conditions—namely, cost-effective and reliable energy—strengthens the attractiveness of industrial clusters for investors and reinforces their

economic role within national and regional economies. However, these conditions are threatened during decarbonization by the relatively high cost of alternative fuels compared to fossil fuels, and by uncertainties surrounding electricity availability in systems dominated by VRES. The operation strategy addresses this through several key mechanisms.

The proposed operation strategy ensures a continuous supply of electricity and hydrogen—even during periods of low renewable power generation—through the integration of storage technologies and the inclusion of ammonia as a wind-independent energy carrier for both power generation and hydrogen production. This approach enhances the energy reliability required for uninterrupted industrial operations.

In addition, the strategy employs a dynamic dispatch approach that minimizes total system costs. Rather than optimizing each energy carrier in isolation, the strategy coordinates system-wide operations to identify the most cost-effective dispatch across all carriers. This integrated approach yields substantial cost savings compared to conventional methods, directly benefiting industrial consumers and supporting their competitive position during the transition.

To enhance economic viability during the early stages of the transition, the strategy includes continuous production of blue hydrogen from natural gas. This contributes to maintaining a relatively low hydrogen market price until green hydrogen achieves cost parity. Furthermore, battery storage can be deployed to buffer price fluctuations and support stable, cost-effective energy prices.

Beyond ensuring energy affordability and accessibility, the strategy facilitates the emergence of new value chains—particularly those centered around alternative carriers such as hydrogen and ammonia. This creates new investment opportunities and attracts additional capital to industrial regions. In turn, these regions can assume a leading role in developing these emerging value chains, strengthening their strategic economic position and fostering leadership in the energy transition.

4.5.5. Broader Socio-Economic Implications

As previously discussed, the proposed strategy supports the preservation of industrial competitiveness and the fostering of attractive investment climates, both of which are essential for the economic strength of industrial clusters. These clusters frequently function as central elements within national economies, thereby contributing to the overall prosperity of society.

The expansion of sustainable industries within industrial clusters, along with the development of new value chains, is expected to stimulate significant workforce growth and job creation. Furthermore, the initiation of new value chains has the potential to positively impact similar developments in other regions, thereby promoting economic activity and employment beyond the immediate clusters.

Furthermore, the strategy also enhances strategic energy autonomy by reducing dependence on fossil fuels, thereby improving energy price stability and reducing vulnerability to geopolitical tensions. This contributes to more secure energy access at stable energy prices, which in turn supports long-term economic resilience and societal well-being.

Lastly, the transition to more sustainable and autonomous energy systems has the potential to serve as a blueprint for other industrial regions seeking decarbonization pathways. This pioneering role, which aims to reconcile industrial competitiveness with energy transition objectives, has the potential to generate novel opportunities for knowledge export and international collaboration in the domain of sustainable industrial development.

4.6. Implications for Operational Planning

The findings of this study reveal several critical implications for the operational planning of MESs in industrial clusters. Achieving cost-effective operation while ensuring a continuous energy supply requires intelligent system design capable of supporting the proposed operation strategy.

4.6.1. Flexibility Prerequisites

Ammonia has been identified as a critical flexibility provider. It is therefore recommended that industrial clusters prioritize the development of ammonia infrastructure as a core component of their integrated energy systems. Maintaining non-intermittent import and flexible export capabilities for at least one energy carrier—particularly ammonia—is a key design recommendation. Rigid export obligations across all carriers would significantly reduce system flexibility and drive the need for costly additional storage investments.

Biomass may also offer comparable flexibility characteristics, such as decoupling from wind variability and enabling cross-network integration. It presents a potential alternative or complement to ammonia in specific roles. To evaluate this, industrial clusters should conduct comprehensive comparative assessments of ammonia and biomass, considering economic viability, technological readiness, safety, environmental impact, and alignment with policy and regulatory frameworks.

4.6.2. Power Plant Preferences

The operational analysis demonstrates a clear preference for ammonia-fired power plants over hydrogen-fired plants across all scenarios. It was observed that hydrogen-fired plants only increase output when ammonia-fired facilities reach maximum capacity. This finding suggests that investment priority should be given to ammonia-fired generation capacity. An alternative operation strategy for hydrogen power plants could involve the elimination of continuous minimum load requirements, with cold-start activation limited to periods of critical need. This would result in a greater reliance on ammonia-fired plants during normal operations, while hydrogen plants would be reserved for infrequent but significant electricity shortfalls.

4.6.3. Strategic Storage Deployment

All modeled storage technologies demonstrate significant system value. It is therefore recommended to invest in a combination of storage types, as no single technology alone can provide the full flexibility required for cost-effective system operation. In the case of hydrogen, tank storage could be avoided if underground storage were enhanced through higher injection and withdrawal capacities—achievable either by assessing daily instead of hourly capacity limits or by deploying multiple caverns in parallel. Industrial clusters are encouraged to investigate the feasibility of such enhancements to reduce dependence on more expensive tank storage solutions.

Moreover, sensitivity analyses indicate that electricity and hydrogen export volumes strongly influence storage requirements. Reducing export volumes lowers storage needs, suggesting that industrial clusters should accurately assess projected export levels using empirical data to minimize investment costs for storages. Reducing export volumes would therefore also spatial constraints and improve overall system feasibility.

To further alleviate spatial limitations, clusters should also explore underground ammonia storage options. Above-ground tanks pose significant space challenges, whereas underground solutions could accommodate the large volumes needed for effective flexibility provision, especially as ammonia was identified as the most cost-efficient carrier for large-scale storage and power generation during VRES fluctuations.

4.6.4. On-Site Batteries for Electricity Price Regulation

Batteries have demonstrated strong potential for stabilizing fluctuating electricity prices. However, when connected to the national electricity system, large-scale batteries are likely to exert only a limited influence on market prices due to their relatively small share in the overall power market. As a result, industrial consumers may see minimal direct financial benefits from grid-level battery installations. In contrast, on-site battery systems at industrial facilities allow consumers to take immediate advantage of electricity price fluctuations by storing energy during low-price periods and using it when prices peak. Therefore, if the primary objective is to reduce electricity costs for industrial users, deploying on-site batteries is recommended. Conversely, to support system-wide stabilization of variable renewable electricity generation, grid-scale batteries remains essential. Their coordinated operation at the system level ensures efficient balancing of supply and demand across the electricity network.

4.6.5. Operational Reserves for Uncertainty

The model demonstrates optimal foresight, creating an optimized system with minimal margins. However, in real-world implementation, the limitations of weather forecasting introduce significant uncertainty, which must be addressed through the implementation of operational storage reserves. Storage systems should be designed to be oversized by an appropriate factor in order to maintain consistent energy supply to demand during unexpected weather variations. While the worst-case scenario analysis provides initial guidance on required storage capacity under challenging conditions, further research is needed to determine optimal reserve margins based on forecasting uncertainty and reliability requirements.

4.6.6. Electrolyzer Expansion Opportunity

Significant curtailment of renewable electricity (38–53% across scenarios) presents a compelling opportunity to expand electrolyzer capacity. To maximize this potential, additional electrolyzers should be coupled with

battery storage or designed to operate without minimum load constraints and response delays. This would avoid electrolyzers drawing electricity from the grid during periods of low wind power generation. Beyond electrolyzers, other P2X technologies could also be considered to utilize surplus renewable electricity, thereby improving system efficiency and reducing curtailment.

4.6.7. Monitoring and Control

To enable the dynamic response in the operation strategy, industrial clusters should invest in advanced monitoring and control systems. These systems must continuously track not only energy market price fluctuations but also storage levels, component capacity utilization, and system reserves across the multiple energy carrier networks. This approach signifies the shift from current operation strategies, necessitating seamless information exchange between formerly isolated energy networks and the implementation of integrated control systems.

4.7. Reflection

This research proposes a new operation strategy for a cost-effective operation of future multi-energy systems in industrial clusters. While the model provides meaningful insights into system behavior and interactions across multiple energy carriers, several limitations and simplifications must be acknowledged to guide future research and practical implementation. This chapter begins with a qualitative reflection on the results in relation to existing literature in Section 4.7.1. Then, Section 4.7.2 discusses key uncertainties related to system characterization and modeling choices that may affect the robustness of the outcomes. Section 4.7.3 examines the simplifications that cause differences between the model and real-world applications that limit direct applicability. These reflections form the basis for identifying future research, which are summarized in the conclusion of this research in Section 5.1.

4.7.1. Qualitative Reflections of Results in Respect to Literature

The necessity of a flexible operation strategy in MESs is acknowledged in literature. Zhou et al. (2024) investigated the optimal operation of a MES in which green ammonia is synthesized from green hydrogen [41]. Due to the variability in renewable energy production, it is shown that operation strategies are required that can dynamically adapt to these fluctuations in order to maintain operational flexibility and continuous system operation. The study highlights that traditional, rigid operation strategies commonly applied in the chemical industry are no longer suitable and must be revised to meet the operational requirements of future MES configurations. Similarly, Wen et al. (2022) explore the optimal operation strategy of a hydrogen-ammonia-based storage system and emphasize the importance of flexible, dynamic strategies that continuously account for storage capacities and output flows [39]. Their findings reinforce the need for adaptive control mechanisms that enable real-time responsiveness to changing system conditions, particularly in energy systems with high shares of VRES.

These findings are consistent with the results of this study, which indicates that a dynamic, cross-sectoral operation strategy is essential for ensuring the cost-effective and flexible operation of MESs. However, the specific operational decisions derived from such strategies are highly dependent on the modeled network configurations and the selection of included energy carriers, which makes a more in-depth comparison between operational results from MES modeling studies challenging.

4.7.2. Uncertainties

A number of underlying uncertainties have the potential to influence the outcomes of the optimal MES operation. Most forward are the future energy carrier prices and technology costs that remain uncertain as they are highly dependent on global market dynamics and policy developments. Sensitivity analyses have been conducted to address some of these uncertainties, particularly those related to energy carrier prices and demand profiles. For instance, the sensitivity analysis has already demonstrated that price variations significantly influence which storage technologies are prioritized. However, these analyses do not cover the uncertainties related to future CAPEX and OPEX of technologies and system components.

Further uncertainties emerge from the evolving regulatory landscape. These not only affect the pricing and costs of system components, but also include environmental and safety regulations. For example, policies on CO_2 emissions and broader environmental legislation will influence the extent to which the energy transition is mandated. This, in turn, will impact the willingness of other companies and stakeholders to align with decarbonization efforts, having a direct impact on the overall investment climate. Additionally, regulations concerning ammonia's toxicity could impose stricter limitations on its large-scale deployment, despite the

flexibility benefits highlighted in this study. This all illustrates how policies and regulations can significantly shape the pathway towards a carbon-neutral energy system.

Moreover, the model predominantly employs the energy hub approach, which involves the simplification of energy network representation through the abstraction of their physical behavior. This is of particular significance for the non-electrical carriers such as ammonia, heat, natural gas, and hydrogen. The exclusion of physic-based network dynamics for these carriers—such as pressure limits, flow constraints, and response times of networks and components—reduces the model's accuracy in evaluating the system's real-world operational viability

In addition, capturing such dynamics would require detailed physics-based network modeling combined with a significantly finer temporal resolution—on the order of seconds to minutes rather than hours—to accurately reflect system behavior. While component response times appear aligned at hourly intervals, finer resolutions could reveal critical mismatches. To exemplify, the natural gas network operates at a typical flow velocity of 10 m/s with propagation speed of potential change equal to speed of sound ($343m/s$), while electricity flows at the speed of light ($3 \cdot 10^8 m/s$) with identical propagation speed of potential change [128]. Chemical conversion processes like hydrogen or ammonia-fueled power generation serve as power balancing mechanisms in the current model, yet their actual response times are thus much slower than required for effective grid stabilization. These chemical and thermodynamic processes operate significantly slower than electrical grid responses, necessitating sub-hourly analysis to identify requirements for fast-responding technologies like batteries to bridge operational gaps until slower processes fully adjust. Therefore, understanding and managing these dynamics is essential for maintaining continuous system operation.

4.7.3. Differences with Real World Applications

A number of significant differences exist between the model setup and the real world implementation. The model operates under the assumption of perfect foresight, a condition that allows technologies such as storages to operate optimally based on known future conditions. However, in real-world scenarios, uncertainties in future renewable generation, demand, and system conditions would require larger storage capacities to ensure sufficient reserves remain available for future periods, unlike the precise optimization possible with perfect foresight.

Furthermore, the model operates under the assumption of seamless collaboration among all stakeholders. However, in reality, such alignment is unlikely due to diverging interests, lack of information sharing, or stakeholder conflict. These factors hinder the development of a unified, centrally coordinated, and transparently operated system.

Thirdly, current market structures for hydrogen, ammonia, and heat are either non-existent or only emerging in limited terms. The model assumes the existence of centralized, well-functioning markets for all these carriers, allowing for consistent price signals and coordinated dispatch. This assumption contrasts the current reality and introduces a considerable degree of uncertainty with regard to the feasibility and applicability of such a market structure in the future.

Fourthly, the model treats market prices as fixed throughout the year, independent of system operation. However, in practice, the dispatch of flexible assets, such as storage or conversion technologies, can influence real-time prices. The exclusion of this feedback loop from the model limits its ability to capture dynamic market interactions and the effect of component dispatch on the market price.

4.8. Summary

This chapter presented a detailed analysis of the optimal operation of the MMES under different scenarios. The normal-case analysis revealed specific system behavior and network interdependencies. The scenario comparison demonstrated operational shifts under varying weather conditions. The sensitivity analysis showed the effect of export volumes and carrier prices on the system's behavior. Based on all findings, an optimal operation strategy was formulated, focusing on cross-sector economic optimization, dynamic dispatch in response to system fluctuations, enhanced flexibility through energy conversion and storage technologies, and sufficient energy supply to industrial consumers. This strategy represented a shift away from conventional siloed, price-driven, static approaches based on constant resource availability assumptions. It addressed key challenges in the transition toward carbon-neutral industrial clusters and offered concrete guidance for operational planning. Finally, several limitations of the current research were acknowledged to inform future studies and practical implementation.

5

Conclusion

This research presented a novel model-based approach for optimizing the operation of MESs in industrial clusters, addressing critical challenges in the transition toward carbon neutrality. The main research objective was to develop a model-based approach to advance the optimization of multi-energy systems in industrial clusters and support decision-making regarding system operation strategies. Focusing on a synthetic, future-oriented MES inspired by the Maasvlakte area in the Port of Rotterdam, five energy carriers networks—electricity, hydrogen, ammonia, natural gas, and heat—were integrated within a unified MES optimization framework to identify cost-effective and flexible operation strategies.

The modeling approach captures both existing infrastructure and potential future developments by combining physics-based power flow modeling, to capture technical feasibility within the existing electrical infrastructure, with the energy hub approach for emerging or unconstrained energy carrier networks. This modeling approach represents a significant advancement in the field of MES modeling. Several methodological contributions further enhance the current state of practice, including the introduction of a new energy system scope by the integration of ammonia as an energy carrier and by the representation of multifunctional roles of alternative carriers, by advancing the modeling approach through the differentiation of heat flows by temperature levels to reflect industrial usability, and by providing new insights on cost-effective system operation strategies. These innovations collectively address the first research sub-question concerning the accurate representation of MESs and the methodological advances it can contribute.

To address the uncertainties associated with weather-dependent renewable energy generation, this research developed a scenario-based optimization framework. This framework was designed to test the system's operation under varying weather conditions. This led to the formulation of three representative scenarios: worst-case, normal-case, and best-case. These scenarios were developed based on varying levels of wind and solar availability, as determined by historical meteorological data. The analysis indicated a notable responsiveness of MES operation to varying weather conditions, underscoring the necessity for operational storage reserves. This framework effectively addresses the second research question regarding the identification of operational constraints and the incorporation of weather-related uncertainties into the optimization model.

Based on the system's optimal operation across all scenarios, a new system operation strategy was proposed that represents a paradigm shift from conventional energy system operation and organization. While traditional energy system operation strategies tend to be siloed, price-driven, static, and assume constant resource availability, the proposed strategy embraces cross-sector economic optimization, dynamic responsiveness, cross-sectoral flexibility, and continuous energy supply to industries. Key elements of this strategy include enabling dynamic dispatch decisions across all sectors, positioning ammonia as a key flexibility provider, facilitating cross-sectoral flexibility through conversion and multifunctional energy carriers, and integrating strategic use of storage technologies across sectors. This comprehensive approach addresses the third research question regarding the enhancement of energy system flexibility and the development of operation strategies that enable flexible and cost-effective operation.

For the operational planning of industrial clusters, the research provided several concrete recommendations. These included the prioritization of ammonia infrastructure as a key element of system flexibility, the preference for ammonia-fired power generation over hydrogen-fired power generation, the investment in a diverse mix of storage technologies rather than a single type, the implementation of on-site battery systems for effective balancing of the electricity price, the incorporation of sufficient operational reserves in storage systems to ensure uninterrupted operation under all weather conditions, the expansion of electrolyzer capacity or other

P2X technologies to enhance renewable energy utilization, and the implementation of system-wide monitoring and control capabilities to enable dynamic, real-time responses to changing system states.

These findings offer valuable insights for policymakers, system operators, and industrial stakeholders navigating the complex transition toward sustainable and carbon-neutral industrial operations. The implementation of the proposed operation strategy has the potential to enhance the energy system flexibility and cost-effectiveness of industrial clusters in conjunction with the increasing integration of renewable energy and decarbonization targets. Through addressing the main research objective of developing a model-based approach to advance the optimization of multi-energy systems in industrial clusters and support decision-making regarding system operation strategies, this research contributes significantly to both the theoretical understanding and practical implementation of multi-energy systems for industrial decarbonization.

5.1. Directions for Future Research

Building upon the model-based approach and operation strategies presented in this research, several areas for potential future research emerge. While this study has made significant contributions to both academic knowledge and practical implementation—advancing the theoretical field of MES modeling and providing actionable insights for operational decision-making and infrastructure development—there remain important opportunities to further enhance the accuracy, applicability, and comprehensiveness of MES optimization models and MES operation strategies.

Future research should concentrate on incorporating more physically detailed representations of energy carrier networks, especially those for natural gas, hydrogen, ammonia, and heat. Such an approach would facilitate more accurate operational modeling by accounting for fluid dynamics, thermodynamics, and reaction kinetics. Furthermore, such an approach would facilitate a more nuanced understanding of the varying response times of these carrier networks, thereby leading to a more accurate representation of system operation and dispatch flexibility.

To adequately capture these physical dynamics, future models should implement finer temporal resolutions—at the minute or even second level rather than hourly intervals—to enable accurate modeling of critical network phenomena. Given that these physical processes operate on timescales significantly shorter than hourly intervals, incorporating them would substantially enhance the operational accuracy of MES models and provide more realistic insights into system flexibility limitations.

Furthermore, the exploration of real-time optimization methods–without perfect foresight–could provide valuable insights into the system's real-world responsiveness. The modeling of the system under uncertainty would reveal the operational consequences for storage sizing, reserve requirements, and the ability to maintain consistent performance during unpredictable events.

In view of the fact that future multi-energy systems are unlikely to be managed by a single central operator, decentralized decision-making in MES operation should also be explored. This encompasses the exploration of market structures that can effectively coordinate independent actors, while facilitating MES operation and its corresponding benefits.

The integration of high-temperature heat networks into industrial MESs is an important area for future research, especially considering trade-offs between using waste heat for power generation, industrial processes, or low-temperature heating networks. These exchanges are often managed through bilateral agreements, limiting system-wide optimization. Exploring centralized coordination models could improve efficiency, support cross-sector heat integration, and enhance decarbonization potential.

Moreover, future studies should integrate investment and operational planning in a unified modeling framework. Coupled with a policy scenario analysis, this would help to identify which combinations of technology pathways and regulatory measures are most effective in advancing toward a resilient, flexible, and sustainable energy system.

Finally, it is recommended that future research efforts concentrate on a comparative analysis of ammonia and biomass as potential alternative carriers within the context of future energy systems. These two options have the capacity to fulfill comparable roles in ensuring flexibility within MESs.

References

[1] United Nations Environment Programme. *Emissions Gap Report 2024: No More Hot Air … Please! With a Massive Gap Between Rhetoric and Reality, Countries Draft New Climate Commitments*. Nairobi: United Nations Environment Programme, 2024. DOI: 10.59117/20.500.11822/46404. URL: https://www.unep.org/emissions-gap-report-2024.

[2] World Economic Forum. *Transitioning Industrial Clusters Towards Net Zero*. World Economic Forum, 2023. URL: https://www3.weforum.org/docs/WEF_Transitioning_Industrial_Clusters_2023.pdf.

[3] Port of Moerdijk. *Cluster Energie Strategie Rotterdam-Moerdijk 2024*. 2024. URL: https://portofmoerdijk.nl/media/4y4dvtbo/cluster-energie-strategie-rotterdam-moerdijk-2024-final.pdf.

[4] Pierluigi Mancarella. "MES (multi-energy systems): An overview of concepts and evaluation models". In: *Energy* 65 (2014), pp. 1–17. DOI: 10.1016/j.energy.2013.10.041.

[5] Qiuwei Wu et al. *Optimal Operation of Integrated Multi-Energy Systems Under Uncertainty*. English. 1st. Elsevier, 2021. ISBN: 9780128241141.

[6] J. Sijm et al. *Energy Transition Implications for Demand and Supply of Power System Flexibility: A Case Study of the Netherlands Within an EU Electricity Market and Trading Context*. Ed. by E. Gawel et al. Springer, Cham, 2019, pp. 358–390. DOI: 10.1007/978-3-030-03374-3_21.

[7] Oliver Schmidt and Iain Staffell. *Monetizing Energy Storage: A Toolkit to Assess Future Cost and Value*. Oxford, UK: Oxford University Press, 2023. ISBN: 9780192888174. DOI: 10.1093/oso/9780192888174.001.0001.

[8] CE Delft. *Welke centrales vervangen de kolencentrales? Analyse van elektriciteitsmarkt zonder kolencentrales*. Delft, Netherlands, 2021. URL: https://cedelft.eu/wp-content/uploads/sites/2/2021/03/CE_Delft_0000_Welke_centrales_vervangen_de_kolencentrales_Def.pdf.

[9] Ailin Asadinejad and Kevin Tomsovic. "Optimal use of incentive and price-based demand response to reduce costs and price volatility". In: *Electric Power Systems Research* (2017). DOI: 10.1016/j.epsr.2016.12.019.

[10] T. Brown et al. "Synergies of sector coupling and transmission reinforcement in a cost-optimised, highly renewable European energy system". In: *Energy* (2018). DOI: 10.1016/j.energy.2018.06.222.

[11] Verena Kleinschmidt et al. "Unlocking Flexibility in Multi-Energy Systems: A Literature Review". In: (2020). DOI: 10.1109/EEM49802.2020.9221927.

[12] Y. Zhang et al. "Linearized Stochastic Scheduling of Interconnected Energy Hubs Considering Integrated Demand Response and Wind Uncertainty". In: *Energies* (2018). DOI: 10.1016/j.enbenv.2022.06.007.

[13] Panagiotis Fragkos, Amanda Schibline, and Andrzej Ceglarz. *Energy System Models: Basic Principles and Concepts*. Presentation, Track 1: Intro to ESMs, organized by E3Modelling and RGI. Oct. 2023.

[14] Pierluigi Mancarella et al. "Modelling of Integrated Multi-Energy Systems: Drivers, Requirements, and Opportunities". In: (2016). DOI: 10.1109/PSCC.2016.7541031.

[15] Matteo Giacomo Prina et al. "Classification and challenges of bottom-up energy system models: A review". In: *Renewable and Sustainable Energy Reviews* 129 (2020), p. 109917. DOI: 10.1016/j.rser.2020.109917.

[16] Andreas Herbst et al. "Introduction to Energy Systems Modelling". In: *Swiss Journal of Economics and Statistics* 148 (2012), pp. 111–135. DOI: 10.1007/BF03399363.

[17] Lukas Kriechbaum, Gerhild Scheiber, and Thomas Kienberger. "Grid-based multi-energy systems—modelling, assessment, open source modelling frameworks and challenges". In: *Energy, Sustainability and Society* 8.35 (2018). DOI: 10.1186/s13705-018-0176-x.

[18] Giulia Mancò et al. "A review on multi-energy systems modelling and optimization". In: *Applied Thermal Engineering* (2024). DOI: 10.1016/j.applthermaleng.2023.121871.

[19] Sannamari Pilpola and Peter D. Lund. “Analyzing the Effects of Uncertainties on the Modelling of Low-Carbon Energy System Pathways”. In: *Energy* 201 (2020). DOI: 10.1016/j.energy.2020.117652.

[20] Jonas Hörsch et al. “PyPSA-Eur: An Open Optimisation Model of the European Transmission System”. In: *Energy Strategy Reviews* 22 (2018), pp. 207–215. DOI: 10.1016/j.esr.2018.09.012.

[21] Hans-Kristian Ringkjøb, Petter Myhre Haugan, and Ida Marie Solbrekke. “A review of modelling tools for energy and electricity systems with large shares of variable renewables”. In: *Renewable and Sustainable Energy Reviews* 96 (2018), pp. 440–459. DOI: 10.1016/j.rser.2018.08.002.

[22] Xiwang Li and Jin Wen. “Review of Building Energy Modeling for Control and Operation”. In: *Renewable and Sustainable Energy Reviews* 37 (2014), pp. 517–537. DOI: 10.1016/j.rser.2014.05.056.

[23] Martin Geidl and Göran Andersson. “A Modeling and Optimization Approach for Multiple Energy Carrier Power Flow”. In: (2005). DOI: 10.1109/PTC.2005.4524640.

[24] OpenMDAO Documentation Team. *Basic Optimization Problem Formulation*. 2024. URL: https://openmdao.github.io/PracticalMDO/Notebooks/Optimization/basic_opt_problem_formulation.html#main-message.

[25] Paolo Gabrielli et al. “Optimal design of multi-energy systems with seasonal storage”. In: *Applied Energy* 219 (2018), pp. 408–424. DOI: 10.1016/j.apenergy.2017.07.142.

[26] Tobi Michael Alabi et al. “A novel optimal configuration model for a zero-carbon multi-energy system (ZC-MES) integrated with financial constraints”. In: *Sustainable Energy, Grids and Networks* (2020). DOI: 10.1016/j.segan.2020.100381.

[27] Dechang Yang and Ming Wang. “Optimal operation of an integrated energy system by considering the multi energy coupling, AC-DC topology and demand responses”. In: *International Journal of Electrical Power and Energy Systems* (2021). DOI: 10.1016/j.ijepes.2021.106826.

[28] Yulong Jia et al. “Optimal Operation of Multi-Energy Systems in Distributed Energy Network Considering Energy Storage”. In: (2017). DOI: 10.1109/EI2.2017.8245261.

[29] Binod Koirala et al. “Integrated electricity, hydrogen and methane system modelling framework: Application to the Dutch Infrastructure Outlook 2050”. In: *Applied Energy* (2021). DOI: 10.1016/j.apenergy.2021.116713.

[30] Enrico Fabrizio, Vincenzo Corrado, and Marco Filippi. “A model to design and optimize multi-energy systems in buildings at the design concept stage”. In: *Renewable Energy* (2010). DOI: 10.1016/j.renene.2009.08.012.

[31] Xuezhi Liu and Pierluigi Mancarella. “Modelling, assessment and Sankey diagrams of integrated electricity-heat-gas networks in multi-vector district energy systems”. In: *Applied Energy* (2016). DOI: 10.1016/j.apenergy.2015.08.089.

[32] Eduardo A. Martínez Ceseña et al. “Techno-economic and business case assessment of multi-energy microgrids with co-optimization of energy, reserve and reliability services”. In: *Applied Energy* (2018). DOI: 10.1016/j.apenergy.2017.08.131.

[33] Li Guangdi et al. “Optimal Operation Strategy of Multi-energy System Considering Energy Supply for Waste Treatment”. In: (2022). DOI: 10.1109/AEEES54426.2022.9759729.

[34] Yuqin Xu and Keyi Xu. “Multi-objective Optimal Dispatching of the Integrated Energy System in the Industrial Park”. In: (2021). DOI: 10.1109/ICPSAsia52756.2021.9621509.

[35] Yanan Wang and Chengcheng Shao. “Optimal Operation Model of the Multi-Energy Network in the Distribution System”. In: (2019). DOI: 10.1109/ICEI.2019.00071.

[36] Qian Zhang, Jingwen Qi, and Lu Zhen. “Optimization of integrated energy system considering multi-energy collaboration in carbon-free hydrogen port”. In: *Transportation Research Part E* (2023). DOI: 10.1016/j.tre.2023.103351.

[37] Changxing Yang et al. “Multi-timescale Optimal Operation Strategy of Electric-Hydrogen Hybrid Energy Storage System”. In: (2023). DOI: 10.1109/CIEEC58067.2023.10166309.

[38] Rasoul Garmabdari et al. “Multi Energy System Modelling and Operation Optimisation for University Research Facility”. In: (2018). DOI: https://doi.org/10.1109/EEEIC.2018.8494607.

[39] Du Wen and Muhammad Aziz. “Flexible Operation Strategy of an Integrated Renewable Multi-Generation System for Electricity, Hydrogen, Ammonia, and Heating”. In: *Energy Conversion and Management* 253 (2022), p. 115166. DOI: 10.1016/j.enconman.2021.115166.

[40] O. Siddiqui and I. Dincer. “Design and Analysis of a Novel Solar-Wind Based Integrated Energy System Utilizing Ammonia for Energy Storage”. In: *Energy Conversion and Management* 195 (2019), pp. 866–884. DOI: 10.1016/j.enconman.2019.05.001.

[41] Jiahui Zhou et al. “Optimal Capacity and Multi-Stable Flexible Operation Strategy of Green Ammonia Systems: Adapting to Fluctuations in Renewable Energy”. In: *Energy Conversion and Management* 302 (2024), p. 118720. DOI: 10.1016/j.enconman.2024.118720.

[42] Shuoshi Yang et al. “Two-Stage Robust Optimization Scheduling for Integrated Energy Systems Considering Ammonia Energy and Waste Heat Utilization”. In: *Energy Conversion and Management* 302 (2024), p. 118922. DOI: 10.1016/j.enconman.2024.118922.

[43] Port of Rotterdam. *CO2-uitstoot Haven Rotterdam daalde 10% in 2023*. 2023. URL: https://www.portofrotterdam.com/nl/nieuws-en-persberichten/co2-uitstoot-haven-rotterdam-daalde-10-2023.

[44] Centraal Bureau voor de Statistiek (CBS). *Hoe groot is onze broeikasgasuitstoot en wat is het doel?* 2024. URL: https://www.cbs.nl/nl-nl/dossier/dossier-broeikasgassen/hoe-groot-is-onze-broeikasgasuitstoot-wat-is-het-doel-.

[45] Port of Rotterdam. *Terugdringen CO2-uitstoot Havenbedrijf*. 2024. URL: https://www.portofrotterdam.com/nl/over-het-havenbedrijf/havenbedrijf-de-samenleving/terugdringen-co2-uitstoot-havenbedrijf#:~:text=Gevalideerde%20klimaatdoelen,maximaal%201%2C5%20graad%20opwarming..

[46] Stewart Robinson. “Conceptual Modeling for Simulation”. In: (2013). DOI: 10.1109/WSC.2013.6721461.

[47] Stewart Robinson. “Conceptual modelling for simulation Part I: Definition and requirements”. In: *Journal of the Operational Research Society* (2008). DOI: 10.1057/palgrave.jors.2602368.

[48] Institute for Sustainable Process Technology (ISPT). *Clean Ammonia Roadmap*. ISPT, 2024. URL: https://ispt.eu/media/2024-ISPT-Clean-Ammonia-Roadmap-report_online-versie.pdf.

[49] International Renewable Energy Agency (IRENA). *Innovation Outlook: Renewable Ammonia*. IRENA, 2022. URL: https://www.irena.org/publications/2022/Sep/Innovation-Outlook-Renewable-Ammonia.

[50] TNO. *Verkenning van Toekomstige Ontwikkelingen in het Elektriciteitssysteem in Nederland 2030–2050*. TNO – Nederlandse Organisatie voor Toegepast Natuurwetenschappelijk Onderzoek, Mar. 2024. URL: https://www.tno.nl.

[51] Guiyan Zang, Edward J. Graham, and Dharik Mallapragada. “H2 Production through Natural Gas Reforming and Carbon Capture: A Techno-Economic and Life Cycle Analysis Comparison”. In: *International Journal of Hydrogen Energy* 49 (2024), pp. 1288–1303. DOI: 10.1016/j.ijhydene.2023.09.230.

[52] Jonas Bollmann et al. “Burner-heated dehydrogenation of a liquid organic hydrogen carrier (LOHC) system”. In: *International Journal of Hydrogen Energy* 48.2023 (2023), pp. 30039–30056. DOI: 10.1016/j.ijhydene.2023.04.062.

[53] WarmtelinQ. *Welke temperatuur heeft het water in WarmtelinQ?* 2025. URL: https://www.warmtelinq.nl/veelgestelde-vragen/overige-vragen/capaciteit-en-temperatuur#:~:text=Welke%20temperatuur%20heeft%20het%20water,onttrokken%20voor%20verwarming%20van%20woningen..

[54] Royal Netherlands Meteorological Institute (KNMI). *Daggegevens van het Weer in Nederland*. 2025. URL: https://www.knmi.nl/nederland-nu/klimatologie/daggegevens.

[55] Global Wind Atlas. *Global Wind Atlas*. 2024. URL: https://globalwindatlas.info/en/.

[56] Global Solar Atlas. *Global Solar Atlas - Map Viewer*. 2024. URL: https://globalsolaratlas.info/map?c=51.98488,4.12262,11&s=51.978536,4.119873&m=site.

[57] Port of Rotterdam. *Waterstof in Een klimaatneutrale haven in 2050*. 2024.

[58] Charlotte Yong and Andrew Keys. *Decarbonisation Options for Large Volume Organic Chemicals Production, LyondellBasell Rotterdam*. The Hague, Netherlands: PBL Netherlands Environmental Assessment Agency and TNO Energy Transition, Jan. 2021. URL: https://www.pbl.nl/en/publications/decarbonisation-options-for-large-volume-organic-chemicals-production-lyondellbasell-rotterdam.

[59] Carl-Fredrik Lindberg et al. “Potential and Limitations for Industrial Demand Side Management”. In: 61 (2014), pp. 415–418. DOI: 10.1016/j.egypro.2014.11.1138.

[60] Mehul Khandelwal and Ton van Dril. *Decarbonisation Options for the Dutch Biofuels Industry*. The Hague, Netherlands: PBL Netherlands Environmental Assessment Agency and TNO Energy Transition, Apr. 2020. URL: https://www.pbl.nl/en/publications/decarbonisation-options-for-the-dutch-biofuels-industry.

[61] Muhammad Arif Budiyanto et al. “Evaluation of CO2 Emissions and Energy Use with Different Container Terminal Layouts”. In: *Scientific Reports* 11 (2021), p. 5476. DOI: 10.1038/s41598-021-84958-4.

[62] Royal HaskoningDHV. *Publiekssamenvatting Milieueffectrapport CCS Porthos*. Amersfoort, Netherlands, June 2020. URL: https://www.rvo.nl/sites/default/files/2020/09/0%20-%20Publiekssamenvatting%20Milieueffectrapport%20CCS%20Porthos.pdf.

[63] PoR Shore Power Team. *Walstroom opportunity’s: info tbv portfolio management*. 2022.

[64] Statistics Netherlands (CBS). *Electricity and Natural Gas Prices for Households and Businesses*. 2025. URL: https://www.cbs.nl/en-gb/figures/detail/84575ENG.

[65] TenneT TSO B.V. *Monitoring Leveringszekerheid 2022 (2025-2030)*. TenneT TSO B.V., Dec. 2022.

[66] Lucas van Cappellen, Marianne Teng, and Frans Rooijers. *Beleid kolencentrales tot 2030: Effect van productiebeperking op CO□-uitstoot en compensatie*. 22.220362.126. In opdracht van Natuur & Milieu. CE Delft, Sept. 2022. URL: https://ce.nl/publicaties/beleid-kolencentrales-tot-2030/.

[67] Frans Rooijers et al. *Elektrificatie en Vraagprofiel 2030: Rapport Experttraject TenneT E-Top*. 20.190446.116. Delft, Netherlands: CE Delft, Sept. 2020. URL: http://www.ce.nl/.

[68] ENTSO-E Transparency Platform. *Total Load Data for the Netherlands*. 2025. URL: https://transparency.entsoe.eu/load-domain/r2/totalLoadR2/show?name=&defaultValue=true&viewType=TABLE&areaType=BZN&atch=false&dateTime.dateTime=14.03.2025+00:00%7CCET%7CDAY&biddingZone.values=CTY%7C10YNL----------L!BZN%7C10YNL----------L&dateTime.timezone=CET_CEST&dateTime.timezone_input=CET+(UTC+1)+/+CEST+(UTC+2).

[69] Bert den Ouden et al. *Blueprinting the Hydrogen Market – Hydrogen Spot Market Simulation*. Analysis of hydrogen market mechanisms and spot market simulations. HyXchange, Jan. 2024. URL: https://hyxchange.nl/document-library/.

[70] Patrick Freitag et al. “A Techno-Economic Analysis of Future Hydrogen Reconversion Technologies”. In: *International Journal of Hydrogen Energy* 77 (2024), pp. 1254–1267. DOI: 10.1016/j.ijhydene.2024.06.164. URL: https://doi.org/10.1016/j.ijhydene.2024.06.164.

[71] Zac Cesaro et al. “Ammonia to Power: Forecasting the Levelized Cost of Electricity from Green Ammonia in Large-Scale Power Plants”. In: *Applied Energy* 282.Part A (2021), p. 116009. DOI: 10.1016/j.apenergy.2020.116009.

[72] Hystock. *Introduction to underground hydrogen storage in cavern*. 2024.

[73] Ember. *European Wholesale Electricity Price Data*. 2025. URL: https://ember-energy.org/data/european-wholesale-electricity-price-data/#explore-this-data.

[74] International Energy Agency (IEA). *Denmark - Country Profile*. 2025. URL: https://www.iea.org/countries/denmark.

[75] Statista. *Distribution of Electricity Production in the Netherlands by Source*. 2025. URL: https://www.statista.com/statistics/1236355/netherlands-distribution-of-electricity-production-by-source/.

[76] U.S. Energy Information Administration (EIA). *Natural Gas Prices - Historical Data*. 2025. URL: https://www.eia.gov/dnav/ng/hist/n9103us3m.htm.

[77] Maarten Afman, Sebastiaan Hers, and Thijs Scholten. *Energy and Electricity Price Scenarios 2020-2023-2030: Input to Power to Ammonia Value Chains and Business Cases*. Delft, Netherlands: CE Delft, Jan. 2017. URL: https://www.ce.nl.

[78] Gemeente Zeewolde. *Memo eindgebruikerskosten en nationale kosten warmtetransitie. Ruimtelijk kader Trekkersveld IV*. Technical report. Gemeente Zeewolde, Nov. 5, 2021.

[79] Booster USA. *Fuel Pricing Dynamics: Understanding the Factors That Affect Fuel Costs*. 2025. URL: https://boosterusa.com/blog/fuel-pricing-dynamics-understanding-the-factors-that-affect-fuel-costs/.

[80] Johannes Hampp, Michael Düren, and Tom Brown. “Import Options for Chemical Energy Carriers from Renewable Sources to Germany”. In: *PLOS ONE* 18.2 (2023), e0262340. DOI: 10.1371/journal.pone.0281380.

[81] Autoriteit Consument & Markt. *Maximumtarieven warmte 2025: Variabel tarief omlaag, vaste kosten bijna gelijk*. 2024. URL: https://www.acm.nl/nl/publicaties/maximumtarieven-warmte-2025-variabel-tarief-omlaag-vaste-kosten-bijna-gelijk.

[82] Tom Brown, Jonas Hörsch, and David Schlachtberger. “PyPSA: Python for Power System Analysis”. In: *arXiv preprint* 1707.09913v3 (2018). URL: https://arxiv.org/abs/1707.09913v3.

[83] DataCamp Team. *Optimization in Python: Scipy’s Optimize Module*. 2024. URL: https://www.datacamp.com/tutorial/optimization-in-python.

[84] PyPSA Development Team. *PyPSA Documentation*. 2024. URL: https://pypsa.readthedocs.io/en/latest/.

[85] *Power Flow Calculation. Ybus Matrix, Power Flow Equations, and Newton-Raphson Method*. TU Delft Open Course Ware. 2021. URL: https://ocw.tudelft.nl/wp-content/uploads/PowerFlow.pdf.

[86] Jonas Hörsch et al. “Linear Optimal Power Flow Using Cycle Flows”. In: *arXiv preprint* 1704.01881v3 (Jan. 2018). URL: http://arxiv.org/abs/1704.01881v3.

[87] Bill Roungas, Sebastiaan Meijer, and Alexander Verbraeck. “A Framework for Optimizing Simulation Model Validation & Verification”. In: *International Journal on Advances in Systems and Measurements* 11.1 & 2 (2018). Published by Delft University of Technology and KTH Royal Institute of Technology, pp. 137–152. URL: http://www.iariajournals.org/systems_and_measurements/.

[88] A. Fernández-Guillamón et al. “Comparison of Different Tools for Power Flow Analysis with High Wind Power Integration”. In: *2019 International Conference on Clean Electrical Power (ICCEP)*. IEEE, 2019. DOI: 10.1109/ICCEP.2019.8890163.

[89] Andreas Schröder et al. *Current and Prospective Costs of Electricity Generation until 2050*. Research Report. Berlin, Germany: German Institute for Economic Research (DIW Berlin), 2013. URL: https://hdl.handle.net/10419/80348.

[90] Ivalin Petkov and Paolo Gabrielli. “Power-to-Hydrogen as Seasonal Energy Storage: An Uncertainty Analysis for Optimal Design of Low-Carbon Multi-Energy Systems”. In: *Applied Energy* 274 (2020), p. 115197. DOI: 10.1016/j.apenergy.2020.115197.

[91] Robin Niessink. *Technology Factsheet: Coal-Fired Power Plant (Co-Firing Biomass) - Electricity Production and District Heating*. Dec. 2018.

[92] Achmed Edianto et al. “Forecasting Coal Power Plant Retirement Ages and Lock-In with Random Forest Regression”. In: *Patterns* 4.7 (2023), p. 100776. DOI: 10.1016/j.patter.2023.100776.

[93] Agora Energiewende. *Flexibility in Thermal Power Plants – With a Focus on Existing Coal-Fired Power Plants*. 2017. URL: https://www.agora-energiewende.de.

[94] Unknown Author. *Flexibility in Thermal Power Plants: HELE and CHP Technologies for Flexibility and Efficiency Improvements*. 2019.

[95] Loes Rutten. *Technology Factsheet: Natural Gas CHP - Electricity Production and District Heating*. May 2020. URL: https://energy.nl/wp-content/uploads/technology-factsheetnaturalgaschp-v2-7.pdf.

[96] Hans Kleinbekman et al. *Techical feasibility study Power to Gas; A detailed analysis of the technical feasibility of P2G for the North Sea Wind Power Hub*. North Sea Wind Power Hub, 2019.

[97] Danish Energy Agency and Energinet. *Technology Data for Renewable Fuels: Technology Descriptions and Projections for Long-Term Energy System Planning*. 2017. URL: https://ens.dk/technologydata.

[98] Alles over Waterstof. *Update Rapport H-Vision: Blauwe Waterstof in Rotterdam*. URL: https://allesoverwaterstof.nl/update-rapport-h-vision-blauwe-waterstof-in-rotterdam/.

[99] Onyx Power. *Voorbereiding Waterstofproductieproject in Rotterdam*. 2025. URL: https://www.onyx-power.com/nl/nieuwtjes-en-pers/voorbereiding-waterstofproductieproject-in-rotterdam/.

[100] FLUOR. *Port of Rotterdam Pre-Feasibility Study*. Tech. rep. Port of Rotterdam, 2023.

[101] Port of Rotterdam. *Large-Scale Ammonia Cracker to Enable 1 Million Tonnes of Hydrogen Imports*. 2025. URL: https://www.portofrotterdam.com/en/news-and-press-releases/large-scale-ammonia-cracker-to-enable-1-million-tonnes-of-hydrogen-imports.

[102] Simon Richard et al. "Techno-economic analysis of ammonia cracking for large scale power generation". In: *International Journal of Hydrogen Energy* 71 (2024), pp. 571–587. DOI: 10.1016/j.ijhydene.2024.05.308.

[103] Loes Rutten. *H2 Industrial Boiler: Technology Factsheet*. Sept. 2020.

[104] Randeep Agarwal et al. "LNG Regasification – Effects of Project Stage Decisions on Capital Expenditure and Implications for Gas Pricing". In: *Journal of Natural Gas Science and Engineering* 78 (2020), p. 103291. DOI: 10.1016/j.jngse.2020.103291.

[105] Haneul Mun, Sihwan Park, and Inkyu Lee. "Liquid Hydrogen Cold Energy Recovery to Enhance Sustainability: Optimal Design of Dual-Stage Power Generation Cycles". In: *Energy* 284 (2023), p. 129229. DOI: 10.1016/j.energy.2023.129229.

[106] DNV GL. *Study on the Import of Liquid Renewable Energy: Technology Cost Assessment*. 2020. URL: https://www.gie.eu/wp-content/uploads/filr/2598/DNV-GL_Study-GLE-Technologies-and-costs-analysis-on-imports-of-liquid-renewable-energy.pdf.

[107] Anthony Wang et al. *European Hydrogen Backbone: How a Dedicated Hydrogen Infrastructure Can Be Created*. Utrecht, The Netherlands: Guidehouse, July 2020. URL: https://ehb.eu/files/downloads/2020_European-Hydrogen-Backbone_Report.pdf.

[108] TNO and EBN. *Haalbaarheidsstudie Offshore Ondergrondse Waterstofopslag*. Netherlands: TNO & EBN, 2022. URL: https://www.rijksoverheid.nl/documenten/rapporten/2022/07/01/22286281bijlage-1-haalbaarheidsstudie-offshore-ondergrondse-waterstofopslag.

[109] Doaa Saleh Mahdi et al. "Hydrogen underground storage efficiency in a heterogeneous sandstone reservoir". In: *Advances in Geo-Energy Research* 5.4 (2021), pp. 437–443. DOI: 10.46690/ager.2021.04.08.

[110] Hendrie Derking, Luuk van der Togt, and Marcel Keezer. "Liquid Hydrogen Storage: Status and Future Perspectives". In: *CHMT'19 Conference Proceedings*. Presented at CHMT'19, November 4, 2019. Cryoworld BV, 2019. URL: https://www.utwente.nl/en/tnw/ems/ecd-2020/Events/chmt/m13-hendrie-derking-cryoworld-chmt-2019.pdf.

[111] "Compressed Hydrogen Storage". In: *Renewable and Sustainable Energy Reviews* (2017). URL: https://www.sciencedirect.com/journal/renewable-and-sustainable-energy-reviews.

[112] PALA Group. *What is the Average Aboveground Fuel Storage Tank's Life Expectancy?* 2025. URL: https://www.palagroup.com/what-is-the-average-aboveground-fuel-storage-tanks-life-expectancy/#:~:text=fuel%20storage%20tanks.-,Average%20Life%20Expectancy%20of%20Aboveground%20Fuel%20Storage%20Tanks,maintenance%20of%20the%20storage%20tank..

[113] Jeffrey Ralph Bartels. "A Feasibility Study of Implementing an Ammonia Economy". Ames, Iowa: Iowa State University, 2008. URL: https://dr.lib.iastate.edu/server/api/core/bitstreams/c0443ee4-2e07-4213-9dbd-ee251dad41ec/content.

[114] Spirit Energy. *Understanding Batteries: A Guide to Battery Technology and Applications*. 2025. URL: https://www.spiritenergy.co.uk/kb-batteries-understanding-batteries.

[115] HoogspanningsNet. *Koppelnet - Het Nederlandse Elektriciteitsnet*. 2025. URL: https://www.hoogspanningsnet.com/hetnet/koppelnet/.

[116] Creos et al. *Analysing Future Demand, Supply, and Transport of Hydrogen*. Supported by Guidehouse. European Hydrogen Backbone Initiative, June 2021. URL: https://www.ehb.eu.

[117] Iza Zuijderwijk. *Interview with Arjan van Voorden, Stedin*. Personal interview conducted on January 15th, 2025. 2025.

[118] Tansu Galimova et al. "Feasibility of Green Ammonia Trading via Pipelines and Shipping: Cases of Europe, North Africa, and South America". In: *Journal of Cleaner Production* 427 (2023), p. 139212. DOI: 10.1016/j.jclepro.2023.139212.

[119] R.M. Nayak-Luke et al. "Techno-Economic Aspects of Production, Storage and Distribution of Ammonia". In: (2021), pp. 191–207. DOI: 10.1016/B978-0-12-820560-0.00008-4.

[120] Energy Transition Model. *Heat Infrastructure Costs*. 2025. URL: https://docs.energytransitionmodel.com/main/heat-infrastructure-costs.

[121] Emma Koster, Florian Hesselink, and Marianne Teng. *Warmtenetten in Vesta MAIS: Update Berekeningsmethoden*. 22.210347.173. Commissioned by Planbureau voor de Leefomgeving (PBL). Delft, Netherlands: CE Delft, Nov. 2022.

[122] Jooyong Kim and Ingo Weidlich. “Identification of Individual District Heating Network Conditions Using Equivalent Full Load Cycles”. In: *Energy Procedia* 116 (2017), pp. 343–350. DOI: 10.1016/j.egypro.2017.05.081.

[123] Robin Niessink. *Heat Networks High Temperature - District Heating: Technology Factsheet*. Mar. 2019.

[124] MAN Energy Solutions. *Industrial Heat Pumps: Efficiency and Lifespan*. 2025. URL: https://www.man-es.com/our-focus/future-technologies/heat-pumps#:~:text=On%20average%2C%20well%2Dmaintained%20heat,it%20continues%20to%20perform%20efficiently..

[125] OCI and FLUOR. *Constructieve uitgangspunten: Ammonia Bunkering Project*. Technical Report 215-DBD-001-001. Version Rev. 5. Issued for authority approval. OCI, Dec. 5, 2023.

[126] M. Torquet. *Underground Storage of Ammonia: Review of Possibilities*. Presentation. Presented under the initiative ”Faire de la Terre le meilleur espace pour le stockage de toutes les énergies”. May 23, 2023.

[127] Rick A. Vreman et al. “The Application and Implications of Novel Deterministic Sensitivity Analysis Methods”. In: *PharmacoEconomics* 39 (2021), pp. 1–17. DOI: 10.1007/s40273-020-00979-3.

[128] Electric Power Research Institute (EPRI) and encoord Inc. *Natural Gas Networks and Hydraulic Modeling: Basic Needs for Gas Data Sets*. Tech. rep. 3002024649. Electric Power Research Institute (EPRI), 2022. URL: https://www.epri.com/research/products/000000003002024649.

[129] Iza Zuijderwijk. *Interview with Wilco van der Lans, Port of Rotterdam*. Personal interview conducted on January 9th, 2025. 2025.

[130] Bo Cai et al. “Operation strategy and suitability analysis of CHP system with heat recovery”. In: *Energy and Buildings* 141 (2017), pp. 284–294. DOI: 10.1016/j.enbuild.2017.02.056.

[131] Subramani Krishnan et al. “Present and future cost of alkaline and PEM electrolyser stacks”. In: *International Journal of Hydrogen Energy* 48.43 (2023), pp. 32313–32330. DOI: 10.1016/j.ijhydene.2023.05.031.

[132] I.P. Koronaki, L. Prentza, and V. Papaefthimiou. “Modeling of CO2 Capture via Chemical Absorption Processes: An Extensive Literature Review”. In: *Renewable and Sustainable Energy Reviews* 50 (2015), pp. 547–566. DOI: 10.1016/j.rser.2015.04.124.

[133] Sandeep Yadav, Rangan Banerjee, and Srinivas Seethamraju. “Thermodynamic Analysis of LNG Regasification Process”. In: *Chemical Engineering Transactions*. Vol. 94. AIDIC Servizi S.r.l., 2022, pp. 919–924. DOI: 10.3303/CET2294153.

[134] Vattenfall. *Hollandse Kust Zuid Wind Park*. 2024. URL: https://hollandsekust.vattenfall.nl/windpark/#:~:text=We%20plaatsen%20139%20super%20krachtige,een%20minimaal%20vermogen%20van%206MW..

[135] Wind-Turbine-Models.com. *Siemens Gamesa SG 11.0-200 DD Turbine*. 2024. URL: https://en.wind-turbine-models.com/turbines/2157-siemens-gamesa-sg-11.0-200-dd.

[136] The Wind Power. *Maasvlakte 2 Wind Farm*. 2024. URL: https://www.thewindpower.net/windfarm_en_21685_maasvlakte-2.php.

[137] Wind-Turbine-Models.com. *Vestas V162-6.2 EnVentus Turbine*. 2024. URL: https://en.wind-turbine-models.com/turbines/2343-vestas-v162-6.2-enventus.

[138] BASF. *BASF News Release*. 2024. URL: https://www.basf.com/global/en/media/news-releases/2024/06/p-24-222.

[139] Wind-Turbine-Models.com. *Vestas V236-15.0 Turbine*. 2024. URL: https://en.wind-turbine-models.com/turbines/2317-vestas-v236-15.0.

[140] Delft University of Technology. *Meteorologisch Data Portal - Dutch PV Portal*. 2024. URL: https://www.tudelft.nl/ewi/over-de-faculteit/afdelingen/electrical-sustainable-energy/photovoltaic-materials-and-devices/dutch-pv-portal/meteorologisch-data-portal.

[141] TKF. *E-YAKrvlwd 87/150 kV*. Twentsche Kabelfabriek (TKF). 2025. URL: https://www.tkf.nl/nl/3110-e-yakrvlwd/58408.

[142] Twentsche Kabelfabriek (TKF). *YMeKrvasdlwd Fca 36/66 kV Cable*. Twentsche Kabelfabriek (TKF). 2025. URL: https://www.tkf.nl/nl/3116-ymekrvasdlwd/58377.

[143] Twentsche Kabelfabriek (TKF). *YMeKrvasdlwd Fca 18/30 kV Cable*. Twentsche Kabelfabriek (TKF). 2025. URL: https://www.tkf.nl/nl/4060-1830-kv/186323.

[144] WarmtelinQ. *Aanlegmethoden*. 2025. URL: https://www.warmtelinq.nl/informatie/aanlegmethoden.

A

Network Single Line Diagrams

A.1. SLD of Electrical Network

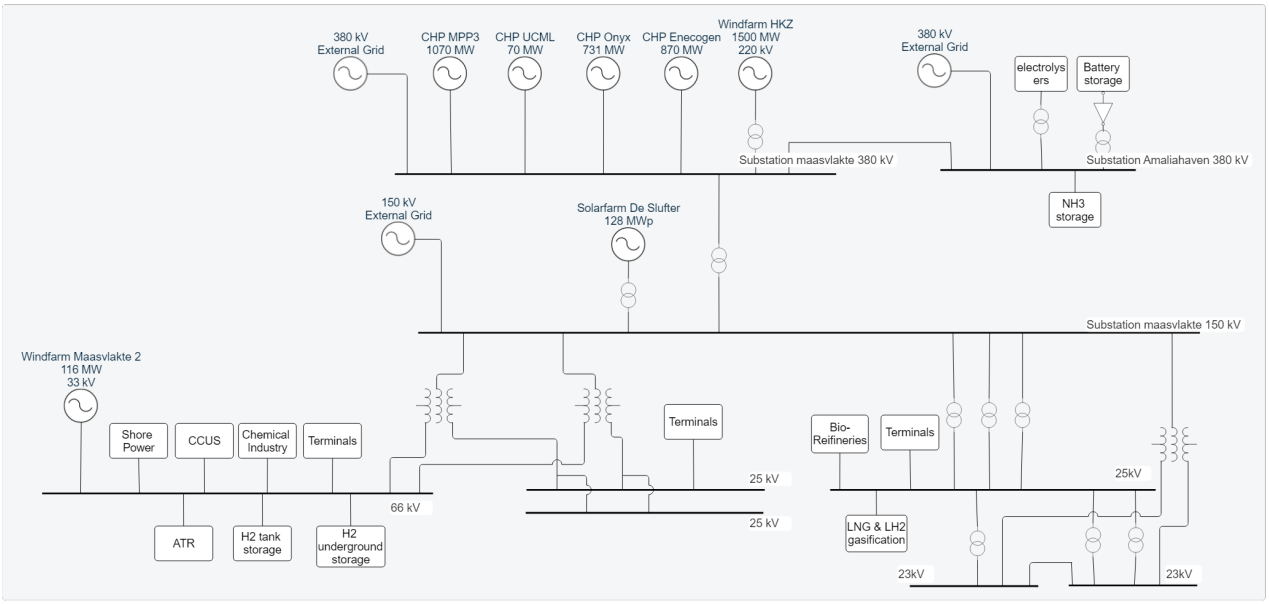

Figure A.1: SLD Electricity Network

A.2. SLD of Natural Gas Network

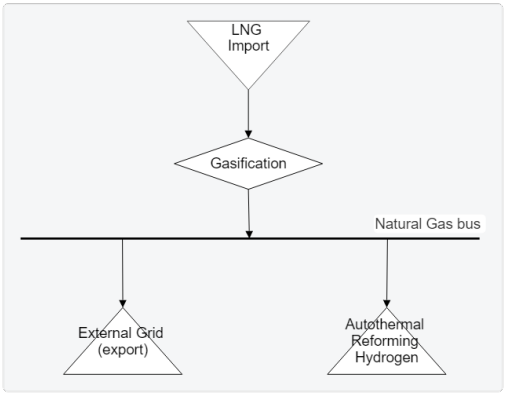

Figure A.2: SLD Natural Gas Network

A.3. SLD of Hydrogen Network

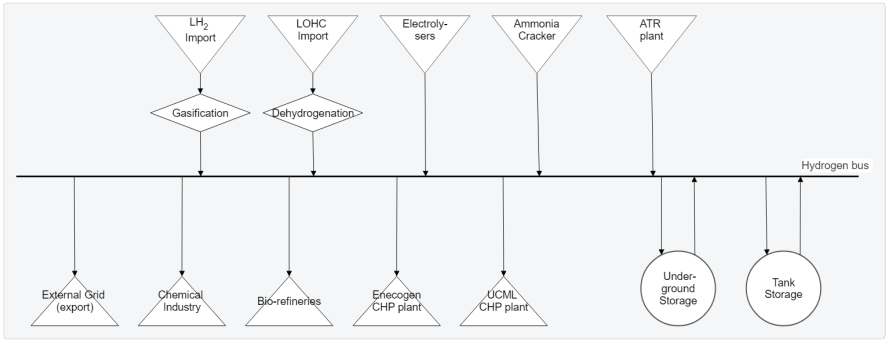

Figure A.3: SLD Hydrogen Network

A.4. SLD of Ammonia Network

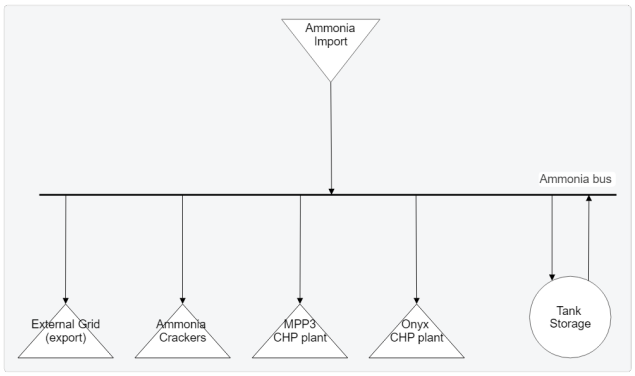

Figure A.4: SLD Ammonia Network

A.5. SLD of Heat Network

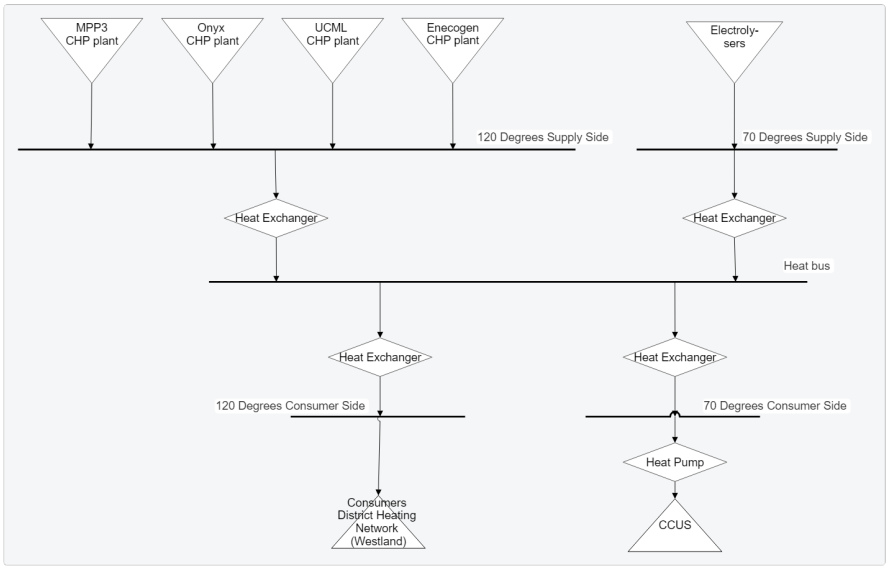

Figure A.5: SLD Heat Network

B

Coordinates of System Components

B.1. Table with Coordinates

Table B.1: Coordinates of system components used in the model.

Component	**x** (lon)	**y** (lat)
LNG import	4.071672	51.972456
LNG gasification	4.071672	51.972456
LH_2 import	4.004544	51.952835
LH_2 gasification	4.004544	51.952835
LOHC import	4.004544	51.952835
LOHC dehydrogenation	4.004544	51.952835
NH_3 import	4.067185	51.943429
Windfarm Hollandse Kust Zuid	4.024975	51.984722
Windfarm Maasvlakte 2	3.973622	51.944582
Windfarm IJmuiden Ver	3.988008	51.923838
Windfarm Nederwiek	3.999687	51.916215
Solarfarm De Slufter	4.009165	51.932253
MPP3 CHP plant	4.023604	51.960293
UCML CHP plant	4.023604	51.960293
Enecogen CHP plant	4.099862	51.952994
Onyx CHP plant	4.069977	51.944741
Electrolysers	3.987434	51.928112
NH_3 cracker	4.057982	51.942170
ATR hydrogen	4.069977	51.944741
BESS	4.015703	51.952148
H_2 underground storage	4.048388	51.978981
H_2 tank storage	3.990320	51.929379
NH_3 storage	4.057982	51.942170
Chemical industry	4.024351	51.968050
Bio-refineries	4.036583	51.968054
CCUS	4.035450	51.981973
Terminals	4.055713	51.953470
Shore Power	4.053309	51.958125
380kV MV bus	4.024634	51.953840
380kV AH bus	4.015703	51.952148
150kV bus	4.024183	51.955315
66kV bus	4.024610	51.954567
25kV bus 1	4.025047	51.954652
25kV bus 2	4.025047	51.954652
NG bus	4.071672	51.972456
H_2 bus	3.987434	51.928112
NH_3 bus	4.057982	51.942170
Heat bus	4.019427	51.953030
External grid connection 380kV	4.039180	51.926241
External grid connection 150kV	4.039180	51.926241
External grid connection NG	4.039180	51.926241
External grid connection H_2	3.989216	51.923726
External grid connection NH_3	4.057982	51.942170
External grid connection Heat	4.039180	51.926241

B.2. Haversine Distance Formula

To compute the great-circle distance between two buses-and thus to obtain lengths of lines, cables, and pipelines in the transmission and distribution system-the Haversine formula is used. This formula accounts for the spherical shape of the Earth and is therefore commonly used to calculate distances between locations on earth. The haversine formula is defined as follows:

$$
\begin{aligned}
a &= \sin^2\left(\frac{\Delta\varphi}{2}\right) + \cos(\varphi_1) \cdot \cos(\varphi_2) \cdot \sin^2\left(\frac{\Delta\lambda}{2}\right) \\
c &= 2 \cdot \arcsin\left(\sqrt{a}\right) \\
d &= R \cdot c
\end{aligned}
$$

Where:

- φ_1, φ_2 are the latitudes of the two points (in radians),
- λ_1, λ_2 are the longitudes of the two points (in radians),
- $\Delta\varphi = \varphi_2 - \varphi_1$,
- $\Delta\lambda = \lambda_2 - \lambda_1$,
- R is the mean radius of the Earth (assumed to be 6371 km),
- d is the resulting distance in kilometers.

Since the coordinates are provided in degrees, they must be converted to radians prior to using the formula. This is done via:

$$\theta_{\text{rad}} = \theta_{\text{deg}} \cdot \frac{\pi}{180}$$

So:

$$
\begin{aligned}
\varphi &= lat \cdot \frac{\pi}{180} \\
\lambda &= lon \cdot \frac{\pi}{180}
\end{aligned}
$$

C

Temperature Analysis

Component	Temperature [°C]	Ref.
Warmtelinqs Heat Supply	110-120	[53]
Warmtelinqs Heat Return	110-120	[53]
Hydrogen-fired CHP's	120	[129] [130]
Ammonia-fired CHP's	120	[129] [130]
Electrolysers	70	[131]
CCUS	40-60	[132]
LH2 Gasification	0-20	[105]
LNG Gasification	0-20	[133]
LOHC Dehydrogenation	280-320	[52]
Chemical Industry Consumption	400	[58]
Bio-refineries Consumption	400	[60]

Table C.1: Temperature of thermal energy flows.

D

Wind Farm Generation Profiles

Table D.1: Windfarm and Turbine Specifications, [134] [135] [136] [137] [138] [139]

Wind Farm	Turbine Type	Mean Wind Speed (m/s)	Cut-in Speed (m/s)	Rated Speed (m/s)	Cut-out Speed (m/s)
HKZ	Siemens Gamesa SG 11.0-200 DD	9.33	4.0	14.0	32.0
MV2	Vestas V162/6.0MW	9.15	3.0	10.5	24.0
IJV	Vestas V236-15.0	9.56	3.0	11.1	31.0
NW	Vestas V236-15.0	9.52	3.0	11.1	31.0

Mean wind speed at Hoek van Holland KNMI weather station is 8.2 m/s.

Generation Profile Calculation

The availability profiles of wind farms were calculated based on turbine specifications, mean wind speed, and hourly wind data. The steps are as follows:

1. The hourly wind speed profile was scaled by a farm-specific scaling factor:

$$\text{Scaled Wind Speed Profile} = \text{Wind Speed [KNMI station]} \times \text{Scaling Factor}$$

   where scaling factors were: HKZ: $\frac{9.33}{8.2}$, MV2: $\frac{9.15}{8.2}$, IJV: $\frac{9.56}{8.2}$, NW: $\frac{9.52}{8.2}$

2. The scaled wind speed profile of each wind farm location was processed based on turbine cut-in, rated, and cut-out speeds:
   - Wind speeds below the cut-in speed were set to zero availability.
   - Wind speeds between the cut-in and rated speeds retained their original values.
   - Wind speeds above the rated but below the cut-out were capped at the rated wind speed.
   - Wind speeds exceeding the cut-out speed were set to zero availability.
3. Availibility profile for each wind farm was obtained by:

$$\text{Availability Profile} = \frac{\text{Scaled Wind Speed Profile}}{\text{Rated Wind Speed}}$$

4. Eventually, the generation profile is generated by:

$$\text{Generation profile} = \text{Availability Profile} \times \text{Nominal Capacity}$$

E

Solar Farm Generation Profile

The generation profile for the solar farm is derived using the following steps:

1. Hourly solar irradiance profile was obtained from the KNMI weather station in Hoek van Holland [140]. This data represents the Global Horizontal Irradiation (GHI) at that location.

2. The solar irradiance profile was scaled by scaling factor based on the mean GHI of both locations [56]:

$$\text{Scaled Solar Irradiance Profile} = \text{Solar Irradiance Profile [KNMI weather station]} \times \frac{\text{GHI [Solar farm]}}{\text{GHI [KNMI weather station]}}$$

$$\text{Scaled Solar Irradiance Profile} = \text{Solar Irradiance Profile [KNMI weather station]} \times \frac{127.8}{126.4}$$

3. The scaled solar irradiance profile is limited to the maximum solar irradiance of 1000 W/m², as from this value the output of the solar panels remains constant.

$$\text{Capped Solar Irradiance Profile} = \min(\text{Scaled Solar Irradiance}, 1000)$$

4. The availability profile is calculated by normalizing the capped solar irradiance using the maximum solar irradiance:

$$\text{Availability Profile} = \frac{\text{Capped Solar Irradiance Profile}}{\text{Maximum Solar Irradiance (1000 } \mathrm{W/m^2})}$$

5. Generation profile is eventually calculated with the installed capacity of the solar farm and the efficiency of the panels.

$$\text{Generation Profile} = \text{Hourly Availibility Profile} \times \text{Installed capacity solar farm } [\mathrm{MW_p}] \times \eta$$

F

Terminal Load Calculation

Data from [61].

- **Terminal A:**
  - **Area:** 455,000 m^2
  - **Electricity Consumption (annual):** 9,000,000 kWh
  - **Fuel Consumption (annual):** 6,000,000 L
  - **Total Energy Consumption:** 261,450 GJ/yr
  - **Consumption per Area:** 0.5746 GJ/m^2*yr
- **Terminal B:**
  - **Area:** 252,000 m^2
  - **Electricity Consumption (annual):** 7,000,000 kWh
  - **Fuel Consumption (annual):** 2,000,000 L
  - **Total Energy Consumption:** 103,621 GJ/yr
  - **Consumption per Area:** 0.4112 GJ/m^2*yr

Average Energy Consumption per Area: 0.493 GJ/m^2*yr (equivalent to 0.493 TJ/km^2*yr)

Areas of Terminals on the Maasvlakte

The areas of key terminals on the Maasvlakte, obtained using ArcGIS, online are provided below:

- **Euromax:** 1,157,027.22 m^2
- **MOT:** 1,270,252.87 m^2
- **GATE:** 361,145.75 m^2 + 42,857 m^2
- **UWT Holding:** 72,976 m^2
- **ECT:** 323,808 m^2
- **RWG:** 1,453,653 m^2
- **APMT:** 1,454,200.66 m^2
- **Hutchi + ECT Delta:** 3,070,000 m^2
- **EMO:** 1,730,559.80 m^2
- **RCT + ECT:** 188,040 m^2

Total Area: 11.068 km^2

Energy Consumption of Terminals on the Maasvlakte

Total Energy Consumption: 5.456 TJ/yr

Conversion to Power:

- Annual energy consumption: 5.452×10^{12} J
- Total operating hours (assuming 8 hours/day): 8 hours/day $\times$ 365 days/yr $= 2920$ hours/yr
- Energy per hour: $\frac{5.452 \times 10^{12}}{2920}$ J/hour $= 1.866 \times 10^9$ J/hour
- Power consumption: $\frac{1.866 \times 10^9}{3600}$ W $= 0.517$ MW

Hourly Power Profile

An hourly power profile was generated based on operational hours (8:00–16:00). During non-operational hours, power consumption is set to zero. The results are shown in the following table:

Time Interval (hour)	Power Consumption (MW)
08:00–16:00	0.517
Other hours	0

Table F.1: Hourly Power Profile for Terminals on the Maasvlakte

G

Porthos Load Calculation

The following analysis includes calculations for the average electricity and heat demand across six CO_2 capture techniques. It is assumed that 2.5 million tonnes of CO_2 will be captured annually. Compressor costs of 0.15 GJ/ton CO_2 are added to the average electricity demand, as all technologies require compression [62].

Capture Techniques and Energy Demand

Table G.1: Energy Demand for CO_2 Capture Techniques

Capture Technique	Electricity (GJ/ton CO_2)	Heat (GJ/ton CO_2)
Cryogenic capture	0.7	0.0
Vacuum pressure	0.8	0.0
Membrane concept	1.2	0.0
Oxyfuel concept	1.7	0.0
Chemical absorption	0.45	2.5
Chemical absorption LJG	0.45	2.5

Average Energy Demand per Ton of CO_2

- **Average Electricity Demand (including compression):**

$$\text{Average Electricity Demand} = \frac{0.7 + 0.8 + 1.2 + 1.7 + 0.45 + 0.45}{6} + 0.15 = 1.03 \text{ GJ/ton } CO_2$$

- **Average Heat Demand:**

$$\text{Average Heat Demand} = \frac{0.0 + 0.0 + 0.0 + 0.0 + 2.5 + 2.55}{6} = 0.84 \text{ GJ/ton } CO_2$$

Annual Energy Consumption for 2.5 Million Tonnes of CO_2

- **Annual Electricity Consumption:**

$$\text{Electricity (Annual)} = 1.03 \times 2.5 \times 10^6 = 2,575,000 \text{ GJ/yr}$$

- **Annual Heat Consumption:**

$$\text{Heat (Annual)} = 0.84 \times 2.5 \times 10^6 = 2,100,000 \text{ GJ/yr}$$

Conversion to Capacities (MW)

- **Electricity Capacity:**

$$\text{Power (MW)} = \frac{2,575,000 \times 10^9}{365 \times 24 \times 3600} = 81.65 \text{ MW}$$

- **Heat Capacity:**

$$\text{Power (MW)} = \frac{2,100,000 \times 10^9}{365 \times 24 \times 3600} = 66.59 \text{ MW}$$

H

Network Specifications

H.1. Line Types

All specifications are based on product data from TKF (Twentsche Kabel Fabriek), except for the 380 kV overhead lines, for which no product specifications were available. According to TenneT, 380 kV lines can carry an apparent power of 2635 MVA [115]. Based on this, the nominal current for the 380 kV line is calculated. For the remaining data required for the 380 kV line, it is assumed to be the same as for the 150 kV line, as these values are the closest in magnitude.

Table H.1: Type specification of single-phase conductors.
"ol" = overhead line, "cs"= cable.

Nom. Voltage [kV]	Nom. Current [kA]	Nom. Frequency [Hz]	Resistance [Ω/km]	Reactance [Ω/km]	Capacitance [nF/km]	Cross Section [mm^2]	Mounting	Ref.
380	4.007	50	0.0149	0.0245	290	2000	ol	[115] [141]
150	2.275	50	0.0149	0.0245	290	2000	ol	[141]
66	1.125	50	0.0621	0.182	260	630	cs	[142]
25	0.825	50	0.0601	0.077	250	300	cs	[143]
23	0.825	50	0.0601	0.077	250	300	cs	[143]

Nominal apparent power of three-phase conductors is caluclated by:

$$S = \sqrt{3} * V * I \tag{H.1}$$

Table H.2: Nominal power of three-phase conductors

Nom. Voltage [kV]	Nom. Apparent Power [MVA]
380	2635
150	590
66	128
25	35.75
23	32.85

H.2. Transformer Types

Actual transformer data was not publicly available. Therefore, the most appropriate standard transformer type from the PyPSA transformer library, based on matching voltage levels, was used. Only the voltage levels and nominal apparent power were adjusted. The chosen transformer's nominal apparent power corresponds to the apparent power of the connected transmission line on the low-voltage side.

Table H.3: Transformer type specifications

Nom. V 0 [kV]	Nom. V 1 [kV]	Nom. S [MVA]	Nom. F [Hz]	V_{SC}	Real Part V_{SC}	OC Iron Losses [kW]	I_{OC} [%]	θ^{shift} [Degrees]	Tap Side	Tap Neutral	Tap min	Tap max	Tap step	PyPSA Type
380	150	590	50	12.2	0.25	60	0.06	0	0	0	-9	9	1.5	160 MVA 380/110 kV
150	66	128	50	12.0	0.26	55	0.06	0	0	0	-9	9	1.5	100 MVA 220/110 kV
150	25	35.74	50	11.2	0.302	31	0.08	150	0	0	-9	9	1.5	40 MVA 110/10 kV
66	25	35.74	50	11.2	0.302	31	0.08	150	0	0	-9	9	1.5	40 MVA 110/10 kV
25	23	32.85	50	11.2	0.302	31	0.08	150	0	0	-9	9	1.5	40 MVA 110/10 kV

H.3. Pipeline Types

Table H.4: Pipeline type specifications

Network	Capacity [MW]	Diameter [mm]	Ref.
Natural Gas	16900	1219	[116]
Hydrogen	13000	1219	[116]
Ammonia (refrigerated)	260	150-250	[118]
Heat (110-120)	300	900	[121] [144]
Heat (60-70)	300	900	[121] [144]

I

Carrier Parameters

Table I.1: Component Properties of Energy Carriers

Component	LHV (MJ/tonne)	Cp (MJ/(tonne*K))	Density (tonne/m^3)	E_{volume} (MJ/m^3)	Temperature (K)	Pressure (bar)	Latent Heat (MJ/tonne)
NG	47,100	2.34	0.0008	37.7	283	1	-
H_2	120,000	14.3	0.0000899	10.8	283	1	-
NH_3	18,600	2.19	0.00073	13.58	283	1	-
LNG	47,100	-	0.450	24975	21,195	1	510
LH_2	120,000	-	0.07085	8,502	20	1	449
LNH_3	18,600	-	0.600	11,160	240	1	1370
CH_2	120,000	-	0.02054	2,465	298	150-700	-

J

Weather Analysis for Scenarios

Based on historical hourly meteorological data from the Hoek van Holland KNMI station over the period 1970–2025 [54].

J.1. Frequency Distributions

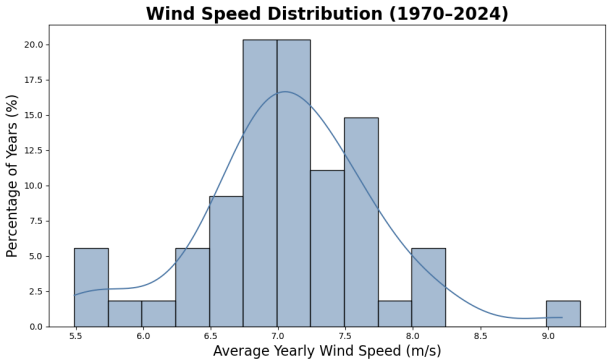

Figure J.1: Wind Speed Distribution.

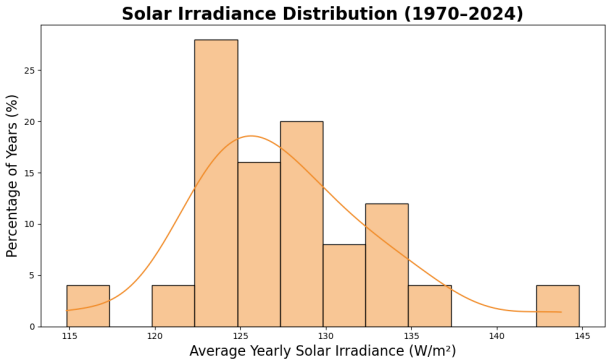

Figure J.2: Solar Irradiance Distribution.

J.2. Yearly Average Wind Speed (1970-2024) and Yearly Average Solar Irradiance (2000-2024)

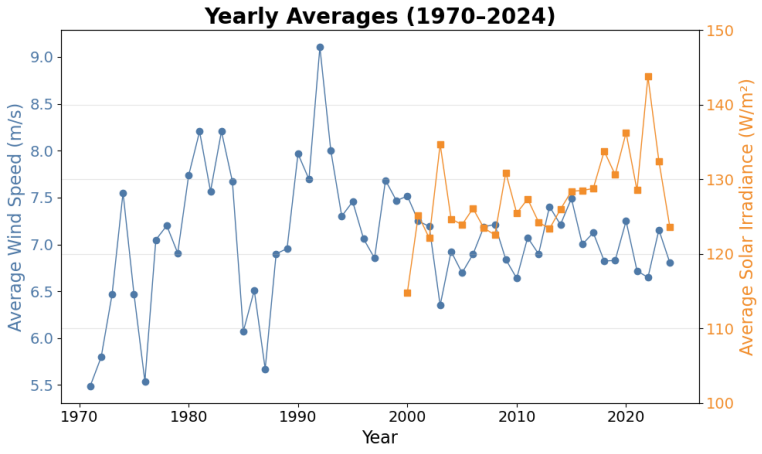

Figure J.3: Yearly averages of wind speed and solar irradiance.

K

Sensitivity Analysis

K.1. Electricity Export Volume

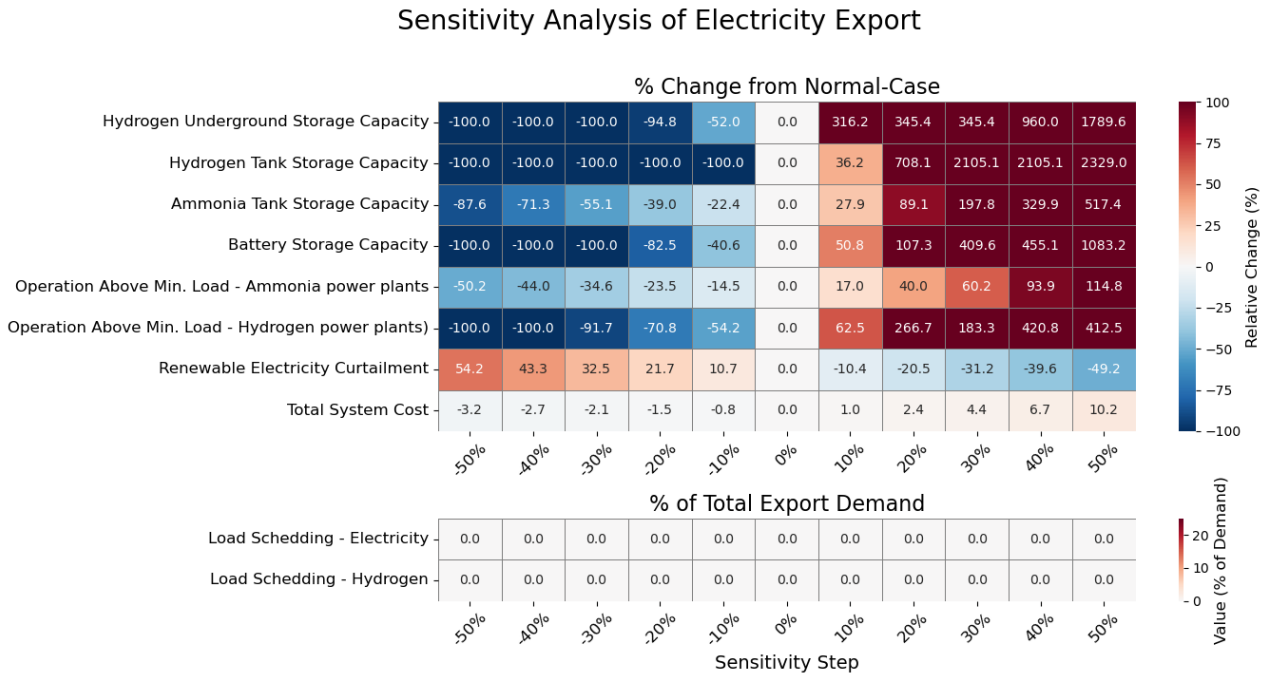

Figure K.1: Heat map of sensitivity analysis on the electricity export volume.

K.2. Hydrogen Export Volume

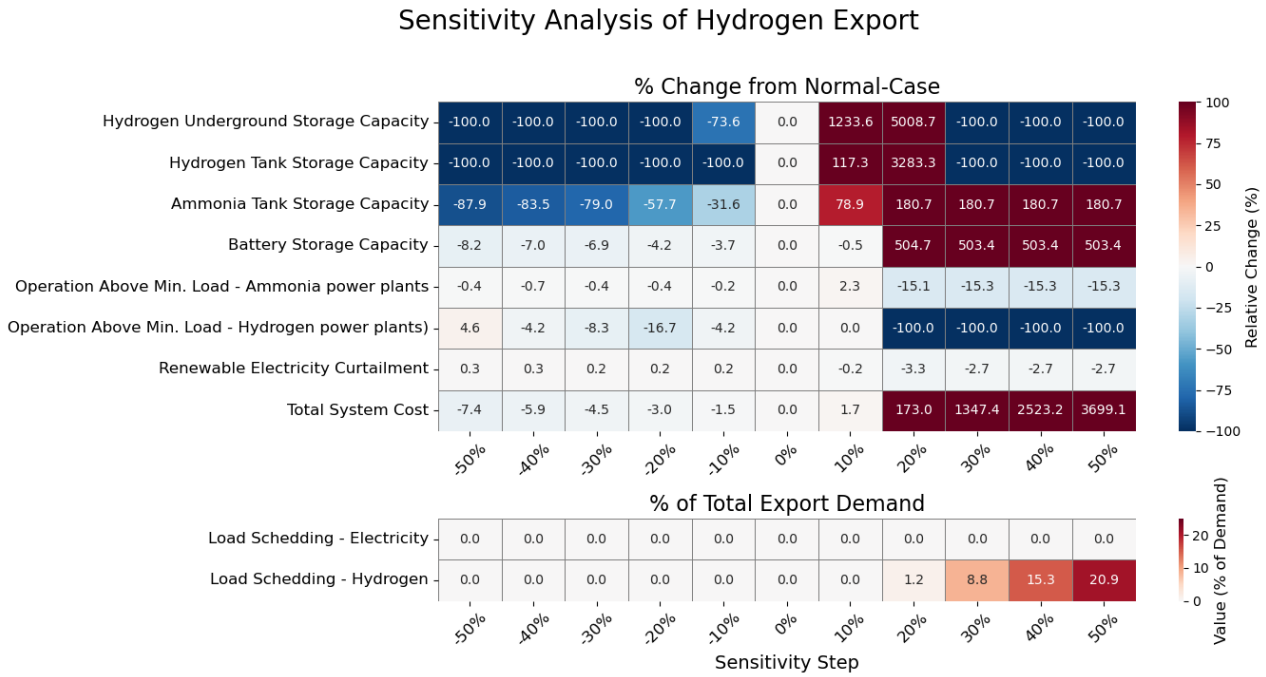

Figure K.2: Heat map of sensitivity analysis on the hydrogen export volume.

K.3. Electricity Market Price

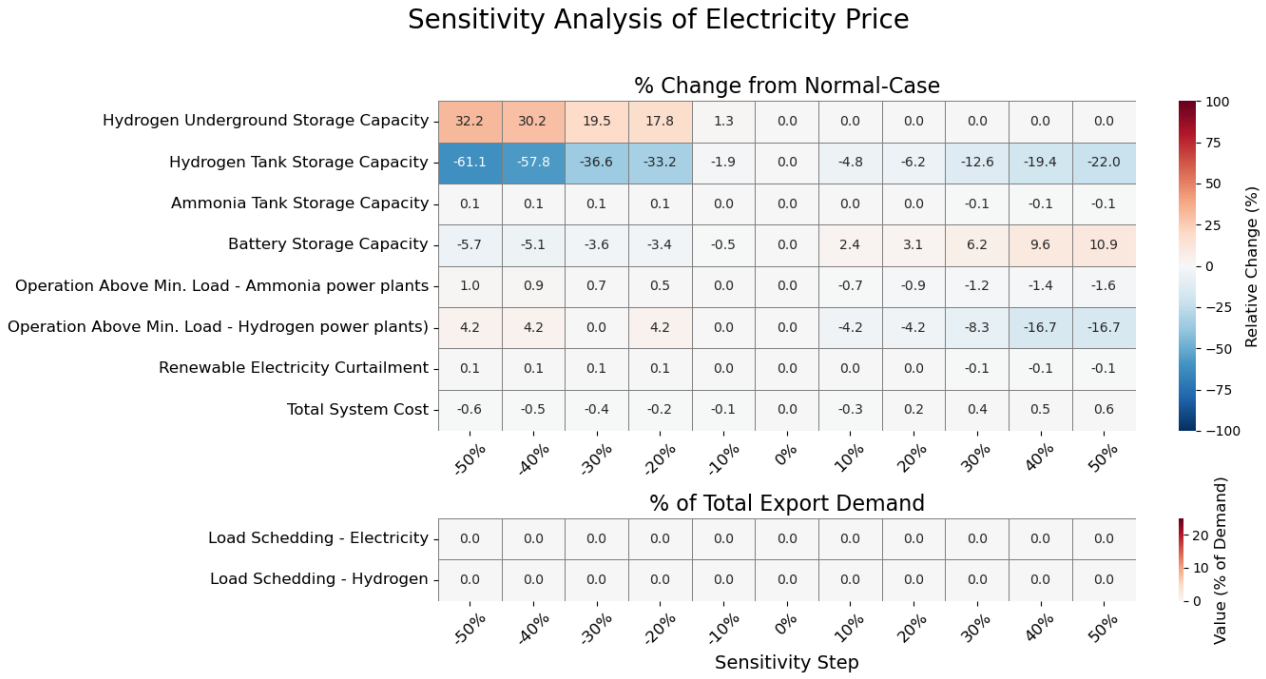

Figure K.3: Heat map of sensitivity analysis on the electricity price.

K.4. Hydrogen Market Price

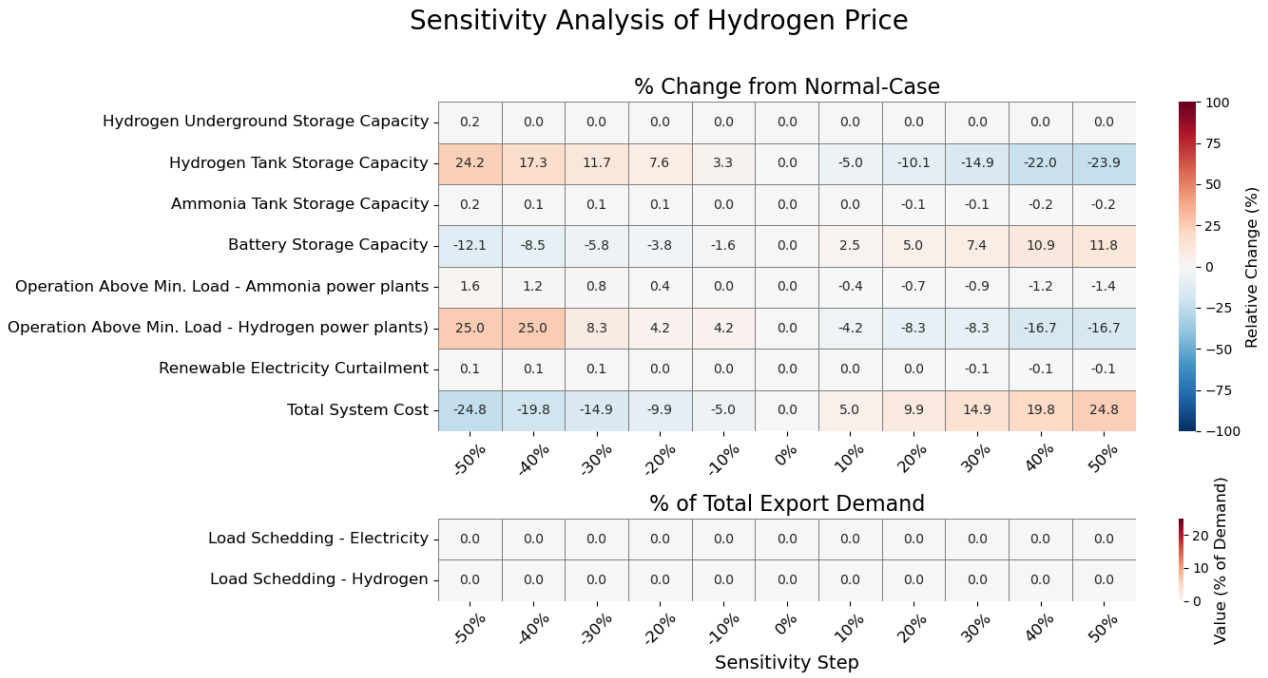

Figure K.4: Heat map of sensitivity analysis on the hydrogen price.

K.5. Ammonia Market Price

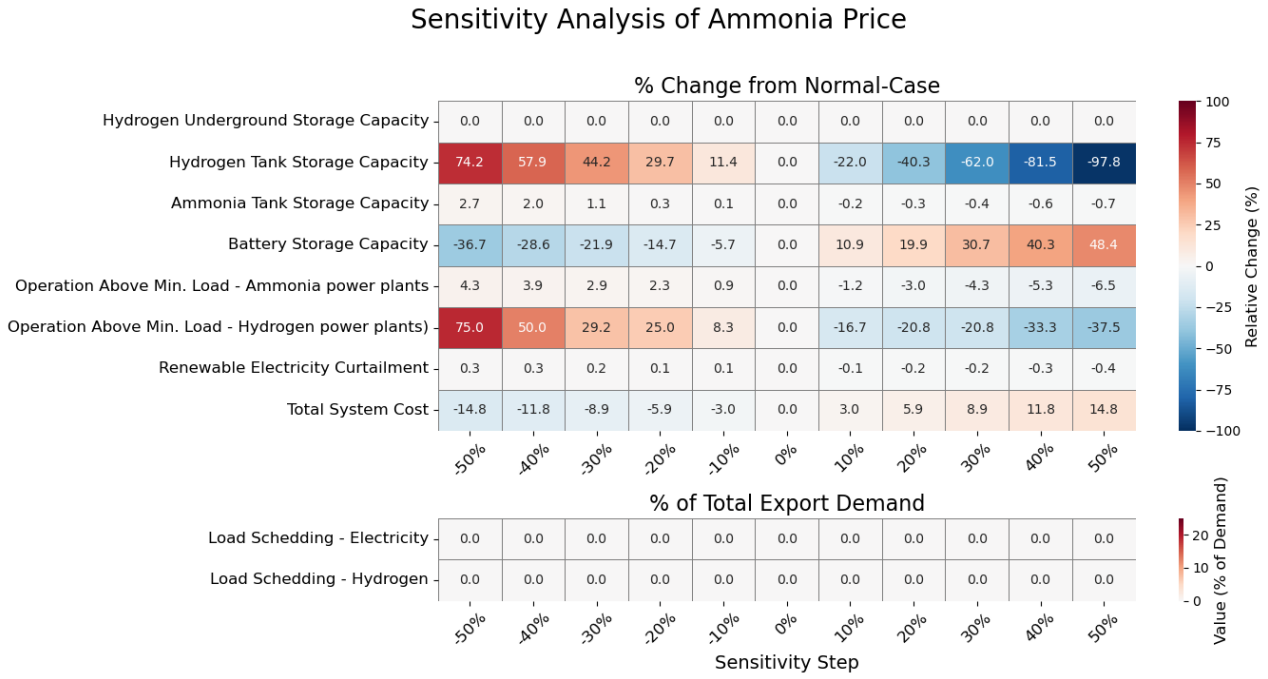

Figure K.5: Heat map of sensitivity analysis on the ammonia price.